



Title	VALENCY CONTROL OF AMORPHOUS SILICON CARBIDE AND ITS APPLICATION TO HETEROJUNCTION SOLAR CELL
Author(s)	太和田, 善久
Citation	大阪大学, 1983, 博士論文
Version Type	VoR
URL	https://hdl.handle.net/11094/2651
rights	
Note	

The University of Osaka Institutional Knowledge Archive : OUKA

<https://ir.library.osaka-u.ac.jp/>

The University of Osaka

VALENCY CONTROL
OF AMORPHOUS SILICON CARBIDE
AND ITS APPLICATION TO
HETEROJUNCTION SOLAR CELL

YOSHIHISA TAWADA

DECEMBER, 1982

FACULTY OF ENGINEERING SCIENCE
OSAKA UNIVERSITY

VALENCY CONTROL OF AMORPHOUS SILICON CARBIDE AND ITS APPLICATION TO HETEROJUNCTION SOLAR CELL

Yoshihisa Tawada

Department of Electrical Engineering

Faculty of Engineering Science

Osaka University

Toyonaka, Osaka 560 Japan

December, 1982

ABSTRACT

A series of systematic study has been carried out on fabrication and valency electron control of the hydrogenated amorphous silicon carbide (a-SiC:H) and its application to the a-SiC:H/a-Si:H heterojunction solar cell. In view of better processability for future mass production lines, p-i-n junction a-Si solar cell might be more promising structure as compared with the Schottky barrier type one. Systematic experimental investigations have been carried out on film deposition conditions and film qualities. Electrical, optical and optoelectronic properties of the film depend much upon geometric parameters of the furnace, injected rf power and also bias potential of the substrate. Presence of hydrogen radicals seems to be an important factor to explain the geometric effects on the film quality and also photovoltaic performances of the solar cells.

It is clearly shown that methane based a-SiC:H films have consider-

ably good valency electron controllability with a good optical transparency. Moreover, an anomalous increase of photoconductivity with doping of the substitutional impurities has been found. Employing these unique properties in the newly developed amorphous material, a-SiC:H/a-Si:H heterojunction solar cells has been developed.

On the basis of these basic parameter characterizations, a-SiC:H/a-Si:H heterojunction solar cell composed of glass/SnO₂/p a-SiC:H/i-n a-Si:H/metal has been developed. Clear step-like improvement on the short-circuit current density and the open-circuit voltage has been obtained with employing p-type a-SiC:H window junction as compared with an ordinary p-i-n a-Si:H homojunction solar cell.

The photovoltaic performances of a-SiC:H/a-Si:H heterojunction solar cells depend upon both the optoelectronic properties and the chemical bonding structure of a-SiC:H. The detailed bonding structure of two kinds of a-SiC:H films has been explored from IR absorption structural analysis. It has been experimentally proved that the methane based a-SiC:H film is a rather ideal amorphous alloy and is superior as a window material. Through these investigations, an 8 % efficiency barrier has been broken through with a-SiC:H/a-Si:H heterojunction solar cells.

A series of technical data on the material constants and cell design parameters for the optimization of this new type solar cell performance are presented, and possibilities of further improvement on the cell efficiency are discussed.

ACKNOWLEDGEMENT

The author would like to express his sincere thanks to Professor Yoshihiro Hamakawa for his kind advice and critical reading of this thesis.

This work has been done at Semiconductor Laboratory, Faculty of Engineering Science, Osaka University, Toyonaka, Osaka, under the direction of Professor Y. Hamakawa, and the author wants to express his greatest gratitude to Professor Y. Hamakawa for his constant advice, suggestion and encouragement throughout this work. The author is also grateful to Professor Y. Sakurai, Professor S. Narita, Professor S. Namba, Professor K. Fujisawa, Professor T. Sueta and Professor S. Yamamoto. The author wishes to give his highest appreciation to Professor A. Hiraki, Dr. T. Imura and Mr. N. Fukada of Osaka University for their useful advice, discussions and measurements.

The author is much indebted to Professor T. Nishino, Dr. M. Okuyama and Dr. H. Takakura for their useful advice and discussions throughout this work. Usual and enjoyable discussions with Drs. Y. Yamazoe, H. Nakayama and Y. Matsui are much appreciated.

The author wishes to express this gratitude to his co-workers in the Semiconductor Laboratory, Dr. H. Okamoto, Messrs. C. Sada, M. Kondo, T. Yamada, T. Yamaguchi and S. Nonomura, for their useful discussions, encouragements, or considerable assistances in this thesis work. The author is much indebted to Messrs. K. Tsuge and K. Nishimura of Kanegafuchi Chemical Industry Co. Ltd., Mr. S. Hotta of Matsushita Electric Industry, Mr. K. Fujimoto of Unitika Co. Ltd. and Mr. N. Nishimoto of Mitsubishi Chemical Industry Co. Ltd., who joined Semiconductor Laboratory, Faculty of Engineering Science. Osaka

University on leave of absence from their companies, for their useful discussions, encouragements, or considerable assistances in this thesis work. In particular, the author takes pleasure in acknowledging the important part played by Messrs. M. Kondo, K. Tsuge, C. Sada and K. Nishimura.

Finally the author wishes to thank his some company members, Messrs. H. Ikeno, Director of R&D-1, M. Yoshino, General Manager of Central Research Laboratory and M. Ohta, Technical Research Division for their supports.

TABLE OF CONTENTS

Chapter I. INTRODUCTION.....	1
1-1. Historical Background.....	1
1-2. Purpose and Significance of This Work.....	4
Chapter II. OPTIMIZATION OF THE FILM DEPOSITION PARAMETERS FOR THE HYDROGENATED AMORPHOUS SILICON SOLAR CELL.....	12
2-1. Introduction.....	12
2-2. Effect of Geometric Parameters on the Film Quality in the Plasma Reaction.....	13
2-3. Effect of Deposition Parameter on the Photovoltaic Performances of a-Si:H p-i-n Junction Solar Cell.....	23
2-4. Optimization of Doped Layers in a p-i-n a-Si:H Solar Cell.....	25
2-5. Discussion and Summary.....	36
Chapter III. PREPARATIONS OF a-SiC:H FILMS AND VALENCY ELECTRON CONTROL.....	44
3-1. Introduction.....	44
3-2. Experimental.....	45
3-3. Preparation and Characterization.....	46
3-3-1. Analysis of carbon content.....	46
3-3-2. Incorporated hydrogen manner in a-SiC:H.....	49
3-3-3. RF power dependence of the deposition.....	53
3-4. Optical and Optoelectronic Properties.....	57
3-4-1. Photoconductivity and optical band gap.....	57
3-4-2. Summary of effects of impurity doping.....	63
3-5. Discussion and Summary.....	66

Chapter IV. WINDOW EFFECTS OF HYDROGENATED AMORPHOUS

SILICON CARBIDE IN a p-i-n a-Si SOLAR CELL.....	70
4-1. Introduction.....	70
4-2. Preparation of a-SiC:H Films and a-SiC:H/a-Si:H Heterojunction Solar Cells.....	71
4-2-1. Fabrication of glass/SnO ₂ /p a-SiC:H/i-n a-Si:H/Al heterojunction solar cells.....	71
4-2-2. Basic properties of doped a-SiC:H as a window material...	73
4-3. Window Effects of a-SiC:H/a-Si:H Heterojunction Solar Cells..	77
4-3-1. Photovoltaic performance dependence on the optical band gap of a-SiC:H.....	77
4-3-2. Effects of J _{sc} and V _{oc}	77
4-3-3. Photovoltaic performances dependence on the thickness of p-type a-SiC:H.....	81
4-3-4. Typical J-V characteristics of a-SiC:H/a-Si:H heterojunction solar cells.....	84
4-4. Discussion and Summary.....	87

Chapter V. PROPERTIES AND CHEMICAL BONDING STRUCTURE

OF a-SiC:H FILMS FOR HIGH EFFICIENCY a-Si SOLAR CELLS.....	95
5-1. Introduction.....	95
5-2. Experimental Details.....	96
5-3. Photoconductivity and Optical Band Gap of Undoped and Boron Doped a-SiC:H Films.....	96
5-3-1. Optical and optoelectronic properties of methane based a-SiC:H films.....	97
5-3-2. Optical and optoelectronic properties of ethylene based a-SiC:H films.....	99

5-4. IR Spectra Analysis and Chemical Bonding	
Structure of a-SiC:H Films.....	101
5-4-1. IR spectra analysis of methane based	
and ethylene based a-SiC:H films.....	101
5-4-2. Hydrogen content and chemical	
bonding structure of a-SiC:H films.....	106
5-5. Effects of Methane Based and Ethylene Based	
a-SiC:H on the Photovoltaic Performances.....	107
5-5-1. Fabrication of methane based and ethylene	
based a-SiC:H/a-Si:H heterojunction solar cells.....	107
5-5-2. Photovoltaic performances of methane	
based a-SiC:H/a-Si:H heterojunction solar cells.....	109
5-5-3. Photovoltaic performances of ethylene	
based a-SiC:H/a-Si:H heterojunction solar cells.....	111
5-5-4. Voltage factor of	
a-SiC:H/a-Si:H heterojunction solar cells.....	114
5-5-5. Typical J-V characteristics of	
a-SiC:H/a-Si:H heterojunction solar cells.....	116
5-6. Discussion and Summary.....	119
Chapter VI. OPTIMIZATION OF a-SiC:H/a-Si:H	
HETEROJUNCTION SOLAR CELLS.....	126
6-1. Introduction.....	126
6-2. Optimization of Deposition Conditions.....	128
6-2-1. rf power dependence.....	128
6-2-2. Substrate temperature dependence.....	131
6-3. Optimization of Design Parameters of	
a-SiC:H/a-Si:H Heterojunction Solar Cells.....	136

6-3-1. i-layer thickness.....	136
6-3-2. Interface between p-layer and transparent electrode.....	140
6-3-3. Typical photovoltaic performances of a-SiC:H/a-Si:H heterojunction solar cells.....	147
6-4. Realistic Estimation of Conversion Efficiency.....	150
6-5. Discussion and Summary.....	156
Chapter VII. CONCLUSIONS.....	163
VITA	

I. INTRODUCTION

1-1. Historical Background

Professor Spear and LeComber first reported the valency electron control of the glow discharge produced amorphous silicon (a-Si:H) in 1976.¹⁾ This discovery made a striking impact in amorphous semiconductor field. At the same year, Carlson and Wronski reported an a-Si:H solar cell,²⁾ and showed as high as 5.5 % conversion efficiency with Schottky barrier solar cells in 1977.³⁾ This high efficiency encouraged the semiconductor field very much, and more than several groups have initiated to research a-Si solar cell, because an excellent optoelectronic properties with high optical absorption for visible light and also large area thin film productivity of a-Si:H match very timely with the strong social needs for the development of low cost solar cells as an energy resource. In 1977, a hydrogenated amorphous silicon carbide (a-SiC:H) was reported by Anderson and Spear,⁴⁾ but a-SiC:H could not be controlled its valency electron at this stage.

The development of p-i-n a-Si:H solar cell by Professor Hamakawa was the second key stage of a-Si solar cell technology. An efficiency of 4.5 % was demonstrated in this junction structure by Professor Hamakawa of Osaka University group in 1978.⁵⁾ Another big impact was an announcement of fluorinated amorphous silicon (a-Si:F:H) in 1978 by Obshinsky of ECD.⁶⁾ According to their report, a-SiF:H films show lower localized density of state with high doping efficiency and higher thermal and optical stability than a-Si:H films. A series of stimulated experimental traces has been initiated by wide groups devoting in not only material sciences but also device fabrication technology.⁷⁾ In the year of 1979, a remarkable progress has been

seen in device application field. A new type of high of high voltage photovoltaic device having a structure of horizontally multilayered p-i-n unit cell has been demonstrated by Osaka University group.^{8, 9)} A very similar cell structure using cermet film has also been postulated by Hanak.¹⁰⁾ A series of tremendous research and development efforts in the device fields comes into blooming in the year of 1980, that is, the conversion efficiency of a-Si solar cells has been improved day by day.

A principal difference in design concepts between single crystal and a-Si solar cell has been pointed out by Hamakawa et al.¹¹⁾ in 1979. That is: a drift type photovoltaic process dominates in a-Si solar cells, because most of photogenerated carriers are produced in the high electric region in the i-layer. Electric field dependence of photogeneration probability has been firstly calculated by Pai and Enck on amorphous selenium.¹²⁾ Recently, the calculations for a-Si have been done by several groups (Yamaguchi et al.¹³⁾, Hamakawa et al.¹⁴⁾ and Silver et al.¹⁵⁾ separately, however, a considerably good coincidence is seen in both results obtained. By using these results, Okamoto et al.¹⁶⁾ have recently revealed the spatial distributions of photocarrier generation probability escaping from geminate recombination and that of photocarrier collection probability in the p-i-n a-Si solar cell. This proves that the internal electric field exceeding 10^4 V/cm give rise to a sufficient drift current, and photovoltaic behavior of a-Si can be referred to "*drift type*" photovoltaic effect in nature. As the quantitative evidence, the drift component current is almost four orders magnitude larger than the diffusion current.

In view of better processability for future mass production system and reducing the effect of the short hole diffusion length in a-Si, the p-i-n structure might be a more promising cell than the Schottky barrier type.¹⁷⁾ However, one deficiency of the p-i-n a-Si homojunction cell is a considerably high optical absorption in the window side p-layer which has a narrow optical band gap with high density of non-radiative recombination centers.¹⁸⁾ The author has carried out some experimental trials to control valency electrons of wide optical band gap materials and found a good valency electron controllability in hydrogenated amorphous silicon carbide prepared by the plasma decomposition of silane and methane gas mixture.^{19, 20)}

New topics in 1981 were a hydrogenated amorphous silicon carbide²¹⁾ and microcrystalline silicon.^{22, 23)} These materials are very useful for the window side junction electrode because their excellent optical transparency with a considerably good photoconductivity. Utilizing p-type a-SiC:H as a front electrode, a-SiC:H/a-Si:H p-i-n heterojunction solar cell has been developed by the author.^{20, 24, 25)} and 8 % efficiency barrier was firstly broken through in the fall of 1981.²⁶⁾ More than 10 % efficiency might be obtained in a near future with the a-SiC:H/a-Si:H heterojunction structure.²⁷⁾

The discovery of valency electron controlled a-SiC:H give an impact in the amorphous semiconductor field.²⁸⁾ However, the researches on the new amorphous materials such as a-SiC:H, a-SiN:H^{29,30)} and a-SiSn^{31, 32)} are at a starting point. New knowledge of these amorphous materials, especially a-SiC:H^{33, 34, 35)} and its related devices have been accumulated day by day.^{36, 37, 38, 39)}

1-2. Purpose and Significance of the Present Work

In view of improving the efficiency of amorphous silicon solar cell, one must well establish at first preparation technology of a-Si:H for solar cell. Furthermore, a wide band gap material which can be controlled its valency electron has to be developed to suppress the optical loss component of p-i-n structure.¹⁸⁾ The purpose of this work is to carry out a series of systematic investigations on the high efficiency amorphous silicon solar cell. Considerable efforts have been paid to explore the mechanism of valency electron control in the hydrogenated amorphous silicon carbide (a-SiC:H) and its application to the a-SiC:H/a-Si:H heterojunction solar cells. Meanwhile, the plasma deposited a-SiC:H has been firstly reported by Anderson and Spear.⁴⁰⁾ However, their work centered only on the compositional dependence of the optical band gap of a-SiC:H. Since their work, photoluminescence study,^{41, 42)} infra-red spectra analysis^{43, 44, 45)} have been released, but no information on the electrical and optoelectronic properties of doped a-SiC:H was given. We have paid our attention on this point, and tried to adopt methane (CH_4) as a carbon source instead of ethylene (C_2H_4) as had been used by Anderson and Spear. It has been clearly shown by the author that the plasma deposition from CH_4 promotes the compiling of tetrahedral bonding of carbon in a-SiC:H network and a large photoconductivity recovery effect has been found by impurity doping on the methane based a-SiC:H.^{20, 21)} Employing the a-SiC:H as a window side junction material, the author has developed a new technology of a-SiC:H/a-Si:H heterojunction solar cell coupled with optimized a-Si:H.

In Chapter II, the author clears up how the geometric parameters in the deposition system make influences on the film quality and on

the photovoltaic performances of a-Si:H p-i-n homojunction solar cell.¹⁹⁾ A series of experimental data on the electrical and optoelectronic properties of a-Si:H films prepared with various geometric parameters is described. Optical emission spectroscopy (OES) measurement was also carried out to evaluate the plasma bombardment effects.^{46, 47)} Film properties depend upon geometric parameters, the rf power and also the bias potential of the substrate. A good correlation between these factors has been found. Presence of hydrogen radicals seems to be an important factor to explain the geometric effect on the film quality and also the photovoltaic performances. Through these optimizations, the efficiency of a-Si:H p-i-n homojunction solar cell has been improved from 4.5³⁾ to 5.7 %.¹⁹⁾

Chapter III discusses the valency electron control of a-SiC:H films prepared by the plasma decomposition of $[\text{SiH}_{4(1-x)} + \text{CH}_{4(x)}]$ or $[\text{SiH}_{4(1-x)} + 1/2\text{C}_2\text{H}_{4(x)}]$. Preparation technology, characterization, and optical, electrical and optoelectronic properties of these films are discussed in details.^{33, 34, 35)} It is verified that a-SiC:H films contain a considerable amount of hydrogen atoms attached to Si and C, and that hydrogen atoms attached to carbon act as an important factor to control its valency electrons. The methane based a-SiC:H films contains almost tetrahedrally bonded carbons with a small number of methyl groups and shows a good valency electron controllability.

Chapter IV deals with the window effects of a-SiC:H on the photovoltaic performances of a-SiC:H/a-Si:H heterojunction structure.²⁵⁾ a-SiC:H/a-Si:H heterojunction solar cells show not only larger short-circuit current density J_{sc} but also larger open-circuit voltage V_{oc}

than ordinary p-i-n a-Si:H homojunction solar cells. The improvement of J_{sc} is caused in a part by a large optical band gap of p-type a-SiC:H which reduces the undesirable absorption in the p-layer and in other part by an enhanced large internal electric field.³⁶⁾ Moreover, a clear correlation is found between V_{oc} and the diffusion potential V_d .²⁵⁾ Utilizing the valency controlled a-SiC:H, the efficiency of a-SiC:H/a-Si:H heterojunction solar cell has been improved to 7.55 %.

Chapter V describes a series of experimental verifications on the electronic properties and the chemical bonding structure of a-SiC:H films for high efficiency solar cells.^{33, 36, 37)} An a-SiC:H film can be fabricated by the decomposition of SiH_4 and hydrocarbons,⁴⁰⁾ or alkylsilane.^{48, 49)} The electrical and optoelectronic properties of a-SiC:H films, as is described in chapter III, significantly depend upon both carbon sources and the deposition conditions. Utilizing ethylene and methane as carbon sources, a series of experimental investigations on the film properties and the structure has been conducted. The photovoltaic performances of methane based and ethylene based a-SiC:H/a-Si:H heterojunction solar cells are also discussed. It comes to the conclusion that a wide band gap material is not always useful as a window material for p-i-n a-Si solar cell and the chemical bonding structure of these materials is an important factor for better junction formation.

In Chapter VI, optimizations of the deposition conditions and the design parameters of a-SiC:H/a-Si:H heterojunction solar cells have been investigated.³⁹⁾ A series of experimental investigation on the deposition conditions and the design parameters of the cells, mainly in view point of interface between the transparent electrode

and p-layer has been carried out.³⁸⁾ Moreover, the actual process in which an 8% efficiency barrier has been broken through with a-SiC:H/a-Si:H heterojunction structure is demonstrated.³⁷⁾ From the surface analysis, it has been found that SnO₂ or ITO are reduced to metallic Sn or In by hydrogen plasma^{38, 39)} and the diffusion of reduced In into p-layer results in harmful influence on cell performances, and Sn does not. To suppress the reduction and the diffusion of In, glass/ITO/SnO₂ substrate has been developed.³⁹⁾ A large area solar cell deposited on this substrate showed more than 7.7% efficiency.

In the final chapter, some conclusions obtained through this thesis work are summarized.

REFERENCES

- 1) W. E. Spear and P. G. LeComber: *Phil. Mag.*, 33 (1976) 935.
- 2) D. E. Carlson and C. R. Wronski, *Appl. Phys. Lett.*, 28 (1976) 671.
- 3) D. E. Carlson: *IEEE Trans. on Electron Devices*, ED-24 (1977) 449.
- 4) D. A. Anderson and W. E. Spear, *Phil. Mag.*, 35 (1977) 1.
- 5) H. Okamoto, Y. Nitta, T. Adachi and Y. Hamakawa: *Surface Sci.*, 86 (1979) 486.
- 6) A. Madan and S. R. Ovshinsky: *Phil. Mag.*, B40 (1979) 259.
- 7) M. Konagai and K. Takahashi: *Appl. Phys. Lett.*, 36 (1980) 559.
- 8) H. Okamoto, Y. Nitta and Y. Hamakawa: *Jpn. J. Appl. Phys.*, 19 (1980), suppl. 19-1, 545.
- 9) Y. Hamakawa, H. Okamoto and Y. Nitta: *J. Non-Cryst. Solids*, 35&36 (1980) 201.
- 10) J. J. Hanak: *J. Non-Cryst. Solids*, 35&36 (1980) 755.
- 11) Y. Hamakawa: *Surface Sci.*, 86 (1979) 44.
- 12) O. M. Pai and R. C. Enck: *Phys. Rev.*, 11 (1975) 5163.
- 13) T. Yamaguchi, H. Okamoto, S. Nonomura and Y. Hamakawa: *Jpn. J. Appl. Phys.*, 20 (1981), suppl. 20-2, 195.
- 14) H. Okamoto, T. Yamaguchi and Y. Hamakawa: *Proc. 8th Int. Conf. on Amorphous and Liquid Semiconductors*, Cambridge (1979) XF-7.
- 15) M. Silver, A. Madan, D. Adler and W. Czubytyj: *Proc. 14th IEEE Photovoltaic Specialists Conf.*, San Diego (1980) p 1062.
- 16) H. Okamoto, T. Yamaguchi and Y. Hamakawa: *J. Phys. Soci. Japan*, 49 (1981) suppl. a, 1213.
- 17) H. Okamoto, Y. Nitta, T. Yamaguchi and Y. Hamakawa: *Solar Energy Mat.*, 2 (1980) 313.

- 18) Y. Hamakawa, H. Okamoto and Y. Nitta: Proc. *14th IEEE Photovoltaic Specialists Conf.*, San Diego (1980) p 1074.
- 19) Y. Tawada, T. Yamaguchi, S. Nonomura, S. Hotta, H. Okamoto and Y. Hamakawa: Jpn. J. Appl. Phys., 20 (1981), suppl. 20-2, 213.
- 20) Y. Tawada, H. Okamoto and Y. Hamakawa: Appl. Phys. Lett., 39 (1981) 237.
- 21) Y. Tawada, M. Kondo, H. Okamoto and Y. Hamakawa: Proc. *9th Int. Conf. on Amorphous and Liquid Semiconductors*, Grenoble (1981) published as J. du Physique, C-4 (1981), suppl. 10, 471.
- 22) T. Hamasaki, H. Kurata, M. Hirose and Y. Osaka: Appl. Phys. Lett. 37 (1980) 1084.
- 23) A. Matsuda, S. Yamasaki, K. Nakagawa, H. Okushi, K. Tanaka, S. Iizima, M. Matsumura and H. Yamamoto: Jpn. J. Appl. Phys., 19 (1980) L305.
- 24) Y. Tawada, M. Kondo, H. Okamoto and Y. Hamakawa: Proc. *15th IEEE Photovoltaic Specialists Conf.*, Florida (1981) p 245.
- 25) Y. Tawada, M. Kondo, H. Okamoto and Y. Hamakawa: Jpn. J. Appl. Phys., 21 (1982), suppl. 21-1, 297.
- 26) Y. Tawada, M. Kondo, H. Okamoto and Y. Hamakawa: Solar Energy Mat., 6 (1982) 299.
- 27) Y. Hamakawa and Y. Tawada: Int. J. Solar Energy, 1 (1982) in press.
- 28) Y. Hamakawa: Proc. *9th Int. Conf. on Amorphous and Liquid Semiconductors*, Grenoble (1981) published as J. du Physique, C-4 (1981) suppl. 10, 1131.
- 29) S. Yokoyama, M. Hirose and Y. Osaka: Jpn. J. Appl. Phys., 20 (1981) L35.
- 30) M. Hirose: Jpn. J. Appl. Phys., 21 (1982), suppl. 21-1, 275.
- 31) C. Verie, J. F. Rochette and J. P. Rebouillat: J. du Physique, C-4 (1981), suppl. 10, 667.

- 32) C. Verie and J. F. Rochette: *Proc. 15th IEEE Photovoltaic Specialists Conf.*, Florida (1982), pp. 251.
- 33) Y. Tawada, K. Tsuge, M. Kondo, H. Okamoto and Y. Hamakawa: *J. Appl. Phys.*, 53 (1982) 5273.
- 34) Y. Tawada, K. Tsuge M. Kondo, K. Nishimura, H. Okamoto and Y. Hamakawa: *Phil. Mag.*, to be published.
- 35) M. Kondo, Y. Tawada, K. Nishinura, H. Okamoto and Y. Hamakawa: *Jpn. J. Appl. Phys.*, 21 (1982) Letter, to be published.
- 36) Y. Tawada, K. Tsuge, K. Nishimura, M. Kondo, H. Okamoto and Y. Hamakawa: *Proc. 3rd Photovoltaic Science and Engineering Conf.*, Kyoto, May, 1982, and *Jpn. J. Appl. Phys.* 21(1982), suppl.21-2, 269.
- 37) N. Fukada, T. Imura, A. Hiraki, Y. Tawada, K. Tsuge, H. Okamoto and Y. Hamakawa: *Proc. 3rd Photovoltaic Science and Engineering Conf.*, May, 1982 and *Jpn. J. Appl. Phys.* 21 (1982), suppl. 21-2, 251.
- 38) Y. Tawada, K. Tsuge, M. Kondo, H. Okamoto and Y. Hamakawa: *Proc. 4th EC Photovoltaic Solar Energy Conf.*, Stressa (1982), pp. 698.
- 39) Y. Hamakawa, Y. Tawada, K. Tsuge, K. Nishimura and H. Okamoto: *Proc. 16th IEEE Photovoltaic Specialists Conf.*, San Diego (1982) in press.
- 40) D. A. Anderson and W. E. Spear: *Phil. Mag.*, 35 (1977) 1.
- 41) D. Engemann, R. Fischer and J. Knecht: *Appl. Phys. Lett.*, 32 (1978) 567.
- 42) R. S. Sussmann and R. Ogden: *Phil. Mag.*, B44 (1981) 137.
- 43) H. Wieder, M. Cardona and C. R. Guarnieri: *Phy. Stat. Sol.*, (b)92 (1979) 99.
- 44) A. Guivarch, J. Richard, M. LeContellec, E. Ligeon and J. Fontenille: *J. Appl. Phys.*, 51 (1980) 2167.

- 45) Y. Catherine, G. Turban and B. Grolleau: Thin Solid Films, 76 (1981) 23.
- 46) S. Hotta, Y. Tawada, H. Okamoto and Y. Hamakawa: Proc. 9th Int. Conf. on Amorphous and Liquid Semiconductors, Grenoble (1981) published as J. du Phisique, C-4 (1981), suppl. 10, 631.
- 47) S. Hotta, N. Nishimoto, Y. Tawada, H. Okamoto and Y. Hamakawa: Jpn. J. Appl. Phys., 21 (1982), suppl. 21-1, 289.
- 48) H. Munekata, S. Murasato and H. Kukimoto: Appl. Phys. Lett., 37 (1980) 536.
- 49) H. Munekata, S. Murasato and H. Kukimoto: Appl. Phys. Lett., 38 (1981) 188.

II OPTIMIZATION OF THE FILM DEPOSITION PARAMETERS FOR THE HYDROGENATED AMORPHOUS SILICON SOLAR CELL

2-1 Introduction

The glow discharge produced amorphous silicon such as a-Si:H and a-Si:F:H have gathered a considerable attention as a promised candidate material for the low cost solar cell.¹⁾ With a recent few year's tremendous R & D efforts, the conversion efficiency of the a-Si solar cell has been improved day by day, and the top data announced in 1980 were 6.1% for the inverted p-i-n a-Si:H cell²⁾ and 6.3% for a-Si:F:H M-I-S type cell³⁾, respectively.

In view of better processability for a future mass production line, the p-i-n heteroface junction a-Si solar cell might be more promising structure as compared with Schottky barrier type one. We have paid our attention on this point, a series of systematic study has been carried out on the film deposition conditions, cell configuration and design parameters for the optimizations of the photovoltaic performance. Optoelectronic properties of the doped and undoped hydrogenated a-Si and their film thickness optimizations for the p-i-n a-Si:H solar cells have been investigated by Okamoto et al.⁴⁾, and through these efforts 4.5% conversion efficiency was announced in the summer of 1978.⁵⁾ On the other hand, an effort to improve the film quality in terms of the cross field technology by which a controllable d.c. electric field is applied to the r.f. sustained plasma perpendicularly to the r.f. field.⁶⁾ An attempt to improve conversion efficiency by reducing a field dependent recombination loss expected in the i-layer has been made with a multiple p-i-n cell structure.⁷⁾ In the course of the study high voltage p-i-n

stacked cell has been developed.⁸⁾

In this chapter, we describe some experimental data on the electrical and optoelectronic properties of the a-Si:H films prepared with various geometric parameters in the furnaces with sustaining plasma discharge conditions. Changes in the photovoltaic performances with the deposition conditions have also been presented.

2-2 Effect of Geometric Parameters on the Film Quality in the Plasma Reaction

Hydrogenated amorphous silicon (a-Si:H) films were prepared by the capacitively coupled r.f. plasma deposition system as shown in Fig. 2-1. The diameter and height of the reaction chamber are 11 cm and 18 cm, respectively, and the diameter of the rotating stage is 9 cm. One of the noticeable merits of the reaction chamber is that we can control the relative position of the substrate to discharge plasma while the energy density of the plasma can be controlled by controlling the r.f. coupling electrode set outside the reaction chamber perpendicularly to the substrate. Therefore, we have investigated at first the effect of the electrode position D to the substrate, that is, the distance between the center of electrode and the substrate surface were settled at 3, 7, 10 and 12.5 cm with a parameter of r.f. power of 13.56 MHz from 10 to 70 watts. Other deposition conditions through the present work are fixed constant as shown in Table 2-1. Under these conditions, it was confirmed firstly that deposition rate increases proportionally to r.f. power P and becomes smaller for higher electrode position as shown in Fig. 2-2. The actual deposition rate was ranging from 1 to 4.5 $\text{\AA}/\text{sec}$.

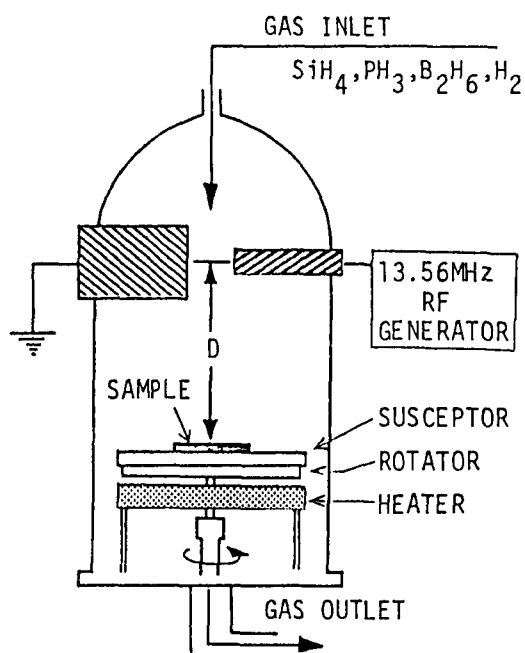


Fig. 2-1 Schematic diagram of plasma deposition equipment; Diameter=11 cm, Height of the chamber=18 cm.

Table 1-1 DEPOSITION PARAMETERS

PRESSURE	2 - 3 Torr.
TOTAL FLOW	40 - 70 sccm
SiH_4	10 % in H_2
PH_3	500 ppm in H_2
B_2H_6	500 ppm in H_2
T_s	260 °C

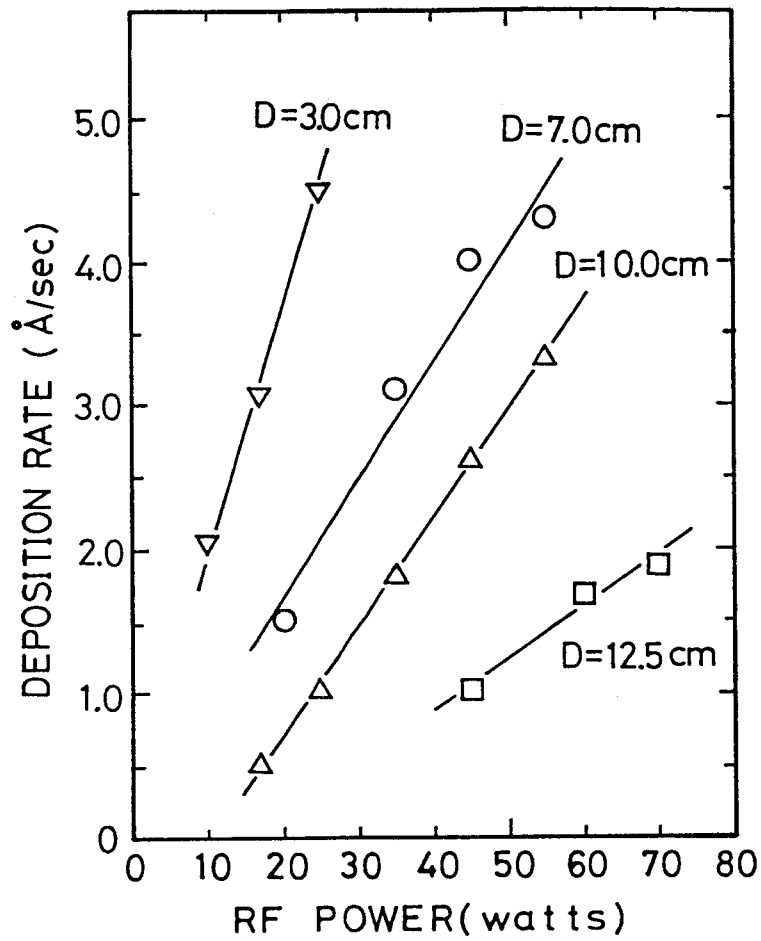


Fig. 2-2 Deposition rate ($\text{\AA}/\text{sec}$) of undoped a-Si:H as a function of r.f. power for electrode position $D=3, 7, 10$ and 12.5 cm.

IR absorption spectrum was measured by utilizing a-Si:H films deposited on high-resistivity crystalline silicon wafer. IR absorption coefficients at 2000 cm^{-1} and 2090 cm^{-1} are shown in Fig. 2-3. The assignments deduced by Knights⁹⁾ and Fritzche¹⁰⁾ indicate that 2000 cm^{-1} and 2090 cm^{-1} band absorption are related to monohydrides (SiH) and dihydrides (SiH₂), respectively. Absorption coefficient at 2000 cm^{-1} increases as r.f. power increases for each electrode position, and absorption coefficient at 2090 cm^{-1} is nearly constant or slightly decreases as r.f. power increases. These results imply that higher r.f. power deposition might be favorable in regard to the incorporated monohydrides. Moreover, one can find an interesting tendency that amount of SiH and SiH₂ depend less on the electrode position D compared with r.f. power. From this point, it is suggested that what kind of decomposed species are yielded in the discharge plasma might well reflect in the composition of deposited films.

Optical band gap $E_g(\text{opt})$ was determined from absorption spectrum at higher absorption region ($\alpha > 10^4\text{ cm}^{-1}$). Both r.f. power P and electrode position D seem to affect the optical band gap slightly, which is around 1.74, 1.76, 1.78 and 1.80 eV for D=3, 7, 10 and 12.5 cm, respectively as shown in Fig. 2-4.

Figure 2-5 shows the dark conductivity $\sigma_d(A)$ and the activation energy $\Delta E(B)$ dependent upon r.f. power and the electrode position D. Dark conductivity is scattered in the range of $10^{-9} - 10^{-8}$ mho/cm with some exceptions found in the higher r.f. power region (45 watts). Activation energy determined from the temperature dependence of dark conductivity is nearly one half of the corresponding

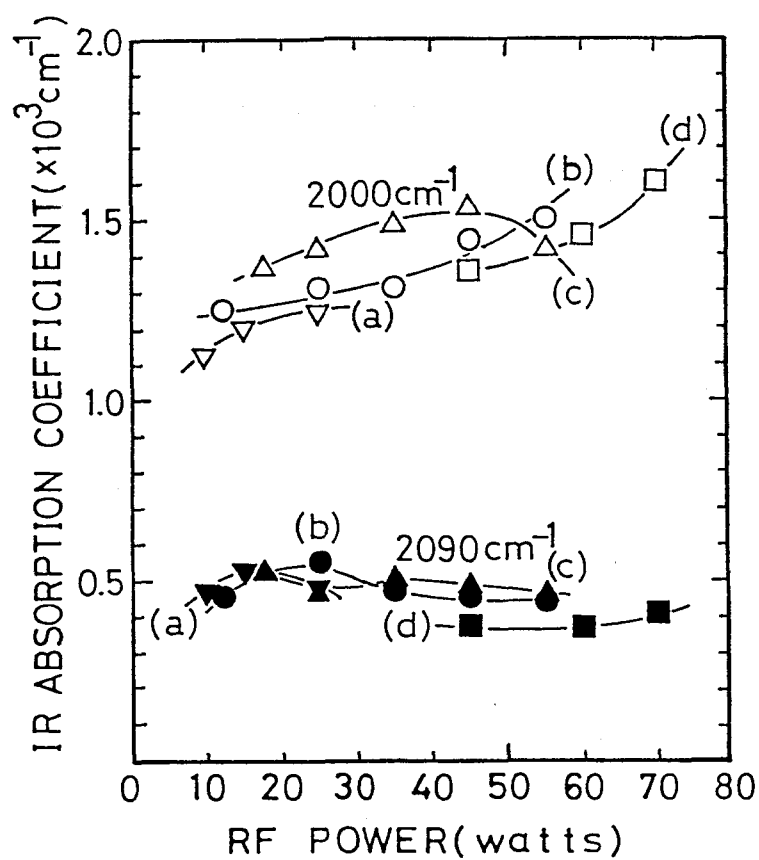


Fig. 2-3 IR absorption coefficient at 2000 cm^{-1} and 2090 cm^{-1} of undoped a-Si:H films as a function of r.f. power for electrode position D=3, 7, 10 and 12.5 cm.

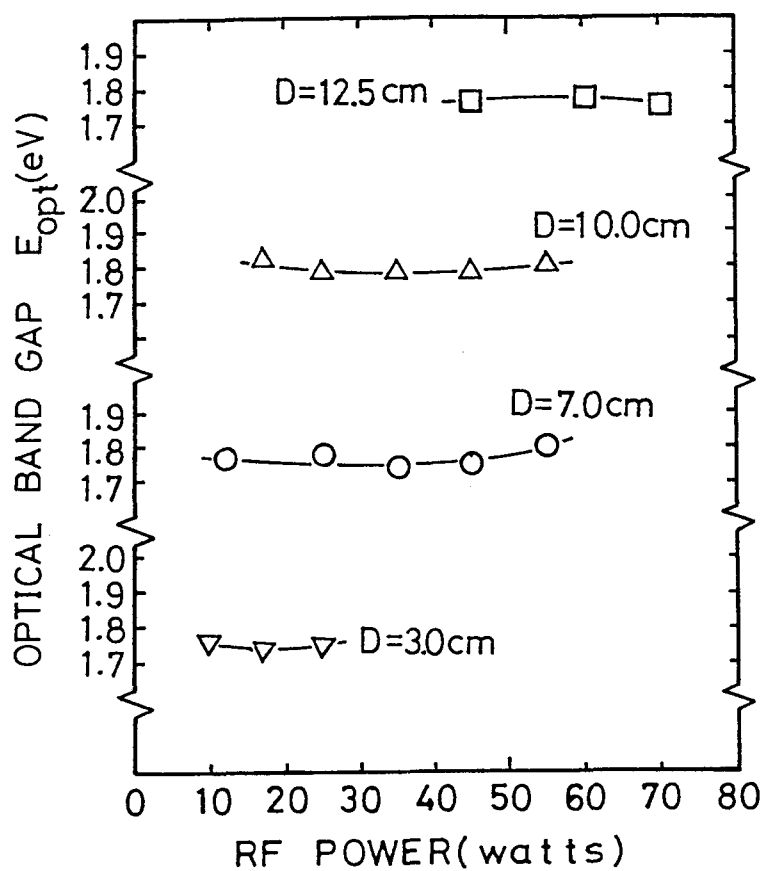


Fig. 2-4 Optical band gap $E_{g(opt)}$ of undoped a-Si:H as a function of r.f. power.

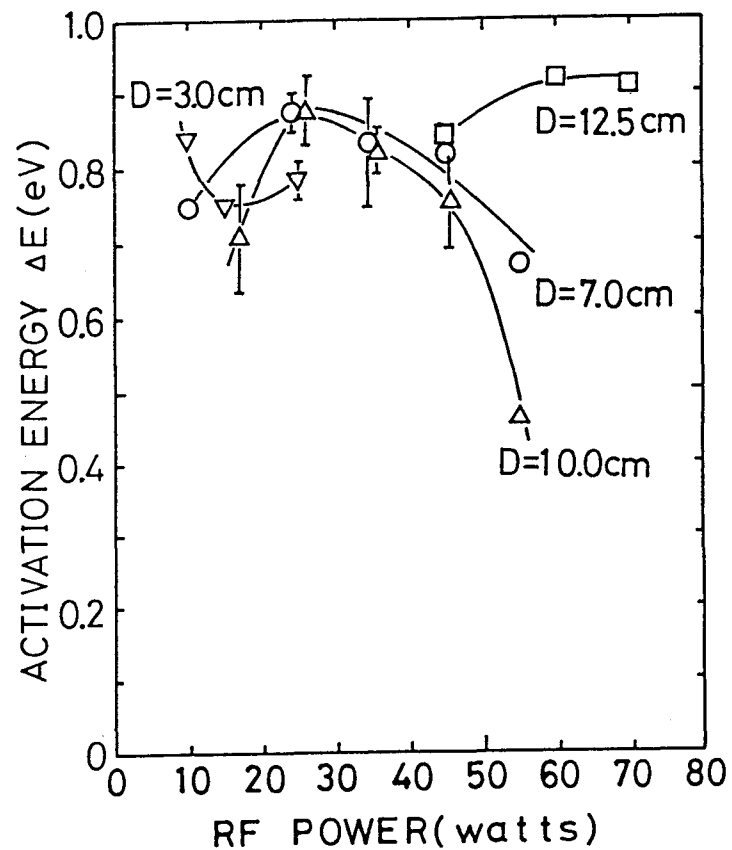
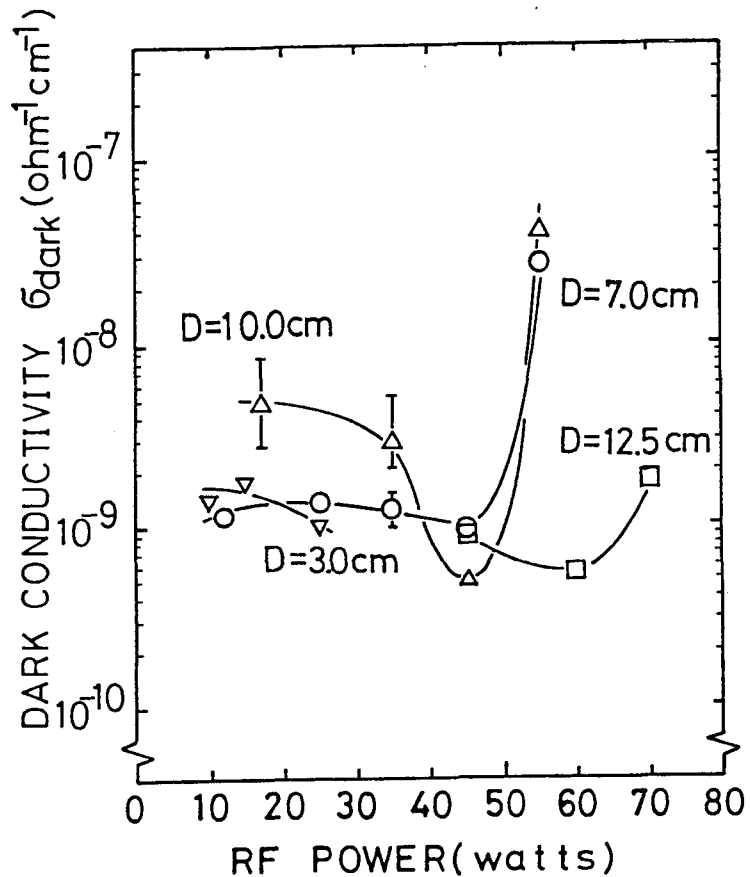


Fig. 2-5 r.f. power dependency on the electric properties of undoped a-Si:H films as a function of r.f power for electrode position $D=3, 7, 10$ and 12.5 cm; (A)= dark conductivity, (B)= activation energy.

optical band gap also with some exceptions at higher power region. A higher r.f. power is considered to induce the following two phenomena, that is, sputtering out of chemically active impurities from the wall of reaction chamber and a bombardment effect of plasma species on the films under the growth. The latter effect can be restricted in our deposition system by controlling the distance between the electrode and surface of the substrate.

For the photovoltaic application, a larger photoconductivity is eagerly requested. One must adjust the deposition conditions to obtain it. Figure 2-6 shows AM-1 photoconductivity (100mW/cm^2) of undoped film. Photoconductivity of undoped a-Si:H is almost fixed at about 10^{-4} mho/cm in the range of r.f. power and electrode position where we could prepare films with a good reproducibility. This value is similar to that previously reported.⁶⁾ However, one should compare normalized photoconductivity $\eta\mu\tau$ to characterize the film quality. Normalized photoconductivity $\eta\mu\tau$ under 1.9 eV illumination (3×10^{14} photons/sec. cm^2), as can be seen in Fig. 2-7, shows a possibility that the desirable r.f. power for each electrode position might exist. Especially, at electrode positions D=7 and 10 cm, the optimum r.f. power of 35 and 45 watts is obscurely recognized. Tanaka¹¹⁾ examined the dependency of r.f. power on the film quality in his capacitively coupled plasma deposition equipment using SiH_4/Ar mixture and concluded that lower r.f. power deposition is favorable. There are few causes for the discrepancy between the two. One of them is a dilute gas of silane. We used only hydrogen against argon which Tanaka used, so the deposited films are not affected by argon including. Another one is a deposition system, particularly, an electrode arrangement. In our deposition system, we can success-

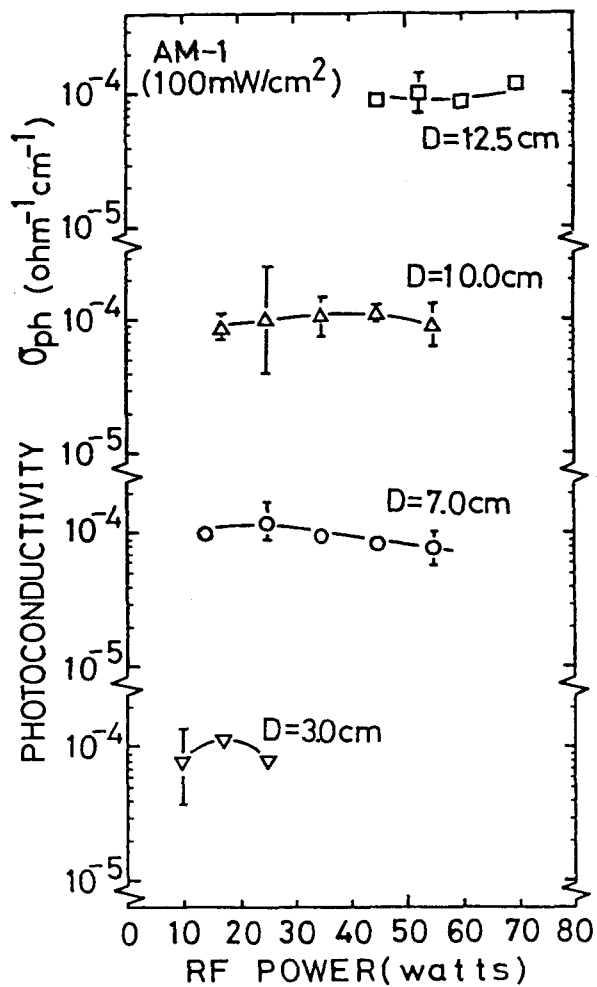


Fig. 2-6 AM-1 photoconductivity (100 mW/cm²) of undoped a-Si:H films as a function of r.f. power for electrode position D=3, 7, 10 and 12.5 cm.

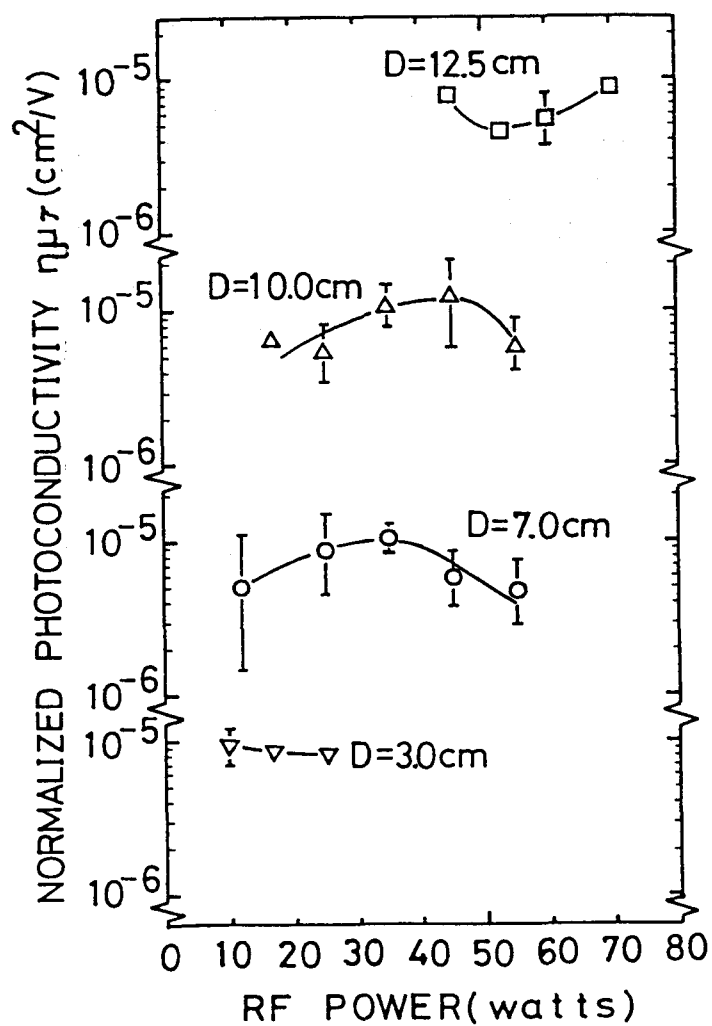


Fig. 2-7 Normalized photoconductivity $\eta\mu\tau$ of undoped a-Si:H films as a function of r.f power for electrode position D=3, 7, 10 and 12.5 cm.

fully avoid the bombardment effects of the plasma species on the grown film by changing the electrode position.

2-3. Effect of Deposition Parameter on the Photovoltaic Performance of a-Si:H p-i-n Junction Solar Cell

In order to examine the dependency of a-Si:H solar cell performance on r.f. power and to improve it, we have fabricated a-Si:H solar cells having a structure of glass/SnO₂(55Ω/□)/p-i-n/metal under various deposition parameters. The layer thicknesses are fixed at 100Å (B₂H₆/SiH₄=0.2%), 6000Å and 500Å (PH₃/SiH₄=0.5%) for p-, i- and n-layers, respectively. At each electrode position D, r.f. power P for p-layer was settled at 10, 25, 35 and 45 watts for 3, 7, 10 and 12.5 cm, respectively, so that deposition rate of p-layer could be the same (about 1.5Å/sec) and the thickness of the p-layer was fixed to be 100Å for each case. Deposition condition of undoped i-layer and n-layer were varied in the same way. Photovoltaic performances of solar cell having a sensitive area of 3.3 mm² were measured under AM-1 sunlight of July, 1980 with about 110mW/cm² and were converted into the value under 100mW/cm².

Figure 2-8 shows typical photovoltaic performances of a-Si:H p-i-n junction solar cells as a function of r.f. power for electrode position of D=10 cm. As can be seen from the figure, photovoltaic performance exhibits a clear dependency on r.f. power. The maximum conversion efficiency and fill factor are 5.5 % and 66 % at r.f. power of 45 watts, and the maximum short circuit current density J_{sc} is 11.7 mA/cm² at r.f. power of 35 watts. On the other hand, as for open circuit voltage V_{oc}, we could not find any distinct correla-

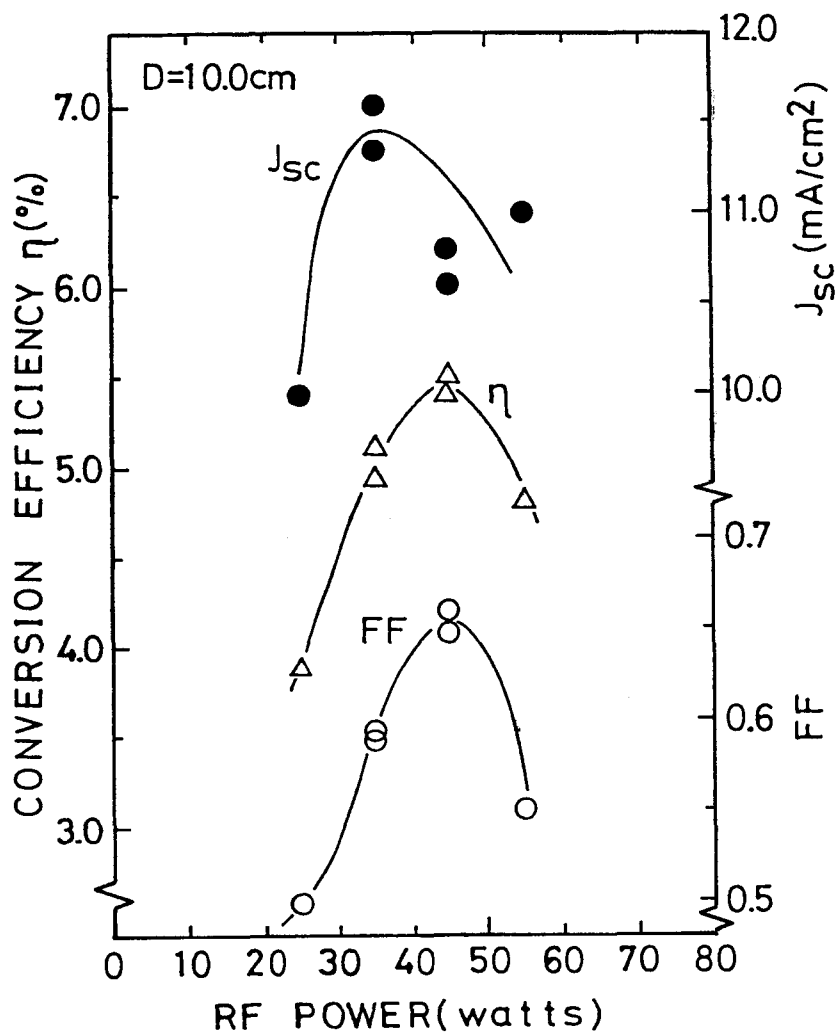


Fig. 2-8 Typical photovoltaic performances of a-Si:H p-i-n homojunction solar cells as a function of r.f. power for electrode position $D=10\text{ cm}$.

tion with each deposition parameter and it is scattered from 0.75 to 0.80 volts. Similar dependency on r.f. power can be seen in the other electrode positions. Figure 2-9 shows the conversion efficiencies of a-Si:H p-i-n junction solar cells as a function of r.f. power for various electrode positions. It is clear from these data that the photovoltaic performance is dependent on both r.f. power and electrode position. Furthermore, the maximum conversion efficiency and the most favorable r.f. power for each electrode position are shown in Fig. 2-10 as a function of electrode position D. It is noted there that the maximum conversion efficiency for each electrode position increases for D beyond 10 cm, and the optimum r.f. power is higher for larger electrode position D. In the case of D=12.5 cm, it should be taken into account that the discharge plasma might be affected by the top of the quartz reaction chamber.

To the extent of the present experiments concerning undoped layer optimization in our own deposition system, it can be concluded that the most favorable condition for solar cell fabrication is D=10 cm and r.f. power P=45 watts with the substrate temperature of 260°C, and under this condition a conversion efficiency of 5.5 % has been obtained with $J_{SC}=10.5 \text{ mA/cm}^2$, $V_{OC}=0.80 \text{ volts}$ and fill factor FF=0.66 as shown in Fig. 2-11.

2-4. Optimization of Doped Layer in a p-i-n a-Si:H Solar Cell

From the experimental studies mentioned above, there exists the most favorable deposition condition for solar cell fabrication. Furthermore, we have also been trying to optimize the phosphorus doped layer ($\text{PH}_3/\text{SiH}_4=0.5 \text{ mole\%}$). Figure 2-12 shows the basic properties of phosphorus doped a-Si:H as a function of r.f. power for electrode

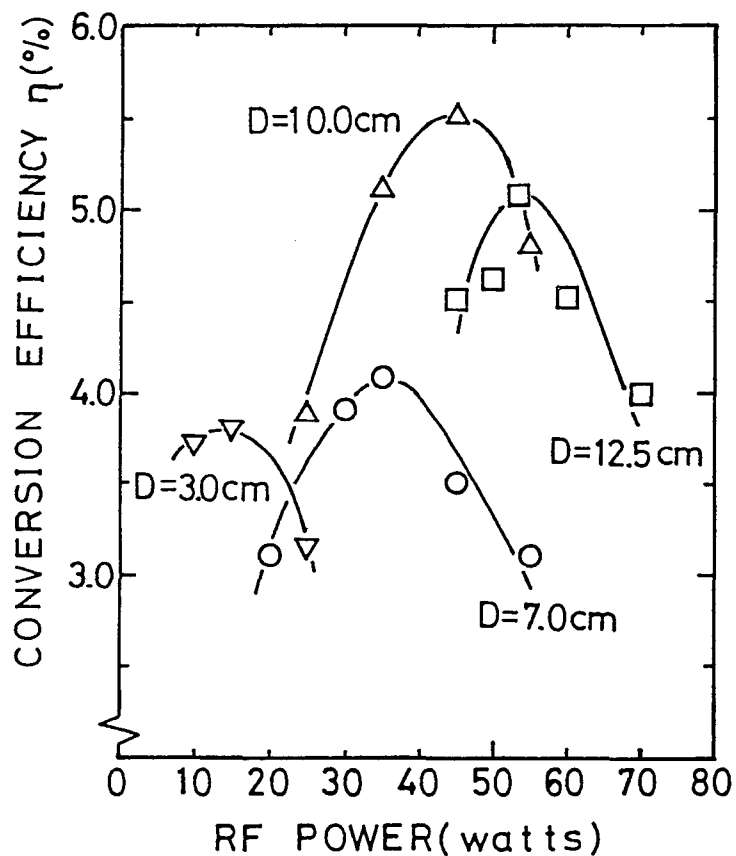


Fig. 2-9 Conversion efficiency of solar cells as a function of r.f. power for various electrode position D.

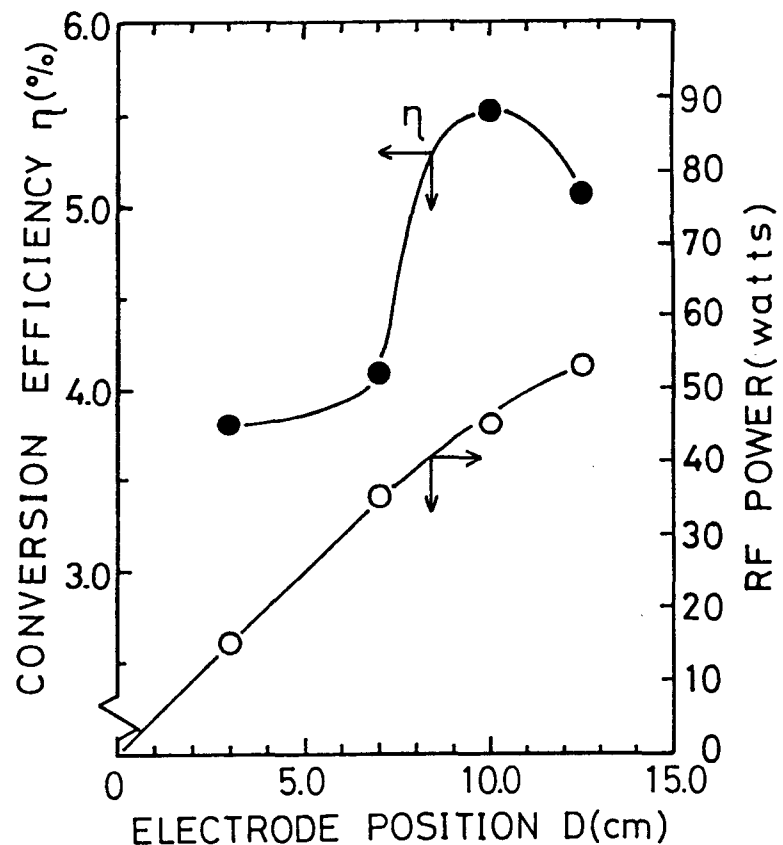


Fig. 2-10 Maximum conversion efficiency and the most favorable r.f. power for each electrode position as a function of electrode position.

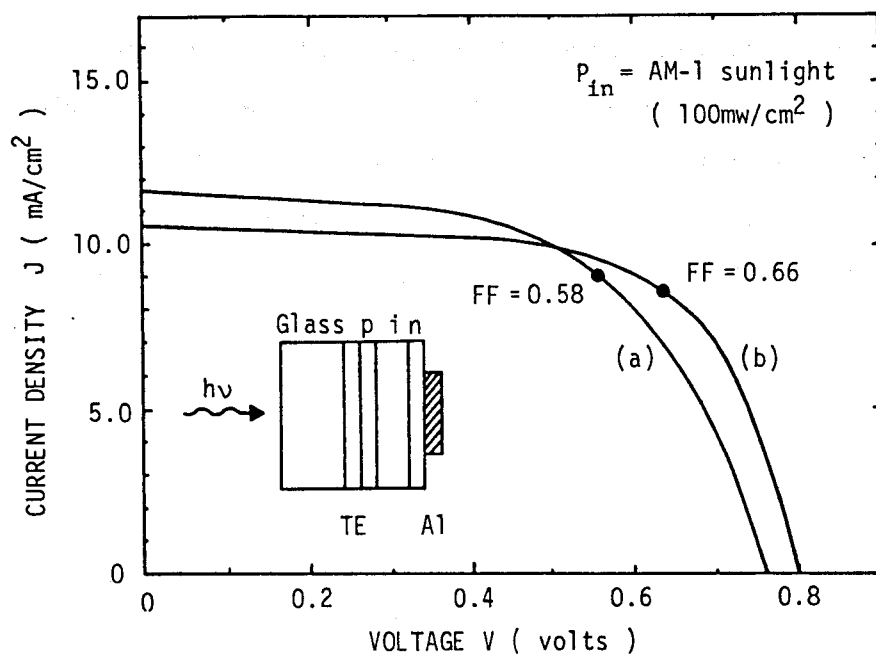


Fig. 2-11 J-V characteristics of glass/SnO₂/p-i-n/Al solar cells (area=3.3 mm²) fabricated under the conditions of $D=10$ cm and $P=35$ watts (a) and 45 watts (b).

position $D=12.5$ cm. As is seen in this figure, the dark conductivity σ_d increases exponentially and the activation energy ΔE decreases with increasing the r.f. power in the region of more than 60 watts. The crystalline structure was observed by the X-ray diffraction patterns in a phosphorus doped a-Si:H decomposed by more than 150 watts r.f. power. Because a high conductive n-layer is favorable to reduce the series resistance of solar cells, the r.f. power dependence of n-layer on the photovoltaic performances has been investigated. The cell structure and layer thicknesses are fixed as is stated above. The deposition conditions of p- and i-layer are settled at the electrode position $D=10$ cm and the r.f. power $P=35$ watts. Figure 2-13 shows the photovoltaic performances of p-i-n a-Si:H solar cells as a function of r.f. power of n-layer depositions. The short circuit current density J_{sc} decreases in the range from 100 to 200 watts r.f. power. On the other hand, the fill factor FF increases in this region, because the series resistance of n-layer increases in this r.f. power region. On the other hand, the open circuit voltage V_{oc} does not change, in spite of changing the activation energy from 0.2 to 0.05 eV. From this result, it might be possible that the fermi level of n-layer does not shift to the conduction band even if the activation energy changes from 0.2 to 0.05 eV.

The conversion efficiency does not so change in the present experiments concerning phosphorus doped layer optimization. However, it can be concluded that more favorable condition for solar cell fabrication is $D=12.5$ cm and r.f. power $P=150$ watts. Because, a good contact has been obtained between the phosphorus doped layer and Al back side electrode under this condition.

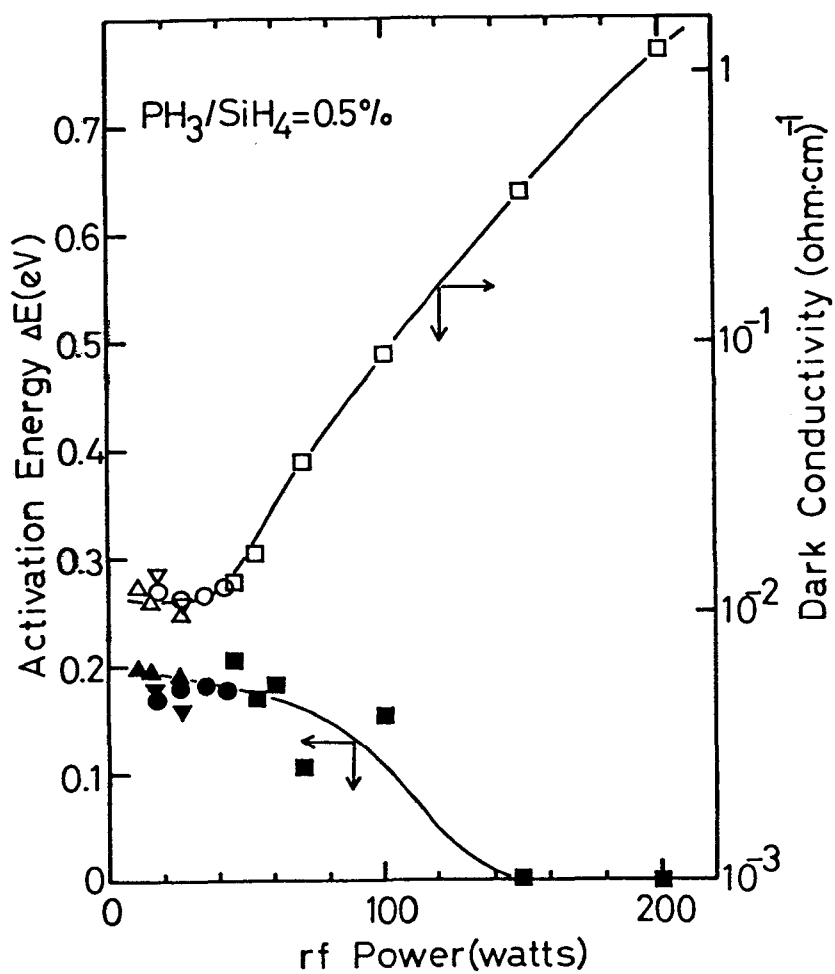


Fig. 2-12 Dark conductivity σ_d at 20 °C and activation energy ΔE of phosphorus doped a-Si:H as a function of r.f. power for electrode position $D=12.5$ cm.

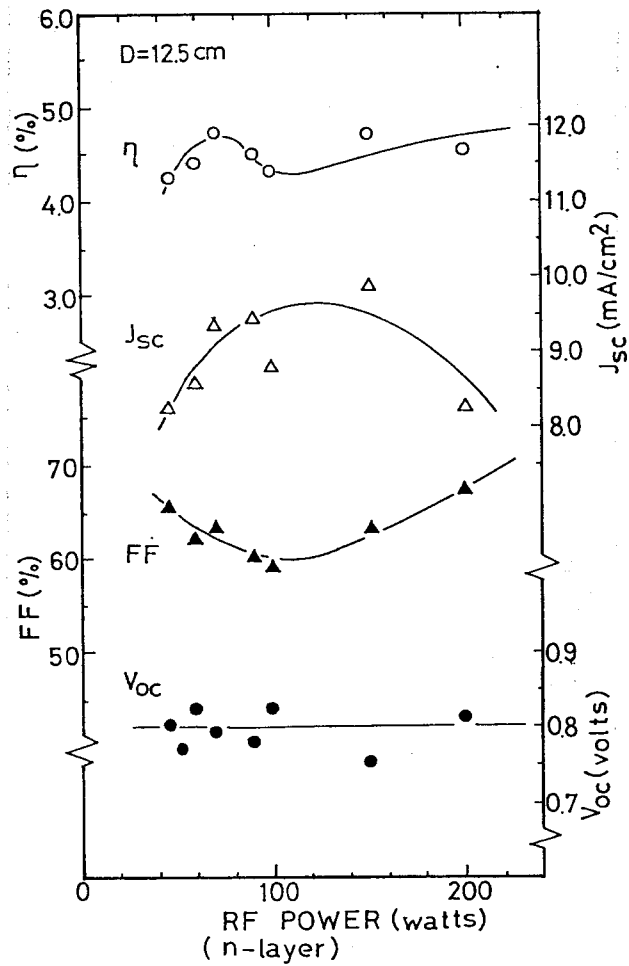


Fig. 2-13 Photovoltaic performances of a-Si:H p-i-n solar cells as a function of p-layer deposition conditions for D=12.5 cm.

Furthermore, we also optimized boron doped a-Si:H. Figure 2-14 shows the activation energy ΔE and the dark conductivity σ_d of boron doped a-Si:H ($B_2H_6/SiH_4=0.2$ mole%) as a parameter of electrode position D. As is seen in this figure, there exists the maximum doping efficiency for electrode position, that is, 15, 35, 35 and 57 watts for D of 3, 7, 10 and 12.5 cm, respectively. At this power, the activation energy and the dark conductivity show the maximum and the minimum values, respectively.

From this result, it is expected that the efficiency of a-Si:H solar cell might show the highest value for each electrode position. Figure 2-15 shows the typical photovoltaic performances of p-i-n a-Si:H solar cell as a function of r.f. power for the electrode position D=7 cm. As can be seen from this figure, the photovoltaic performances exhibit a clear dependency on r.f. power, as well as the undoped a-Si:H layer dependency. Similar dependency on r.f. power can be seen in other electrode positions. Figure 2-16 summarized the maximum efficiency and the most favorable r.f. power for each electrode positions as a function of electrode position D. In this case, the most favorable r.f. power for solar cells agrees with the r.f. power at which the doping efficiency is maximum. Furthermore, comparing this figure with Fig. 2-9, it is recognized that the boron doped layer dependency shows the same tendency as undoped one. In other word, one can select the most favorable deposition condition of undoped a-Si:H as the p-layer deposition condition.

Through these optimization of a-Si:H p-i-n homojunction solar cell, a conversion efficiency up to 5.7 % has been attained as shown in Fig. 2-17. The corresponding performance is $J_{SC}=11.0 \text{ mA/cm}^2$, $V_{OC}=0.801$ volts and FF=64.7 %. However, there is one clear deficiency

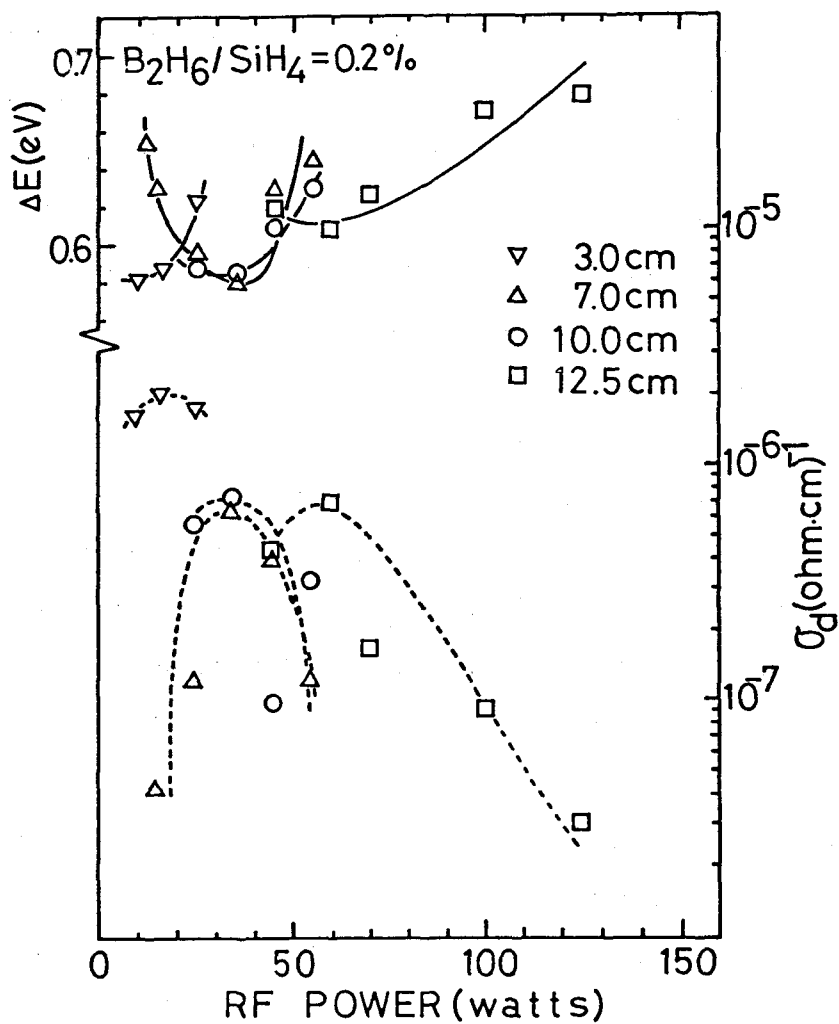


Fig. 2-14 Activation energy ΔE and dark conductivity σ_d at 20 °C of boron doped a-Si:H as a function of r.f. power for various electrode positions D.

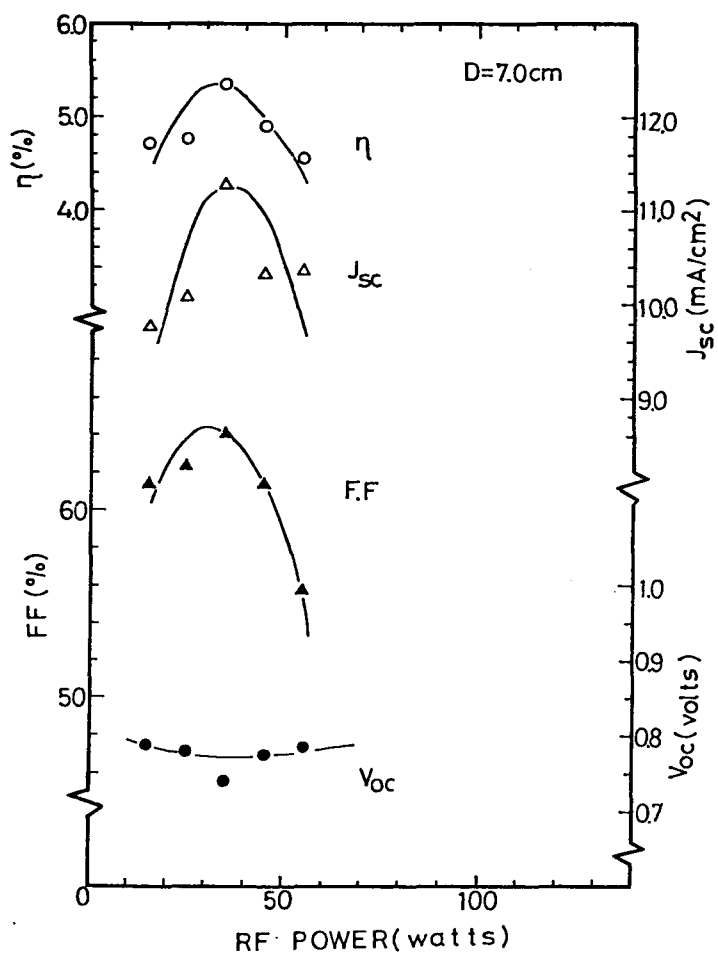


Fig. 2-15 Typical photovoltaic performances of a-Si:H p-i-n solar cells as a function of p-layer deposition conditions for electrode position $D = 7 \text{ cm}$.

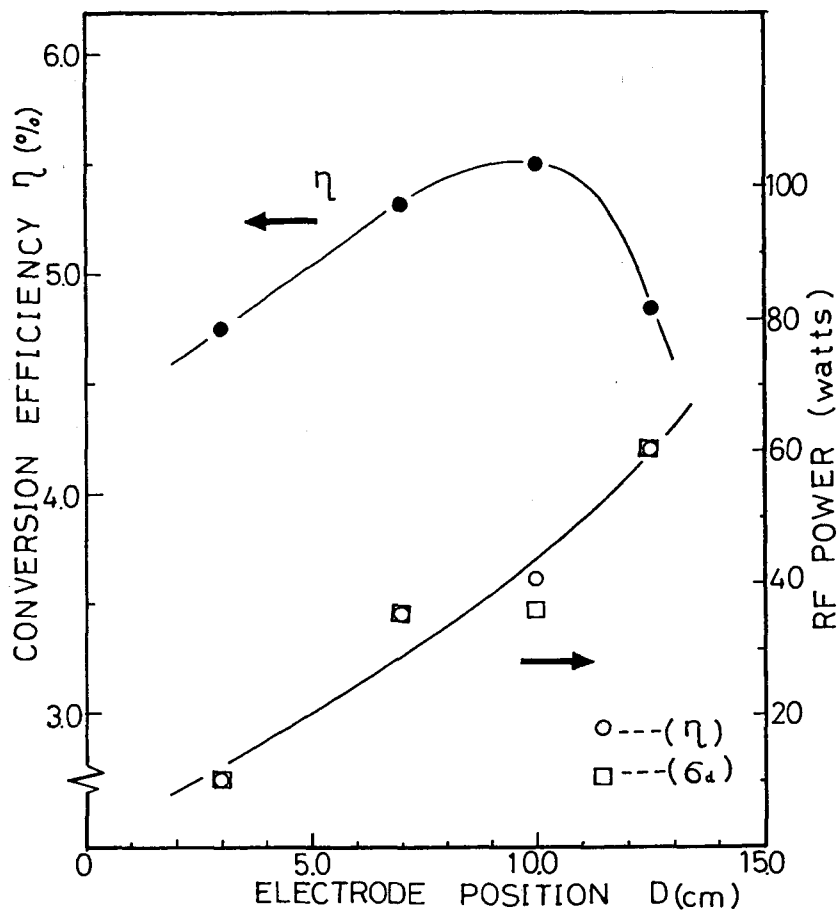


Fig. 2-16 Maximum conversion efficiency and the most favorable r.f. power of p-layer deposition as a function of electrode position D.

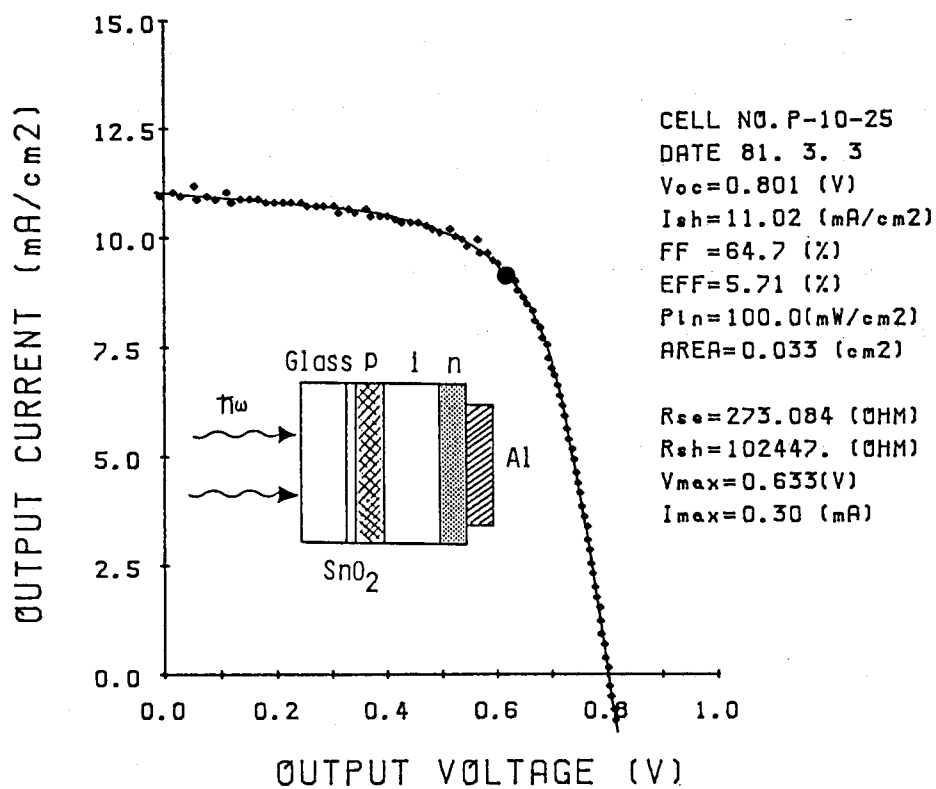


Fig. 2-17 J-V characteristics of the highest efficiency a-Si:H p-i-n solar cell.

of this p-i-n a-Si:H homojunction solar cell which is the unavailability of an optical absorption in the window side p-layer⁴⁾. To further improve the efficiency of a-Si solar cell, one must suppress this loss component. One of the ways is to apply a wide-band gap a-SiC:H films doped with boron for p-layer by coupling an optimized undoped a-Si:H layer with a low resistivity n-layer. At the present stage, more than 8 % conversion efficiency has been obtained with a-SiC:H/a-Si:H heterojunction solar cell¹²⁾. The detailed results are discussed in the following chapters.

2-5 Discussions and Summary

It is widely accepted that the properties of a-Si:H films are strongly influenced by the manner in which hydrogen is incorporated in amorphous silicon net work structure. In the course of our experiments, it is confirmed that r.f. power makes an important role on determining the hydrogen incorporation as well as other deposition parameters. IR absorption at 2000 cm^{-1} which is related to isolated silicon-monohydrides (SiH) increases and absorption at 2090 cm^{-1} which is related silcondihydride (SiH₂) is almost constant or slightly decreases as r.f power increases. This results suggest the possibility that the composition of deposited films might be mainly determined by the decomposed species of SiH₄ in plasma discharge. So far as the local arrangement of the incorporated hydrogen atoms is concerned, higher r.f. power deposition seems to be favorable. On the other hand, it is considered that higher r.f. power deposition might bring about an impurity inclusion and also bombardment effect on the films, which can be found in the r.f. power dependence of dark conductivity and its activation energy. In our deposition

system, however, the latter bombardment effect can be made smaller by controlling the distance between the electrode and substrate.

To confirm this bombardment effect on undoped a-Si:H, the optical emission spectroscopy (OES) measurement¹³⁾ has been carried out just on the substrate by S. Hotta, et al. Figure 2-18 shows the correlation between the OES peak ratio $[\text{SiH}]/[\text{H}_\beta]$ and $[\text{H}_2]/[\text{H}_\beta]$, and the normalized photoconductivity $\eta_{\mu\tau}$ as a function of electrode position D. From this figure, it is recognized that OES $[\text{H}_2]/[\text{H}_\beta]$ ratio is well consistent with $\eta_{\mu\tau}$ product, that is, the increase of $[\text{H}_2]/[\text{H}_\beta]$ corresponds to the increase of $\eta_{\mu\tau}$ product. The concentration of H_2 might be almost constant even if r.f power changes from 15 to 55 watts. Therefore, the increase of $[\text{H}_2]/[\text{H}_\beta]$ ratio means the decrease of concentration $[\text{H}_\beta]$. In other word, this results show that the hydrogen radical concentration influences the film quality. Furthermore, this hydrogen radical seems to be an important factor to explain the geometric effects on the photovoltaic performances. The decrease of photovoltaic performance in the high power deposition region of p-layer might be caused by hydrogen radical bombardment. High power deposition increases the concentration of hydrogen radical which is a strong reduction reagent. H radical is used to reduce ITO and SnO_2 to metallic In and Sn, respectively. These metallic In or Sn not only reduces the transparency of ITO or SnO_2 but also diffuses to p-layer to reduce the electrical properties of this layer. The detailed results are discussed in other chapter.

It is of a good use to examine the relationship between the properties of undoped a-Si:H films and photovoltaic performance of a-Si:H p-i-n homojunction solar cells. Figure 2-19 shows relation-

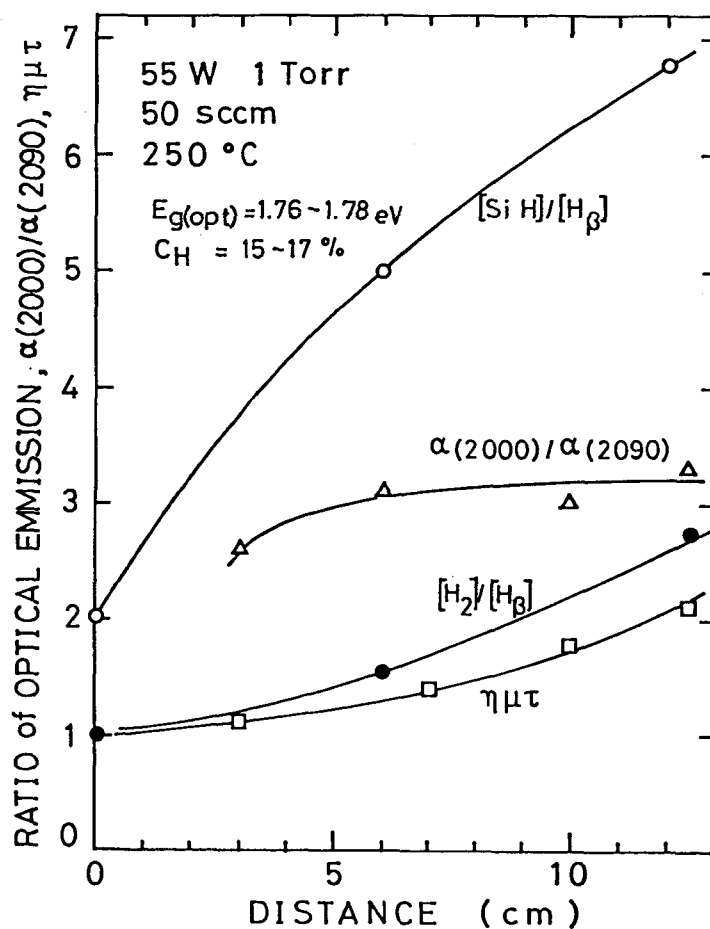


Fig. 2-18 Correlation between the OES peak ratio $[SiH]/[H_\beta]$ and $[SiH_4]/[H_\beta]$, normalized photoconductivity $\eta\mu\tau$ and IR absorption coefficient ratio of $[2090 \text{ cm}^{-1}]/[2000 \text{ cm}^{-1}]$ as a function of electrode position D.

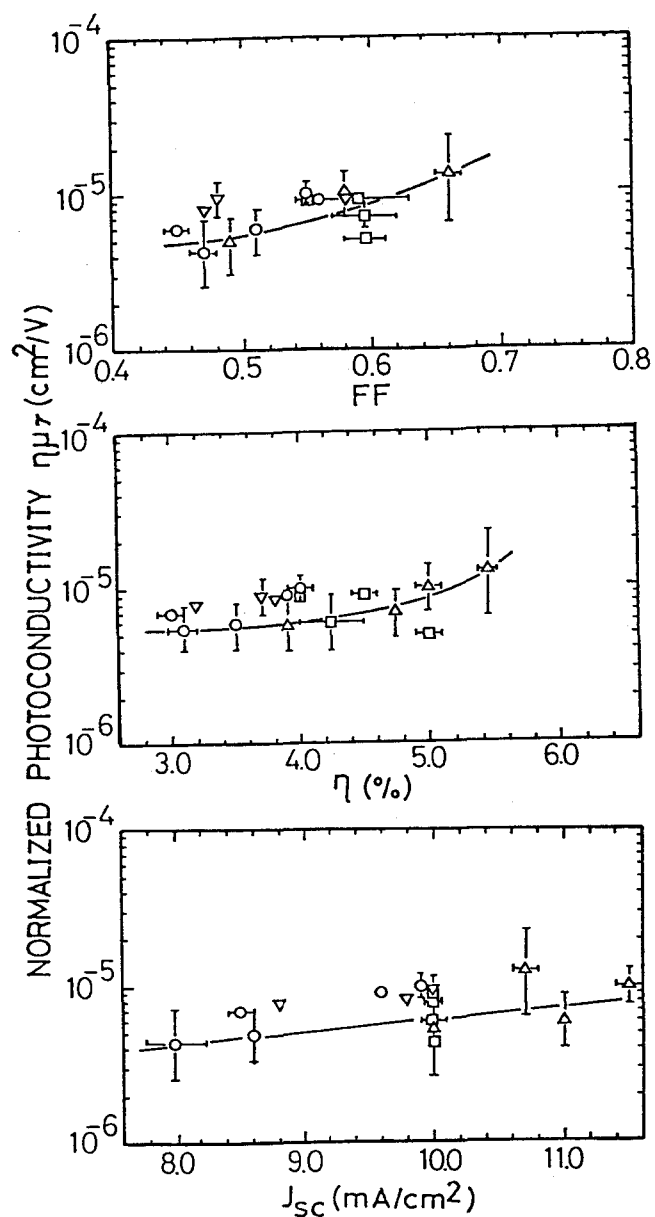


Fig. 2-19 Relationships between normalized photoconductivity $\eta_{\mu\tau}$ of undoped a-Si:H films and photovoltaic performances of solar cells fabricated under the same deposition condition.

ships between normalized photoconductivity of undoped a-Si:H produced with various deposition conditions and photovoltaic performances. From this figure, one can find not large but clear positive correlation between them. Especially, fill factor FF varies well corresponding to normalized photoconductivity $\eta_{\mu\tau}$ and it strongly influences conversion efficiency. There are several factors which limit fill factor, that is series resistances come from transparent electrode, a-Si:H layer and its interface, and free carrier generation and collection factor sensitive to the internal electric field. If normalized photoconductivity $\eta_{\mu\tau}$ reflects film quality including not only gap states density but also hole diffusion length, it is reasonable that there exists a clear correlation between $\eta_{\mu\tau}$ and fill factor FF.

Furthermore, we have examined a dependency of photovoltaic performances on undoped i-layer thickness in a-Si:H p-i-n homojunction solar cells which were fabricated under the conditions of r.f. power $P=35$ watts and electrode position $D=10$ cm. As can be seen in Fig. 2-20, the dependency of J_{sc} on the thickness of undoped i-layer is rather smaller than previous reported.⁴⁾ J_{sc} for 3200 Å i-layer thickness is 9.8 mA/cm^2 against the largest J_{sc} which is obtained for the thickness of 5500 Å. The result agrees approximately with the theoretical expectation demonstrated by Yamaguchi et al.¹⁴⁾ On the other hand, fill factor slightly increases as the thickness of undoped i-layer decreases. As a consequence, the conversion efficiency is slightly dependent on the i-layer thickness and is ranging from 4.5 to 5.1 % with in the i-layer thickness from 3200 to 8000 Å. These results indicate the possibility that our optimized solar cell might not be affected by interface recombination. Therefore, an improvement

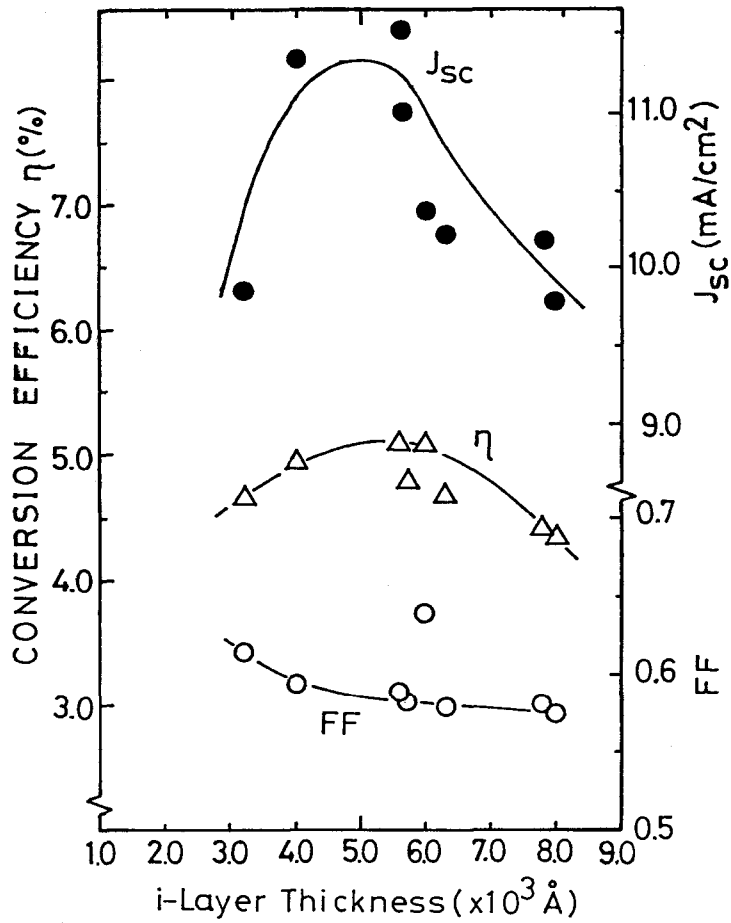


Fig. 2-20. Photovoltaic performances dependency of undoped i-layer thickness in a-Si:H p-i-n homojunction solar cell fabricated under the condition of r.f power $P=35$ watts and electrode position $D=10$ cm.

of conversion efficiency from the previous value of 4.5 %⁵⁾ might be ascribed to the improvement of the junction property, which enable the film quality to directly reflect the photovoltaic performance.

Through these optimization of a-Si:H p-i-n homojunction solar cells, a conversion efficiency has been improved to be 5.7 % with J_{sc} of 11.0 mA/cm², V_{oc} of 0.801 volts and FF of 64.7 %.

The p-i-n a-Si:H homojunction solar cell might be a more promising cell structure than the Schottky barrier type and also the inverted p-i-n a-Si:H solar cell, in view of better processability for future mass-production system and reducing the effect of short hole diffusion length. However, one clear deficiency of this p-i-n a-Si:H homojunction solar cell is the unavailability of an optical absorption in the window side p-layer, which has a narrow optical band gap with a high density of non-radiative recombination centers.⁸⁾ To suppress this loss component and improve the efficiency, I have made experimental efforts to obtain the valency controlled wide gap material. Finally, I have found the good valency electron controllability in hydrogenated amorphous silicon carbide (a-SiC:H) prepared by the plasma decomposition of $[SiH_4(1-x) + CH_4(x)]$. Utilizing this wide gap a-SiC:H as a window side p-layer, at the present stage, more than 8 % efficiency has been obtained with a-SiC:H/a-Si:H heterojunction structure by coupling the optimized undoped a-Si:H and the low resistivity phosphorus doped layer. The detailed results are discussed in the following chapters.

REFERENCES

- 1) See for example on the cost analysis etc., Y. Hamakawa: *Surface Sci.* 86 (1979) 444.
- 2) D. E. Carlson: *Trieste Semiconductor Symposium, Amorphous Silicon Physics and Application, Trieste (1980) 21-25 July.*
- 3) A. Madan, J. MacGill, W. Czubytyj, J. Yang and S. R. Ovshinsky: *Appl. Phys. Lett.* 37 (1980) 826.
- 4) H. Okamoto, Y. Nitta, T. Yamaguchi and Y. Hamakawa: *Solar Energy Mat.* 2 (1980) 313.
- 5) H. Okamoto, Y. Nitta, T. Adachi and Y. Hamakawa: *Extended Abstract of Int. Conf. on Solaid Films and Surfaces, July (1978) and Proc. published as Surface Sci.* 86 (1979) 486.
- 6) H. Okamoto, T. Yamaguchi and Y. Hamakawa: *J. Non-Cryst. Solids* 35&36 (1980) 201.
- 7) Y. Hamakawa, H. Okamoto and Y. Nitta: *Appl. Phys. Lett.* 35 (1979) 187.
- 8) Y. Hamakawa, H. Okamoto and Y. Nitta: *Proc. 14th IEEE Photovoltaic Specialists Conf., San Diego (1980), 1074.*
- 9) J. C. Knights: *Jpn. J. Appl. Phys.* 18 (1979) suppl. 18-1, 101.
- 10) C. C. Tsai and H. Fritzche: *Solar Energy Mat.* 1 (1979) 29.
- 11) K. Tanaka et al.: *J. Non-Cryst. Solids* 35&36 (1980) 475.
- 12) Y. Tawada, M. Kondo, H. Okamoto and Y. Hamakawa: *Solar Energy Mat.* 6 (1982) 299.
- 13) F. J. Kampas and R. W. Griffith: *Solar Cells* 2 (1980) 385.
- 14) T. Yamaguchi, H. Okamoto, S. Nonomura and Y. Hamakawa: *Jpn. J. Appl. Phys.* 20 (1981) suppl. 20-2, 195.

III PREPARATIONS OF a-SiC:H FILMS AND VALENCY ELECTRON CONTROL

3-1. Introduction

A hydrogenated amorphous silicon (a-Si:H) prepared by the glow discharge technique has attracted a great deal of attentions in view of low cost solar cells,¹⁾ thin film transistors²⁾ and also imaging devices.³⁾ A similar attention has been devoted to hydrogenated amorphous silicon carbides (a-SiC:H). The electrical and optical properties of a-SiC:H films prepared by the glow discharge technique was first studied by Anderson and Spear.⁴⁾ They concluded that a-SiC:H films have an appreciably lower density of gap state than a-SiC films. Since thier work, several attempts have been made to exploit the properties of a-SiC:H films. Engemann, Fischer and Knecht⁵⁾ observed the double peaks in photoluminescence of a-SiC:H films and suggested that their films contained Si clusters and C clusters. Recent results of Wieder et al.⁶⁾ showed from the analysis of IR vibrational spectra that Si and C atoms are randomly distributed without chemical ordering. Similar results were reported by Munekata et al.⁷⁾ and Sussmann et al.⁸⁾ However, any information on electrical, optoelectronic properties of doped a-SiC:H films has not been reported.

Recently, we found a good valency electron controllability in a-SiC:H films prepared by the decomposition of $\{\text{SiH}_{4(1-x)} + \text{CH}_{4(x)}\}$ gas mixture.^{9,10)} Utilizing this valency electron controlled a-SiC:H as a p-side window junction in p-i-n a-Si cells, a new type solar cell, a-SiC:H/a-Si:H heterojunction solar cell, has been developed.^{11,12)} Through the optimizations of a-SiC:H/a-Si:H heterojunction solar cell, an 8 % efficiency barrier has been first broken through by our group

and the efficiency of more than 10 % might be one of the most near future targeted efficiency with a-SiC:H/a-Si:H heterojunction cells.¹³⁾

Valency electron controllability of a-SiC:H depends upon both carbon sources and deposition conditions. We have conducted a series of experimental investigations of the dependence of carbon sources and deposition conditions on optical, optoelectronic properties, chemical bonding structure and the correlation between these properties.¹⁴⁾

In this chapter, we discussed the reason why methane was selected as a carbon source, and the results of Auger Electron Spectroscopy (AES) and infra-red (IR) absorption measurement are also discussed in terms of chemical bonding structure. Optical, electrical and optoelectronic properties of a-SiC:H films are also demonstrated.

3-2. Experimental.

Amorphous SiC:H films were prepared by the decomposition of $\{\text{SiH}_{4(1-x)} + \text{CH}_{4(x)}\}$ (methane based a-SiC:H) or $\{\text{SiH}_{4(1-x)} + \frac{1}{2}\text{C}_2\text{H}_{4(x)}\}$ (ethylene based a-SiC:H) in the plasma deposition system as described in the previous chapter. Corning #7059 glass, quartz, stainless steel and high resistive single crystalline silicon wafer were used as substrates. Substrate temperature and rf power were changed from 200 to 300°C and from 25 to 80 watts, respectively. Total gas flow was fixed at 100 sccm, and the used gases, SiH_4 , CH_4 , C_2H_4 , B_2H_6 and PH_3 were diluted with H_2 . The thicknesses of deposited films were 100 Å for AES measurement and 5000 Å for electrical, optoelectronic and ESR measurement, and 10000 Å for IR measurement.

3-3. Preparation and Characterization

3-3-1. Analysis of carbon content

The carbon content of the deposited films was determined by an Auger Electron Spectroscopy (AES).¹⁵⁾ The composition of $a\text{-Si}_{(1-x)}\text{C}_{(x)}$ is described by the composition parameter (x) which indicates the atomic fraction of C in the films. Figure 3-1 shows a typical AES spectra of $a\text{-SiC:H}$ films as a parameter of Ar^+ sputtering time. To eliminate an error originated in adsorbed O_2 , the surface cleaning was carried out by Ar^+ sputtering. As can be seen in the figure, O(KLL) peak does not be seen in the spectrum after 180 sec. Ar^+ sputtering. Then, C/Si ratio is calculated by the peak to peak of Si(LVV) and C(KLL) using a crystalline SiC as a standard material.

Figure 3-2 shows the film composition determined by AES measurement as a function of gas composition. As can be seen in the figure, there is a noteworthy difference between methane based and ethylene based $a\text{-SiC:H}$ films. That is, ethylene based $a\text{-SiC:H}$ films contain a larger amount of carbon than methane based films. This difference is caused by the reactivity of C_2H_4 and CH_4 . C_2H_4 has π -electrons which is reactive in plasma, so that ethylene based $a\text{-SiC:H}$ films contain a large amount of $-\text{C}_2\text{H}_5$ group as is discussed later. On the other hand, methane has σ -electrons as well as silane but its reactivity is rather lower than silane's one.¹⁶⁾ From the viewpoint of valency electron control, not only the carbon content but also the hydrogen content, especially attached to carbon are very important factors.

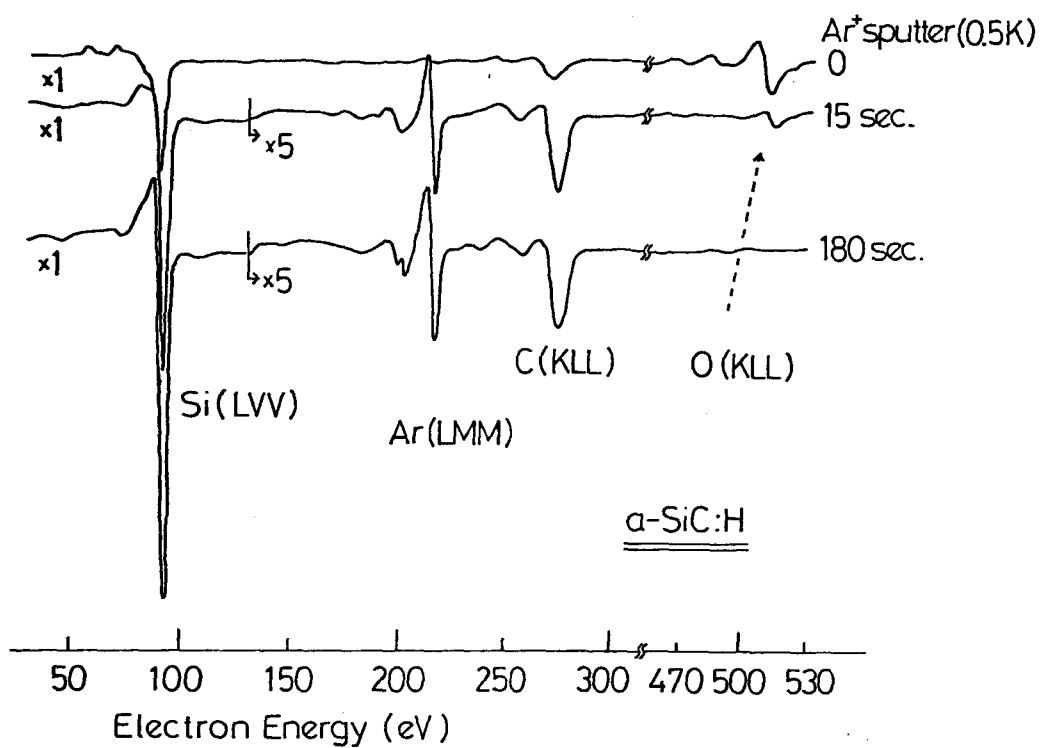


Fig. 3-1. Typical AES spectra of a-SiC:H as a parameter of Ar⁺ sputtering time.

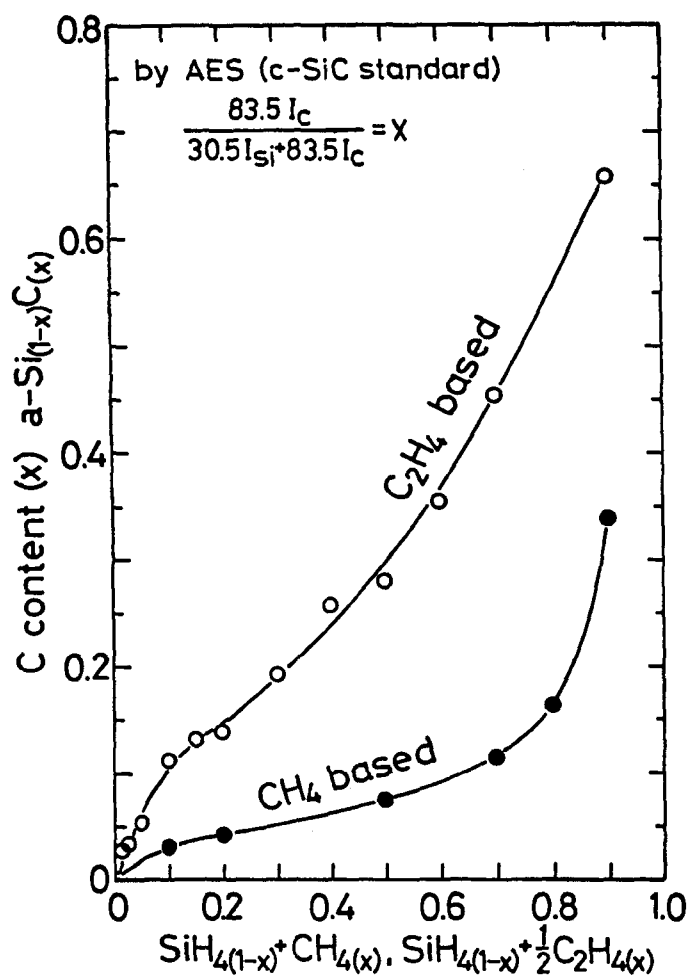


Fig. 3-2. Composition of carbon in methane based and ethylene based a-SiC:H films.

3-3-2. Incorporated hydrogen manner in a-SiC:H

Hydrogen contents in a-Si:H can be estimated by IR,¹⁷⁾ Rutherford Back Scattering (RBS)¹⁸⁾ or nuclear reaction.¹⁹⁾ Guivarc'h et al.¹⁹⁾ estimated a hydrogen content in nearly stoichiometric a-SiC:H films by (¹¹B, α)αα nuclear reaction. However, hydrogen content in a-SiC:H films has not been estimated exactly by IR method, because the absorption cross section of C-H stretching mode absorption is not given exactly. We measured exact IR spectra by Fourier Transfer IR spectrometer (FT-IR, Digilab, FTC-15c) and total hydrogen content by ¹H(¹⁵N, αγ)¹²C nuclear reaction.²⁰⁾ ¹⁵N ions were accelerated by 5 MV tandem type accelerator (University of Tokyo, Nuclear Centre). Ion energy and ion current were 6.7 MeV (energy resonance nuclear reaction=6.38 MeV) and 5 mA, respectively. Intensity of γ-ray was measured by NaI counter. Total hydrogen content in a-SiC:H films was obtained by comparison with hydrogen content in polyester film. On the other hand, hydrogen content attached to Si can be determined by IR Si-H stretching absorption, with the following expression.²¹⁾

$$N_H = A_S \int_{\nu_S} \frac{\alpha(\nu)}{\nu} d\nu$$

$A_S = 1.4 \times 10^{20} / \text{cm}^2$, α =absorption coefficient, ν =wave number

Subtracting the content of hydrogen attached to Si determined by IR method from the content of hydrogen determined by the nuclear reaction, the A_S value for the C-H stretching mode was evaluated. Assuming $A_S = 1 \times 10^{21} / \text{cm}^2$ in the C-H stretching, the total hydrogen determined by IR method is well consistent with that determined by

nuclear reaction, as shown in Fig. 3-3. Using the A_s value, a series of experimental investigations on the incorporated hydrogen manner has been carried out.

Figure 3-4 shows the incorporated hydrogen manner of methane based a-SiC:H films as a function of methane fraction. As can be seen in this figure, the content of hydrogen attached to Si slightly increases with increasing CH_4 gas fraction. While, the content of hydrogen attached to carbon increases as the increase of methane fraction, but for the fraction of less than 0.7 it is small. Hydrogen content of boron doped a-SiC:H is smaller than undoped one. This tendency is consistent with optical band gap narrowing of boron doped a-SiC:H. More clear correlation between $E_{g(opt)}$ and hydrogen content can be seen in the ethylene based a-SiC:H. Figure 3-5 shows the total hydrogen content, the content of hydrogen attached to Si and to C in undoped and boron doped ethylene based a-SiC:H. The content of hydrogen attached to Si slightly decreases with increasing C_2H_4 fraction and is not affected by doping. The content of hydrogen attached to C in boron doped a-SiC:H increases for less than 0.5 gas fraction and decreases for more than 0.5 gas fraction as compared with undoped one. The result is well consistent with the optical band gap widening or narrowing of the ethylene based a-SiC:H, and suggests that the hydrogen attached to C plays an important role for optical and optoelectronic properties. The substantiation of this suggestion can be seen in the incorporated hydrogen or carbon manner in the film. H^C/C ratio of the ethylene based a-SiC:H is about 3, contrary to that of less than 1 in the methane based one. If the carbon is incorporated as $-C_2H_5$ and $-CH_3$ groups, H^C/C ratios are 2.5 and 3, respectively. That is, large

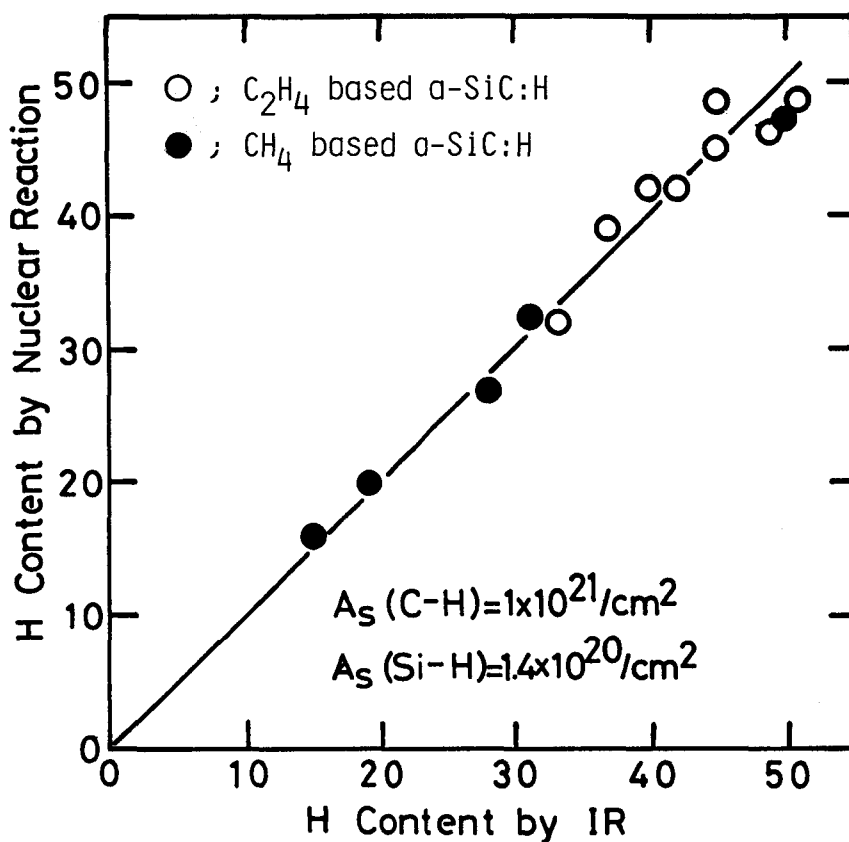


Fig. 3-3. Comparison of hydrogen contents determined by nuclear reaction and IR method in which A_S value is assumed to be $1 \times 10^{21} / \text{cm}^2$.

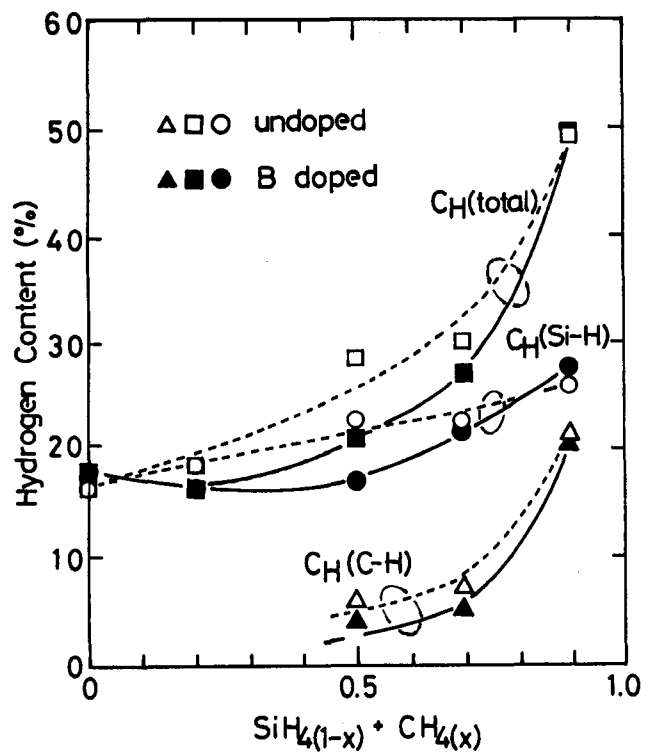


Fig. 3-4. Hydrogen contents attached to carbon and silicon in methane based a-SiC:H films.

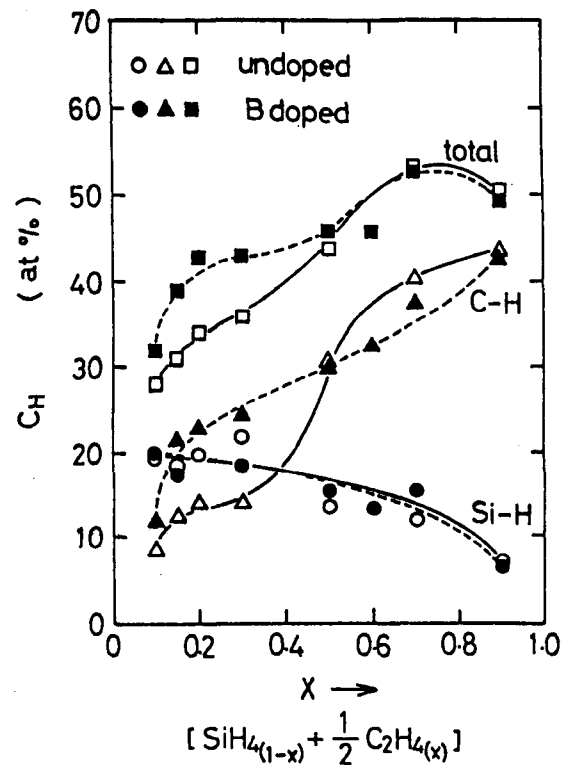


Fig. 3-5. Incorporated hydrogen manner of ethylene based a-SiC:H films.

H^C/C ratio means that the carbon is incorporated as alkyl groups. From this point, methane based a-SiC:H films are recognized to be a rather ideal a-SiC alloy than ethylene based films. The distinction of photoconductivity recovery effect between the two, as is mentioned latter, may originate in these structural differences.

3-3-3. RF power dependence of the deposition

The optoelectronic properties and the chemical bonding structure are also influenced by the deposition conditions. The RF power dependence of methane based and ethylene based a-SiC:H films were examined. Figure 3-6 shows the basic properties of the methane based a-SiC:H films as a function of RF power. The dark conductivity sharply decreases, and the activation energy and the optical band gap increases with increasing RF power. While, carbon content increases from 6 to 18 % with increasing RF power. Figure 3-7 shows the incorporated hydrogen manner of methane based a-SiC:H films as a function of RF power. The content of hydrogen attached to silicon decreases and the content of hydrogen attached to carbon increases with increasing RF power. At every RF power, H^C/C ratio is less than 1. The result means that the incorporated hydrogen manner of methane based a-SiC:H films is not affected by RF power condition.

On the other hand, ethylene based a-SiC:H films show a different RF power dependence. Figure 3-8 shows the basic properties of ethylene based a-SiC:H films as a function of RF power. Photoconductivity and dark conductivity in this case increase by about one order with increasing RF power. While, optical band gap decreases from 2.1 to 1.87 eV. This tendency is contrary to that of methane based a-SiC:H.

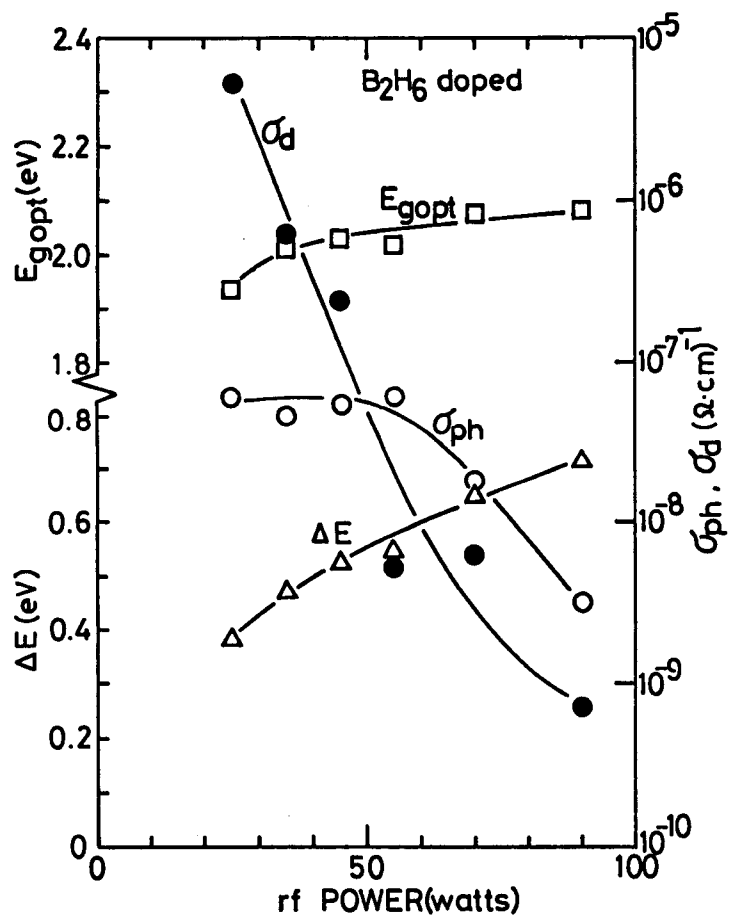


Fig. 3-6. Basic properties of methane based a-SiC:H as a function of RF power.

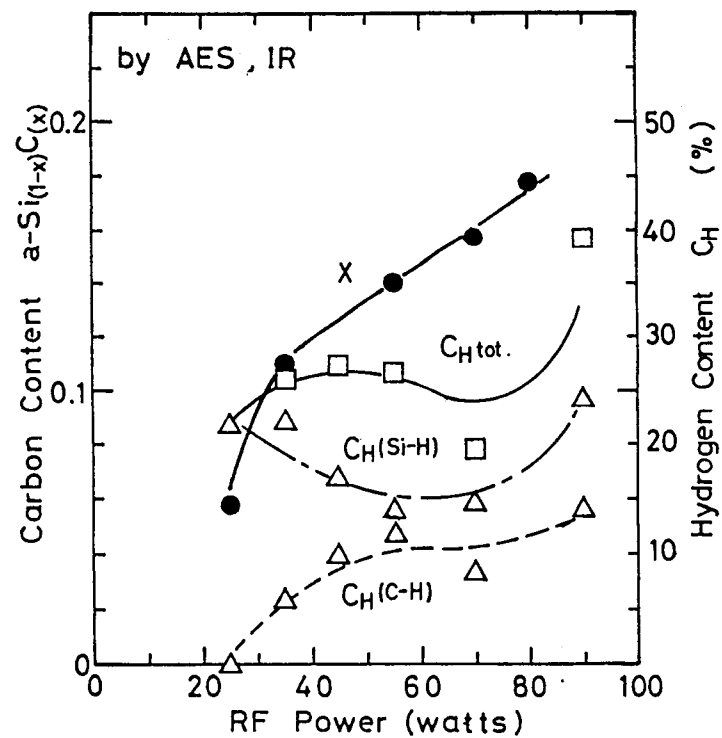


Fig. 3-7. Incorporated hydrogen manner of methane based a-SiC:H as a function of RF power.

The incorporated hydrogen and carbon manner is also contrary to that of methane based one, as shown in Fig. 3-9. The content of hydrogen attached to C continuously decreases and the content of hydrogen attached to Si slightly decreases with increasing RF power from 25 to 90 watts. At the higher RF power condition, IR spectra shows the methane like structure, that is, small H^C/C ratio is observed. This results mean that the ethylene reacts with hydrogens in high RF power condition to be ethane or methane and then the resulted hydrocarbons react with silane to be a-SiC:H film. Therefore, ethylene based a-SiC:H films are expected to show the same window effects as methane based a-SiC:H emplying p-layer in p-i-n a-Si solar cells, when it is fabricated at high RF power condition.

From the viewpoint of solar cell fabrications, the lower RF power deposition condition is favourable, especially p- and i-layer. At the present stage, it is concluded that methane based a-SiC:H is good for p-layer, because it is rather ideal amorphous SiC alloy and can be fabricated at the lower RF power condition

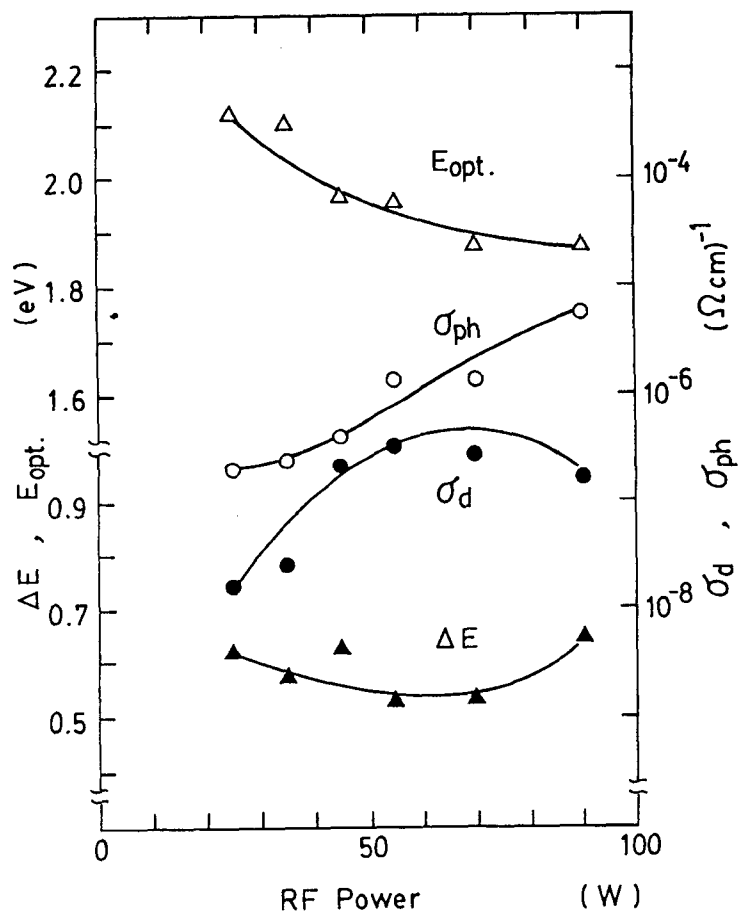


Fig. 3-8. Basic properties of ethylene based a-SiC:H as a function of RF power.

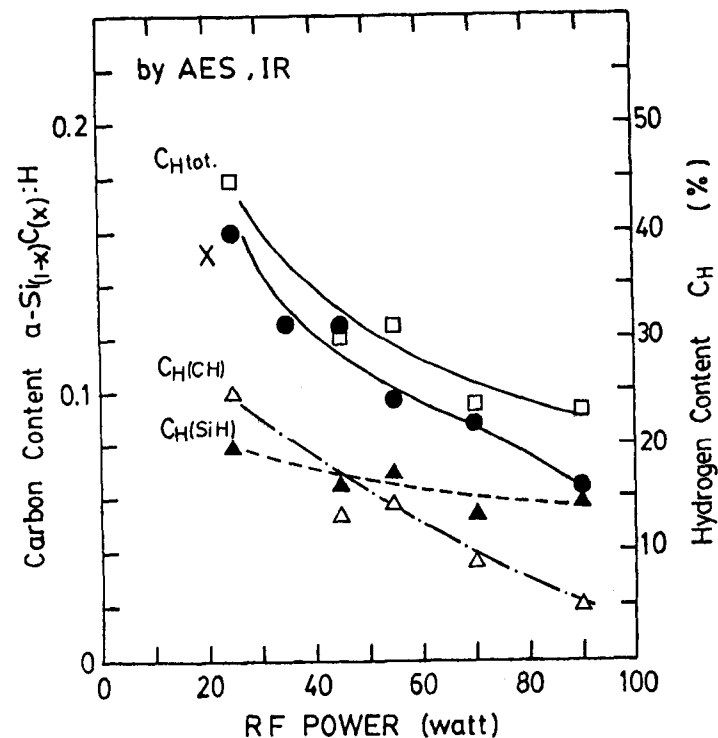


Fig. 3-9. Incorporated hydrogen manner of ethylene based a-SiC:H as a function of RF power.

3-4. Optical and Optoelectronic Properties

3-4-1. Photoconductivity and optical band gap

The optical band gap $E_{g(opt)}$ of a-SiC:H films was determined from the straight line intercept of $(\alpha h\nu)^{1/2}$ versus $h\nu$ curve at high absorption region ($\alpha > 10^4/\text{cm}$) following the analysis of Davis and Mott.²²⁾ It seems unreasonable to measure the photoconductivity of a-SiC:H having a wide band gap ranging from 1.76 to 2.2 eV under the same monochromatic illumination. Therefore, photoconductivity of various compositional a-SiC:H films was measured under AM-1 (100 mW/cm^2) illumination and monochromatic illumination at which a-SiC:H films have an optical absorption coefficient of $10^4/\text{cm}$. The monochromatic photoconductivity was normalized to $\eta_{\mu\tau}$ proposed by Zanzucchi et al.²³⁾ Figure 3-10 shows the correlation between the AM-1 photoconductivity σ_{ph} and the normalized photoconductivity $\eta_{\mu\tau}$ for various compositional a-SiC:H films which have an optical band gap from 1.76 to 2.2 eV. As is seen in the figure, there exists an obvious relation between AM-1 photoconductivity and normalized photoconductivity. From these results, AM-1 photoconductivity measurement is recognized as a quick judging method for optoelectronic properties of a-SiC:H films.

Figure 3-11 shows the AM-1 photoconductivity σ_{ph} and optical band gap $E_{g(opt)}$ of undoped and boron doped methane based a-SiC:H films as a function of methane fraction. AM-1 photoconductivity of undoped a-SiC:H films significantly decreases with increasing methane fraction. On the other hand, boron doped one shows one or three orders of magnitude larger photoconductivity as compared with undoped films. These photoconductivity recovery effect has been similarly seen in

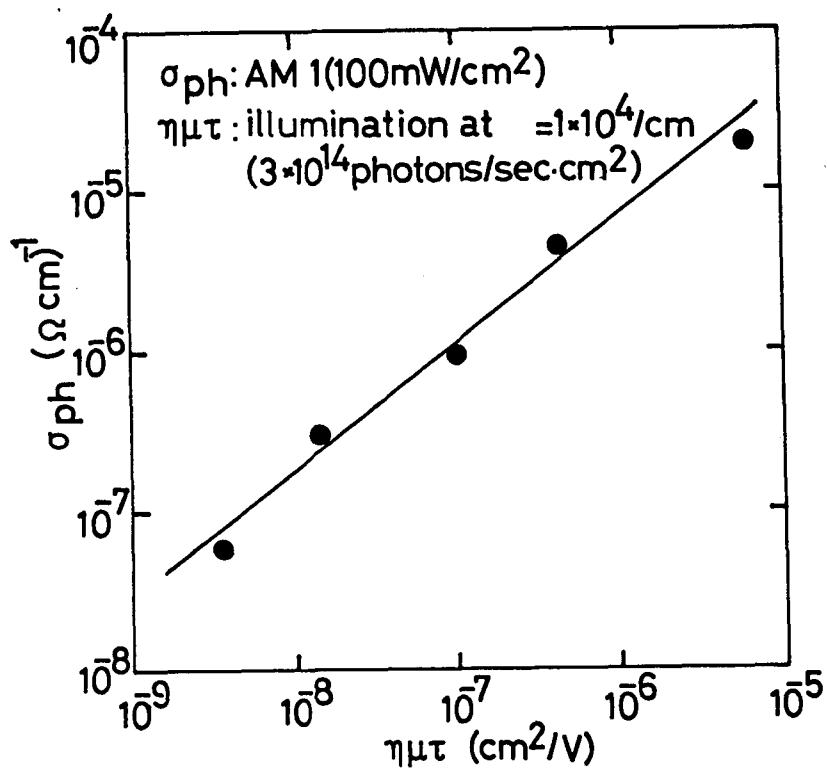


Fig. 3-10 Correlation between AM-1 photoconductivity σ_{ph} and normalized photoconductivity $\eta\mu\tau$.

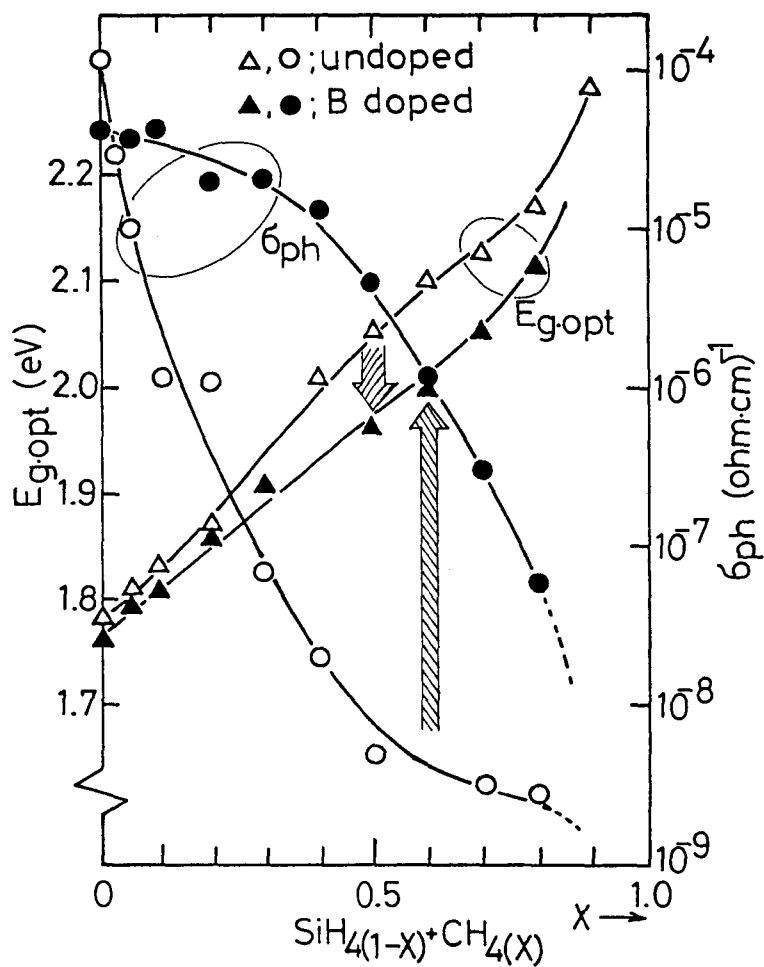


Fig. 3-11 Photoconductivity σ_{ph} and optical band gap $E_{g(opt)}$ of undoped and boron doped methane based a-SiC:H.

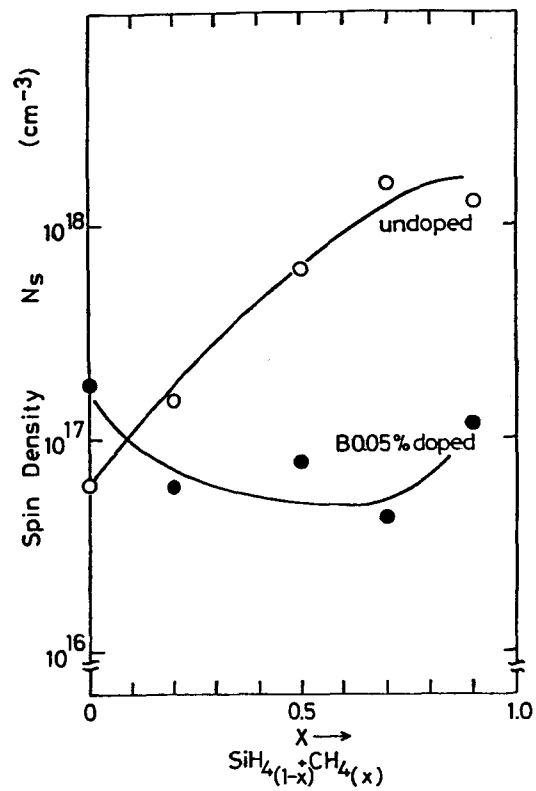


Fig. 3-12. ESR spin density of undoped and boron doped methane based a-SiC:H

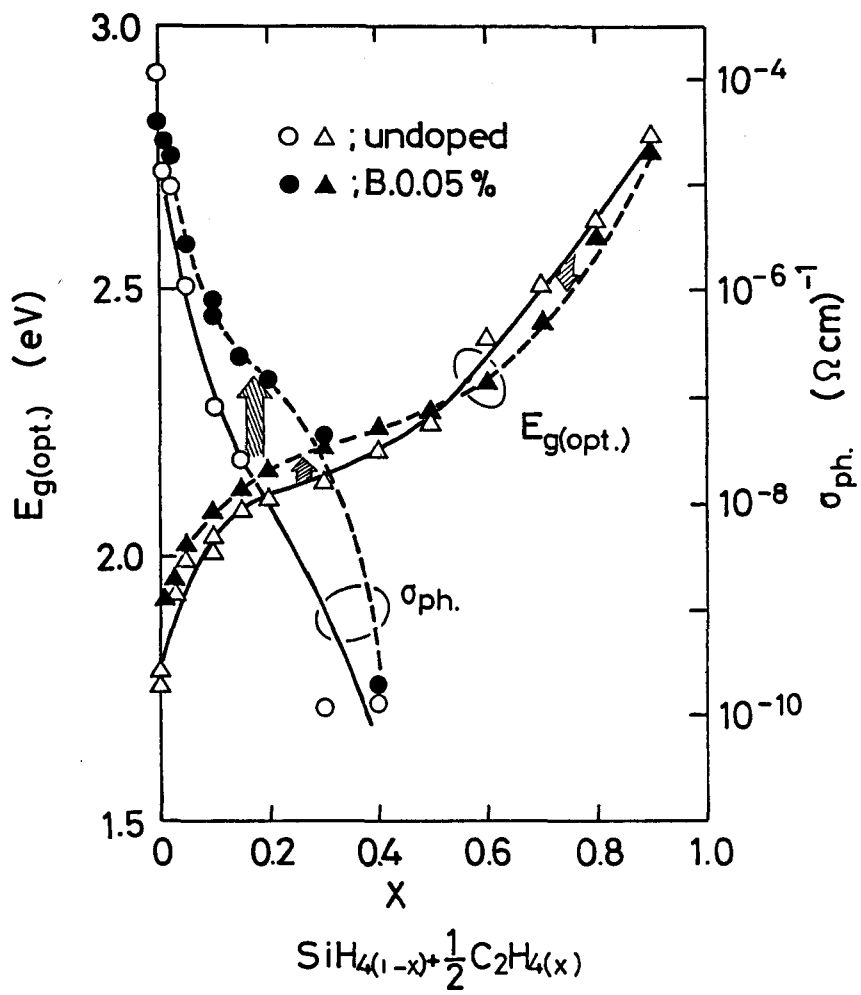


Fig. 3-13. Photoconductivity σ_{ph} and optical band gap $E_{g(opt)}$ of undoped and boron doped ethylene based a-SiC:H.

phosphorus doped a-SiC:H films. These effects are accompanied by the decrease of ESR spin density by doping, as shown in Fig. 3-12. In other word, boron or phosphorus atoms compensate the dangling bond in amorphous SiC network and enhance the carrier life time.

The optical band gap of undoped and boron doped a-SiC:H increases monotonically with increasing methane fraction, but $E_{g(opt)}$ of boron doped one is little bit narrower than undoped film. The narrowing of $E_{g(opt)}$ by boron doping is mainly caused by the decrease of hydrogen attached to carbon.

Figure 3-13 shows the optical band gap $E_{g(opt)}$ and AM-1 photoconductivity σ_{ph} of undoped and boron doped ethylene based a-SiC:H films as a function of ethylene fraction. The optical band gap of ethylene based a-SiC:H films increases from 1.76 to 2.8 eV with increasing gas fraction. One of the reason why ethylene based a-SiC:H films shows a larger optical band gap in the same gas fraction is that the carbon content in ethylene based film is larger than that of methane based one. Photoconductivity recovery effect in this case is only one order. Comparing ethylene based and methane based a-SiC:H films, the latter one shows one or two orders larger magnitude of photoconductivity recovery effect than the former one. The distinction between the two may be due to the incorporated hydrogen manner, especially attached to C which is a factor responsible for the photoconductivity recovery effect.

3-4-2. Summary of effects of impurity doping

Figure 3-14 shows a summary of the effects of impurity doping on the basic properties of typical methane based a-SiC:H films. As is seen in the figure, the dark conductivity σ_d at room temperature is of the order of $10^{-5}(\Omega\text{cm})^{-1}$ for 0.2 % diborane doping and of the order of $10^{-3}(\Omega\text{cm})^{-1}$ for only 0.02 % phosphine doping. In contrast with these, the dark conductivity of undoped film is of the order of $10^{-12}(\Omega\text{cm})^{-1}$. That is, the controllable range of conductivity is from 10^{-12} to 10^{-5} or $10^{-3}(\Omega\text{cm})^{-1}$ for p- and n-type, respectively. The activation energy ΔE also changes from 1.05 to 0.4 eV for boron doping and to 0.3 eV for phosphorus doping. So far as ascertained in terms of electrical conductivity and thermoelectrical power measurement, p-n control of a-SiC:H is well achieved. The most important feature in the methane based a-SiC:H can be seen in the photoconductivity recovery effect by impurity doping. The photoconductivity of undoped film is of the order of $10^{-9}(\Omega\text{cm})^{-1}$, while that of doped a-SiC:H is of the order of $10^{-6}(\Omega\text{cm})^{-1}$ for diborane doping and of the order of $10^{-4}(\Omega\text{cm})^{-1}$ for phosphine doping. The optical band gap of doped a-SiC:H decreases with increasing doping fraction. The narrowing of $E_{g(\text{opt})}$ is caused by the decrease of hydrogen attached to carbon.

The same valency controllability can be seen in ethylene based a-SiC:H films, as shown in Fig. 3-15. The dark conductivity of this case changes from $10^{-13}(\Omega\text{cm})^{-1}$ of undoped film to $10^{-8}(\Omega\text{cm})^{-1}$ of 2% diborane or phosphine doped films. As compared with methane based a-SiC:H films, ethylene based a-SiC:H films need the sufficient doping fraction to get a high conductivity. The photoconductivity recovery in this case is only one order for diborane doping and one or two orders

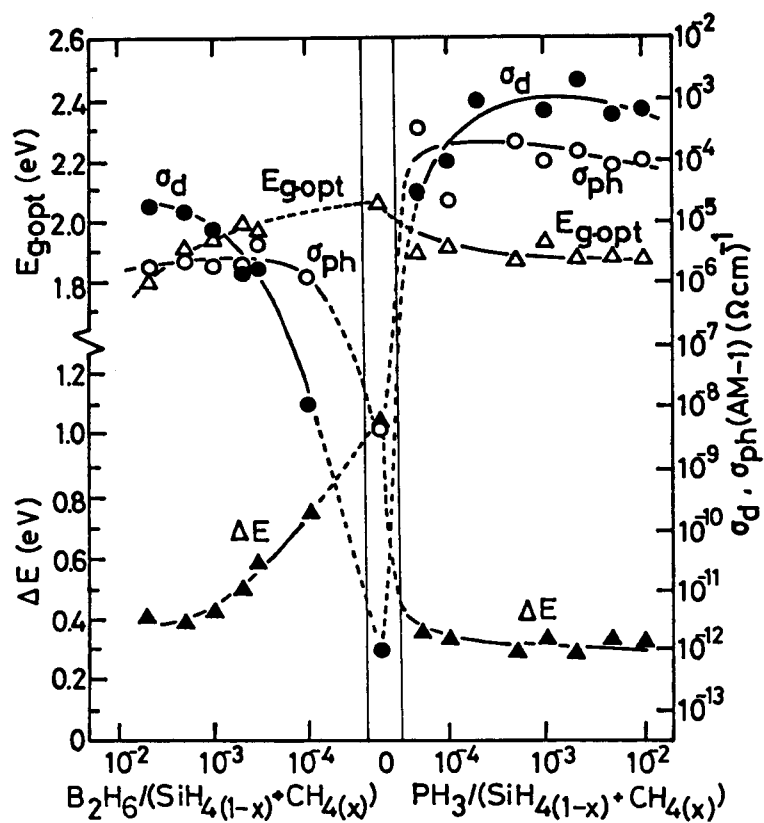


Fig. 3-14. Summary of the effects of impurity doping on the basic properties of methane based $a\text{-SiC:H}$.

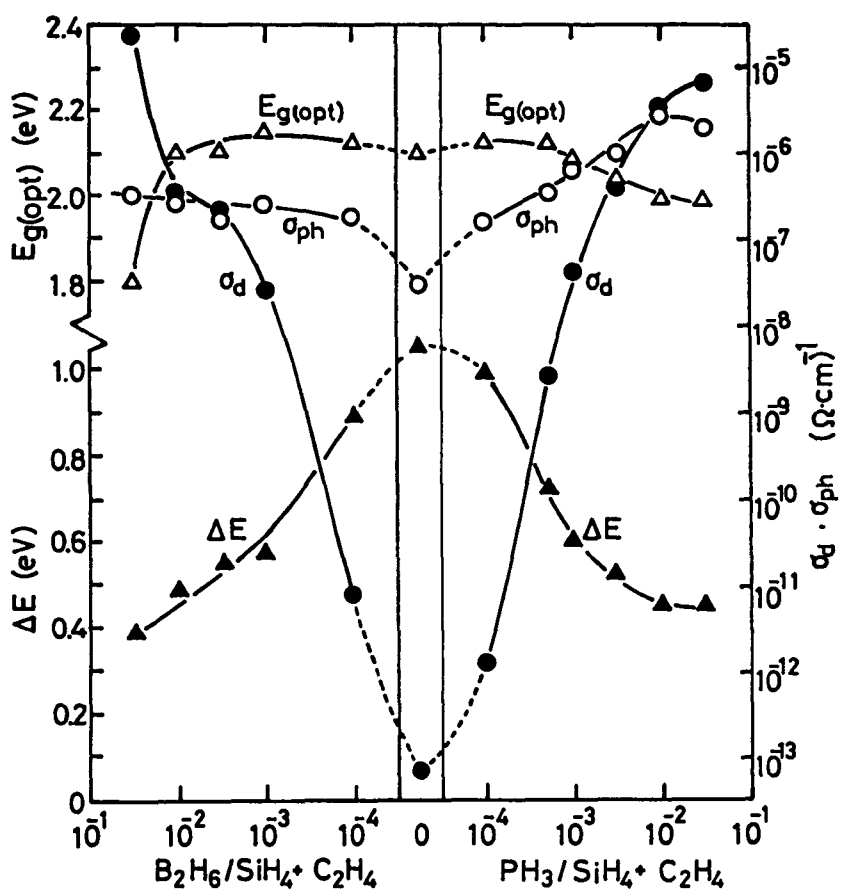


Fig. 3-15. Summary of the effects of impurity doping on the basic properties of ethylene based a-SiC:H.

for phosphine doping. The result is very different from that of the methane based film. The hydrogen attached to C in ethylene based a-SiC:H films increases by adding dopant. Therefore, the optical band gap slightly increases by adding both dopant. The increase of hydrogen attached to carbon makes the valency controllability difficult.

3-5. Discussion and Summary

A series of experimental verifications has been carried out on the valency electron control of a-SiC:H. First of all, carbon sources were examined to obtain an ideal a-SiC alloy. Methane (CH_4) and ethylene (C_2H_4) were selected as carbon sources, and film composition and hydrogen content were verified. The carbon content of the deposited films was determined by an Auger Electron Spectroscopy (AES). There is a noteworthy difference between methane based and ethylene based a-SiC:H films. That is, ethylene based a-SiC:H films contain a larger amount of carbon than methane based films. This is caused to the reactivity of ethylene and methane. Incorporated hydrogen manner of a-SiC:H films is also important in view of valency electron control. However, hydrogen content of a-SiC:H films could not be exactly estimated by IR method, because the absorption cross section of C-H stretching absorption has not been given exactly. We determined the absorption cross section of C-H stretching by $^1\text{H}(^{15}\text{N}, \alpha\gamma)^{12}\text{C}$ nuclear reaction, and A_s value of $1 \times 10^{21}/\text{cm}^2$ was obtained. Using this A_s value, a series of experimental investigation has been carried out on the incorporated hydrogen manner of a-SiC:H films. It is shown that ethylene based a-SiC:H films contain carbons as $-\text{C}_2\text{H}_5$, but methane based films contain carbons as tetrahedral atoms. From this

point, methane based a-SiC:H films are recognized to be a rather ideal a-SiC alloy. However, ethylene based a-SiC:H films show methane like structure when the deposition is carried out at high RF power condition.

Photoconductivity of undoped a-SiC:H films significantly decreases with increasing carbon fraction. However, boron doped methane based films show one or three orders of larger magnitude of photoconductivity as compared with undoped film. The photoconductivity recovery effect is similarly seen in phosphorus doped a-SiC:H films. It is recognized from ESR study that the effect is accompanied by the decrease of ESR spin density. In other word, boron or phosphorus atoms compensate the dangling bond in amorphous SiC network and thus enhance the carrier life time. The photoconductivity recovery effect of ethylene based a-SiC:H films is rather smaller than that of methane based films. It might be possible that the difference between the two types is caused by the hydrogen attached to carbon.

Valency electron controllability can be seen in both methane based and ethylene based a-SiC:H films. The latter one needs the sufficient doping fraction to get a high conductivity as compared with the former one. The most important feature in methane based a-SiC:H films can be seen in the photoconductivity recovery effect by impurity doping. The photoconductivity of methane based a-SiC:H films increases by three and six orders for boron and phosphine doping, respectively.

Using methane based a-SiC:H films as a p-layer in p-i-n a-Si solar cells, an excellent window effect was found, and a new technology of a-SiC:H/a-Si:H heterojunction solar cell has been developed.

REFERENCES

- 1) Y. Hamakawa: J de Physique 42 (1981), suppl. 10, C4-1131.
- 2) P. G. LeComber, A. J. Snell, K. D. Mackenzie and W. E. Spear: J de Physique 42 (1981), suppl. 10, C4-423.
- 3) I. Shimizu, S. Oda, K. Saito, H. Tomita and E. Inoue: J de Physique 42 (1981), suppl. 10, C4-1123.
- 4) D. A. Anderson and W. E. Spear: Philos. Mag. 35 (1977) 1.
- 5) D. Engemann, R. Fischer and J. Knecht: Appl. Phys. Lett. 32 (1978) 567.
- 6) H. Wieder, M. Cardona and C. R. Guanieri: Phys. Stat. Sol. (b)92 (1979) 99.
- 7) H. MuneKata, S. Murasato and H. Kukimoto: Appl. Phys. Lett. 37 (1980) 536.
- 8) R. S. Sussmann and R. Ogden: Philos. Mag. B44 (1981) 137.
- 9) Y. Tawada, T. Yamaguchi, S. Nonomura, S. Hotta, H. Okamoto and Y. Hamakawa: Jpn. J. Appl. Phys. 20 (1981), suppl.20-2, 219.
- 10) Y. Tawada, H. Okamoto and Y. Hamakawa: Appl. Phys. Lett. 39 (1981) 237.
- 11) Y. Tawada, M. Kondo, H. Okamoto and Y. Hamakawa: Proc. 15th IEEE Photovoltaic Specialists Conf., Florida (1981) p-245.
- 12) Y. Tawada, M. Kondo, H. Okamoto and Y. Hamakawa: Jpn. J. Appl. Phys. 21 (1982), suppl. 21-1, 297.
- 13) Y. Tawada, M. Kondo, H. Okamoto and Y. Hamakawa: Solar Energy Mat. 6 (1982) 299.
- 14) Y. Tawada, K. Tsuge, M. Kondo, H. Okamoto and Y. Hamakawa: J. Appl. Phys. 53 (1982) 5273.
- 15) Wen-Yaung Lee: J. Appl. Phys. 51 (1980) 3365.

- 16) G. Turban, Y. Catherine and B. Grolleau: Phys. Thin Solid Films
77 (1981) 287.
- 17) M. H. Brodsky, M. Cardona and J. J. Cuomo: Phys. Rev. B16 (1977)
3556.
- 18) K. Kubota, T. Imura and A. Hiraki: Nucl. Instrum & Methods
168 (1980) 211.
- 19) A. Guivarc'h, J. Richard, M. LeContellec, E. Ligeon and
J. Fontenille: J. Appl. Phys. 51 (1980) 2167.
- 20) H. Fujimoto, A. Otsuka, K. Komaki, A. Iwata, S. Hashimoto, I. Yamane,
H. Yamashita, K. Osawa, Y. Tawada, M. Kondo, H. Okamoto and
Y. Hamakawa: Jpn. J. Appl. Phys. (to be published).
- 21) C. J. Faung, K. J. Gruntz, L. Ley and M. Cardona: J. Non-Cryst.
Solids 35&36 (1980) 255.
- 22) E. A. Davis and N. F. Mott: Philos. Mag. 22 (1970) 903.
- 23) P. J. Zanzucchi, C. R. Wronski and D. E. Carlson: J. Appl. Phys.
48 (1977) 5227.

IV WINDOW EFFECTS OF HYDROGENATED AMORPHOUS SILICON CARBIDE IN A p-i-n a-Si SOLAR CELL

4-1. Introduction

Amorphous silicon is actively investigated as one of the most promising low cost photovoltaic materials.¹⁾ A great deal of R&D efforts paid for improving the conversion efficiency of an a-Si solar cell has included adjustments of material science, fabrication technology and cell parameter designs. In view point of material science, new amorphous materials such as a-Si:F:H,²⁾ a-SiGe:H,³⁾ a-SiC:H⁴⁾ and a-SiSn⁵⁾ have been investigated. As for new fabrication technologies, for example, cross field biased glow discharge,^{6,7)} proximity dc glow discharge⁸⁾ and glow discharge under magnetic field⁹⁾ have been proposed. Efforts to improve cell design have also been made; p-i-n heteroface solar cells,¹⁰⁾ inverted p-i-n solar cells,¹¹⁾ metal insulator(MIS) solar cells,¹²⁾ multilayer¹³⁾ or stacked¹⁴⁾ solar cells, graded heterojunction solar cells¹⁵⁾ and a-SiC:H/a-Si:H heterojunction solar cells⁴⁾ have been developed. Through these technological efforts, a remarkable improvement of the conversion efficiency has been seen, that is, 6.1 - 6.9% with an inverted p-i-n a-Si:H solar cell,¹⁶⁻¹⁸⁾ 6.6% with an a-Si:F:H MIS cell,¹⁹⁾ 5.9% with an a-Si:H/a-SiGe:H stacked cell²⁰⁾ and 7.55% with an a-SiC:H/a-Si:H heterojunction solar cell.²¹⁾

The p-i-n heteroface solar cell is one of the best cell constructions and might provide better producibility, as well as being amenable to future mass production and design control when put into practical applications.²²⁾ However, the p-i-n heteroface solar cell has one demerit, that is, a large optical absorption coefficient in the

window side p-layer which has a narrow optical band gap with high density of non-radiative recombination centers.²³⁾ For the purpose of decreasing this absorption loss, some kinds of experimental trials have been made for a few years. Recently, we have found a valency electron controllability in hydrogenated amorphous silicon carbide prepared by the plasma decomposition of $[\text{SiH}_{4(1-x)} + \text{CH}_4(x)]$ with the dopant gas of B_2H_6 or PH_3 system²⁴⁾.

The compositional dependence of the optical band gap in amorphous silicon carbide was demonstrated by Anderson and Spear²⁵⁾ and they showed that the optical band gap of a-SiC:H prepared by the decomposition of $[\text{SiH}_{4(1-x)} + \text{C}_2\text{H}_4(x)]$ continuously increases with increasing carbon content. However, no information on the electrical, optical and optoelectronic properties of doped a-SiC:H have been reported. We have made a series of experiments on a-SiC:H over the deposition parameter dependence of the film quality, and the effects of substitutional impurity doping on electrical, optical and optoelectronic properties.²⁶⁾

Utilizing this doped a-SiC:H as a wide gap window material, we have developed a new type of a-SiC:H/a-Si:H heterojunction solar cell having more than 7.5% conversion efficiency. The purpose of this chapter is to present window effects of hydrogenated amorphous silicon carbide in this new type solar cell structure.

4-2 Preparation of a-SiC:H Films and a-SiC:H/a-Si:H Heterojunction Solar Cells

4-2-1 Fabrication of glass/ SnO_2 /p a-SiC:H/i-n a-Si:H/Al heterojunction solar cells

Various types of junction structure are now in progress all over

the world.¹⁷⁾ We have paid our attention particularly on the junction structure of the p-i-n heteroface type²²⁾ with a view to better process controllability and reproducibility for the low cost solar cell production in the future. There are two types in the p-i-n heteroface solar cell. One is glass/ITO(or SnO_2)/p-i-n/Metal and another one is ITO/p-i-n/Metal substrate. In the present experiment, glass/ SnO_2 /p-i-n/Al structure were employed because the fluctuation of series resistance originated in a transparent electrode in a solar cell was successfully suppressed. The substrate temperature during deposition was settled at 250°C. A boron doped a-SiC:H layer of 100Å was deposited on the substrate. Then an undoped a-Si:H of 5000Å and a phosphorous doped a-Si:H of 500Å were succesively deposited. An alminium electrode was evaporated onto the surface of n-layer as a back side contact.

It is widely accepted that the properties of a-Si:H films are strongly influenced by rf power.^{27, 28)} Therefore, we optimized the deposition condition of undoped and phosphorous doped a-Si:H⁴⁾ in the p-i-n a-Si:H heteroface solar cell. One of the noticeable merits of our reaction system is that we can control the relative position D of the substrate to the discharge plasma while the energy density of the plasma can be controlled by adjusting the position of the rf coupling electrodes set outside the reaction chamber perpendicularly to the substrate .

To the extent of the experiment concerning the undoped a-Si:H layer optimization in our deposition system, the most favorable condition for solar cell fabrication is D of 10cm and rf power of 35watts. Therefore, the conditions of D=10cm and rf power of 35 watts were chosen for the deposition of the undoped a-Si:H layer in

a-SiC:H/a-Si:H heterojunction cells.

We examined the basic properties of phosphorous doped a-Si:H ($\text{PH}_3/\text{SiH}_4=0.5\text{mol}\%$) as a function of rf power for the electrode position D of 12.5cm. The dark conductivity increases exponentially and the activation energy decreases with increasing rf power in the region of more than 60watts. The crystalline structure was observed by the X-ray diffraction patterns in a phosphorous doped a-Si:H decomposed by more than 150watts rf power. A high conductive n-layer is favorable to reduce the series resistance of solar cells, but a higher rf power deposition might bring about impurity inclusion and also bombardment effects on the film. Therefore, we deposited phosphorous doped a-Si:H in a-SiC:H/a-Si:H heterojunction solar cell under the condition of rf power=150watts and D=12.5cm.

The sensitive area of solar cell is 3.3mm^2 which was carefully evaluated to be about 5% larger than the deposited area of aluminum bottom electrode (area= 3.14mm^2) by taking account of the experimentally confirmed edge effect to the photocurrent. J-V characteristics measurements were carried out under the AM-1 solar simulator. The solar simulator was calibrated by the standard a-Si solar cell. The performance of this standard cell was measured under the sun light (near AM-1 sun light, at Toyonaka, Osaka, Japan, July 1980). At this time, the solar radiation energy was measured by the NASA-calibrated c-Si solar cell and the pyroheliometer.

4-2-2. Basic properties of doped a-SiC:H/a-Si:H as a window material

Amorphous SiC:H were prepared by the plasma decomposition of $[\text{SiH}_4(1-x) + \text{CH}_4(x)]$ gas mixture. The methane based a-SiC:H film

showed not only a photoconductivity recovery effect by doping but also a good valency electron controllability for both donors and acceptors. This valency controlled a-SiC:H is a useful window material for both p-i-n and inverted p-i-n structures. In the p-i-n cell structure, the activation energy ΔE and the dark conductivity σ_d of p-layer are generally required to be less than 0.6eV and more than $10^{-7}(\Omega \cdot \text{cm})^{-1}$, respectively. Therefore, p-type a-SiC:H having a wide band gap ranging from 1.8 to 2.1eV was made use of, whose activation energy ΔE and dark conductivity σ_d , as shown in Fig. 4-1, were settled to be about 0.55eV and on the order of $10^{-7}(\Omega \cdot \text{cm})^{-1}$, respectively. The photoconductivity of these a-SiC:H, however, decreases as the increase of the optical band gap.

Figure 4-2 shows the optical absorption spectra of these a-SiC:H as a function of wave length. As is seen in this figure, the optical absorption spectra of these a-SiC:H shift to higher energy region as compared with a-Si:H. An essential matter required for high efficiency a-Si solar cell is to effectively introduce the incident photons into the i-layer, where the photocurrent is mainly produced. The calculated optical absorption loss in p-layer is shown in Table 4-1. As can be seen in this table, the ineffective absorption in the window side p-layer having an optical band gap of more than 2eV for p-i-n junction cell is negligibly small; on the other hand, there might be about 10% ineffective absorption in a p-layer of p-i-n a-Si:H solar cell. Utilizing these a-SiC:H as a p-side window material, we have fabricated a-SiC:H/a-Si:H heterojunction solar cells.

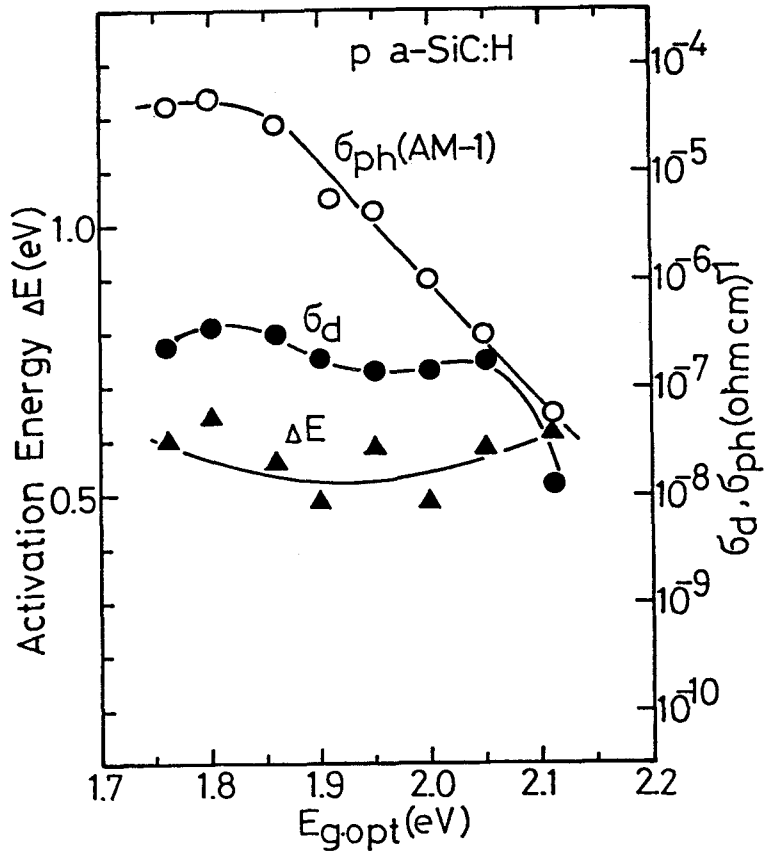


Fig. 4-1. Basic properties of boron doped a-SiC:H as a function of optical band gap $E_{g.(opt)}$.

Table 4-1 Absorption loss in the p-layer

$E_{g,opt}$	1.76eV	2.02eV	2.1eV
$\lambda=4500\text{\AA}$	17.3%	6.1%	1.9%
$\lambda=5000\text{\AA}$	11.7%	4.1%	1.2%
$\lambda=5500\text{\AA}$	6.1%	2.1%	0.6%

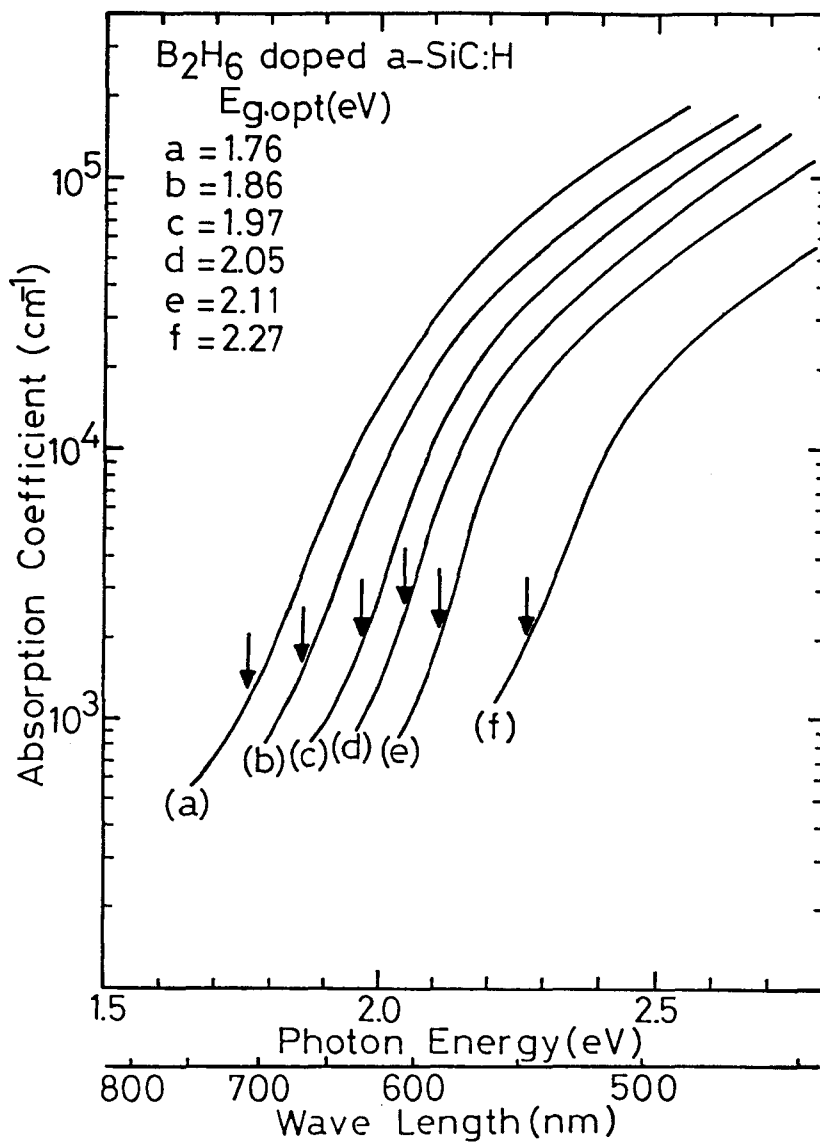


Fig. 4-2 Optical absorption spectra of boron doped a-SiC:H as a parameter of optical band gap $E_{g.(opt)}$.

4-3 Window Effects of a-SiC:H in an a-SiC:H/a-Si:H Heterojunction Solar Cell.

4-3-1 Photovoltaic performance dependence on the optical band gap of a-SiC:H

We have examined the photovoltaic performance dependence on the optical band gap of boron doped a-SiC:H in a-SiC:H/a-Si:H heterojunction solar cells. Figure 4-3 shows the photovoltaic performances of a-SiC:H/a-Si:H heterojunction solar cells as a function of the optical band gap $E_{g(opt)}$ of p-type a-SiC:H. As is seen in this figure, not only the short circuit current density J_{sc} but also the open circuit voltage V_{oc} increase with increasing the optical band gap $E_{g(opt)}$ of p-layer. The short circuit current density J_{sc} shows a tendency to saturate for $E_{g(opt)}$ of more than 2 eV. The open circuit voltage V_{oc} also increases up to 0.91volts as the increase of E_{gopt} of p-layer. The fill factor FF is almost constant except for E_{gopt} of more than 2.1eV. Therefore, there exists an optimum E_{gopt} of p-layer, that is, about 2eV. For this optimum $E_{g(opt)}$ of p-layer, the conversion efficiency of 7.14% was obtained with J_{sc} of 12.22mA/cm^2 , V_{oc} of 0.89volts and FF of 65.6%, as shown in Fig. 4-4.

4-3-2 Effects of a-SiC:H on J_{sc} and V_{oc} .

a-SiC:H/a-Si:H heterojunction solar cells show not only larger J_{sc} but also larger V_{oc} than ordinary p-i-n a-Si:H homojunction solar cells. More direct experimental evidence can be seen in the collection efficiency data as shown in Fig. 4-5. As is seen in this figure, the collection efficiency of these cells is extremely improved, especially near around the peak of solar energy spectrum with increasing $E_{g(opt)}$

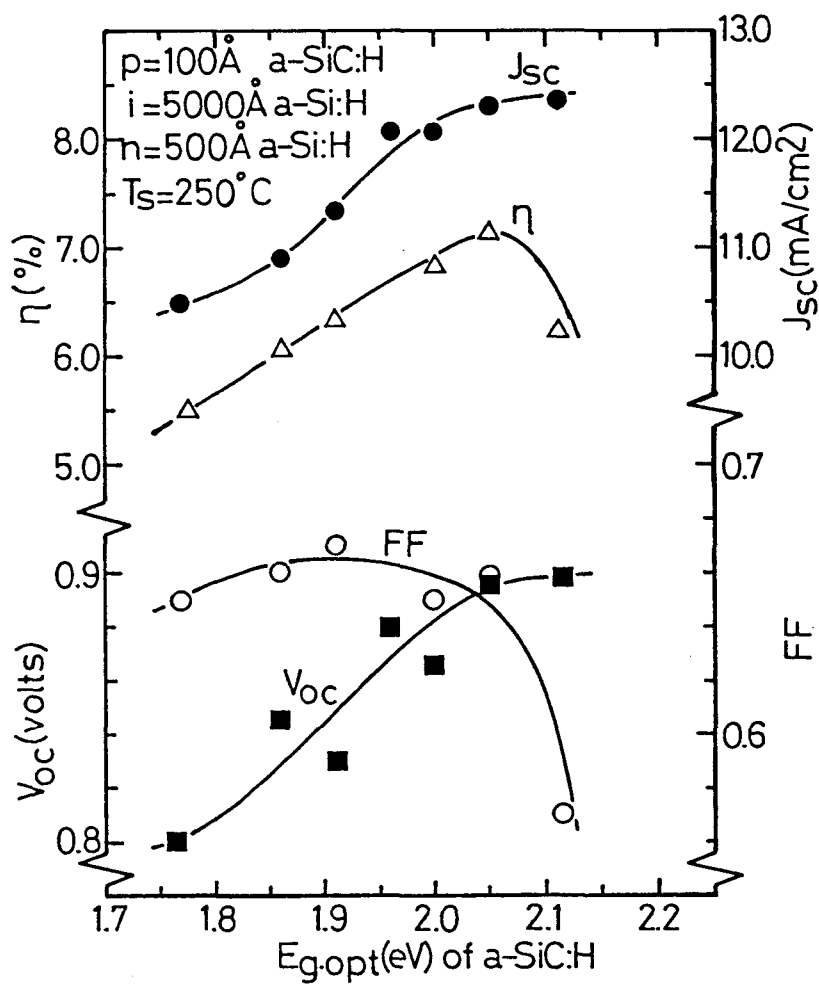


Fig. 4-3. Photovoltaic performances of a-SiC:H/a-Si:H heterojunction solar cells as a function of optical band gap of window side a-SiC:H.

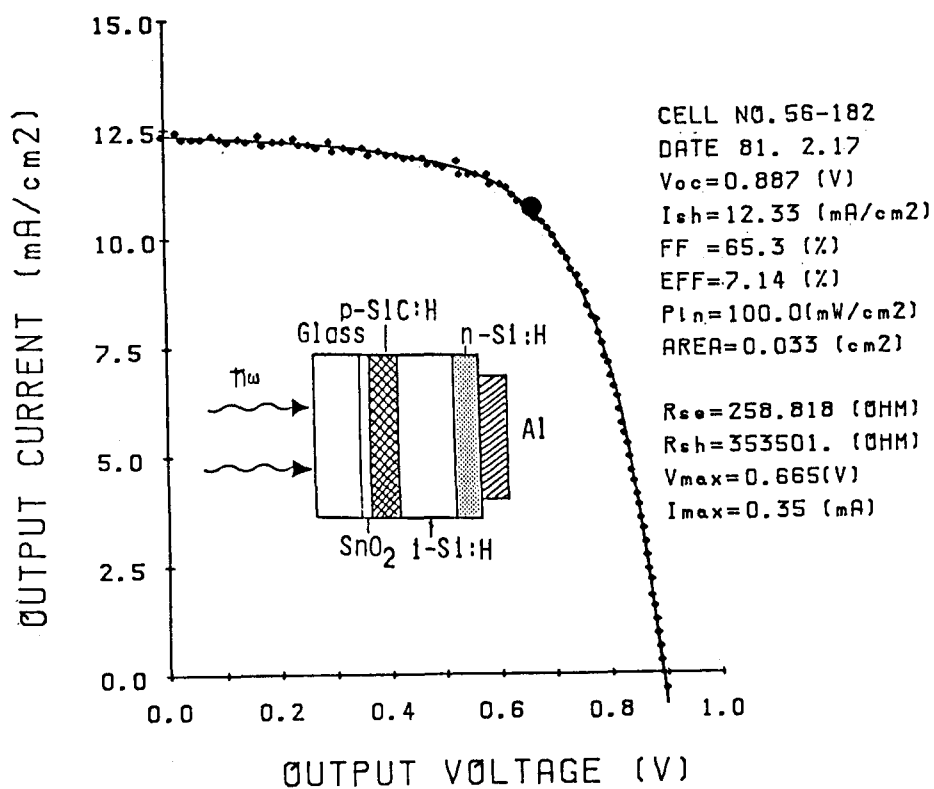


Fig. 4-4. J-V characteristics of a-SiC:H/a-Si:H heterojunction solar cell having the sensitive area of 3.3mm^2 .

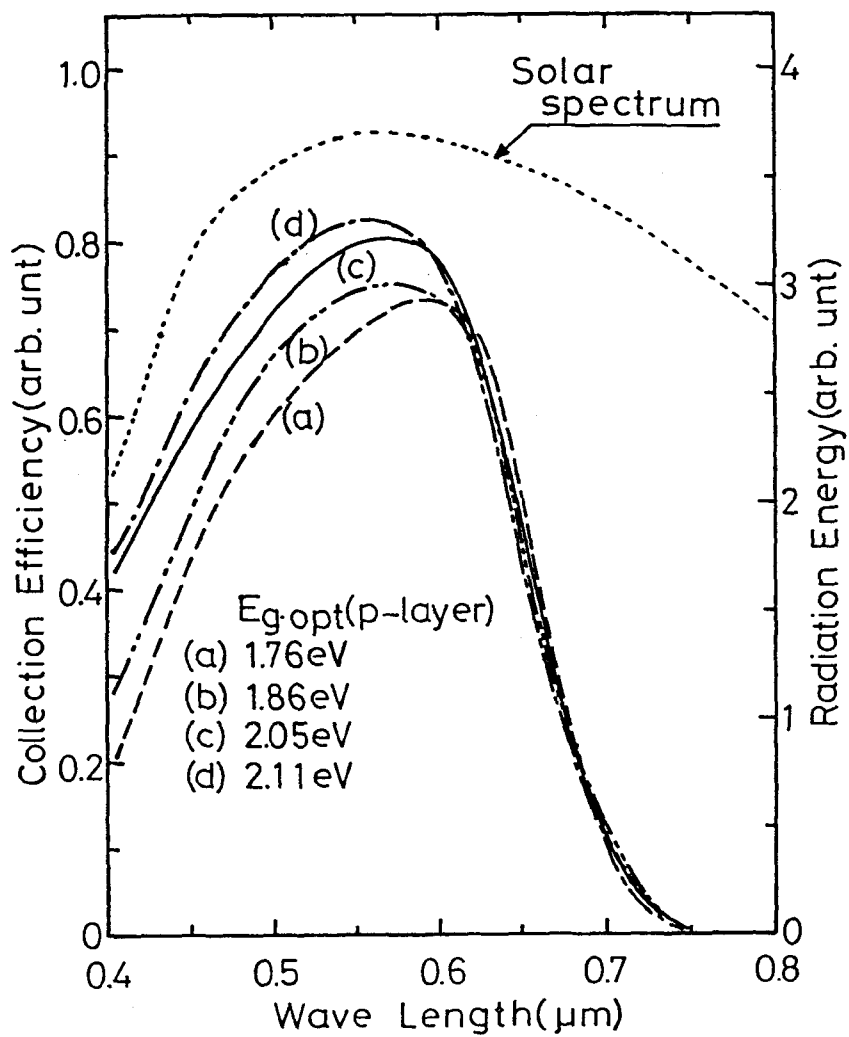


Fig. 4-5. Collection efficiency spectra of a-SiC:H/a-Si:H heterojunction solar cells as a parameter of optical band gap of window side p-layer.

of a p-layer. These improvements are caused by a large optical band gap of a p-layer which reduces the optical absorption loss in a p-layer, and the large internal electric field which increases the collection probability of free carrier.

As for effects of a-SiC:H on the open circuit voltage V_{oc} , there exists a clear correlation between the open circuit voltage V_{oc} and the diffusion potential V_d in a p-i-n junction, as shown in Fig. 4-6. With p-type a-SiC:H, we can increase the diffusion potential of a p-i-n junction, and 1/3 of the increased diffusion potential contributes to the increase of the open circuit voltage V_{oc} . This result shows us that it might be possible to obtain a larger open circuit voltage by optimization of p-layer.

4-3-3 Photovoltaic performance dependence on the thickness of p-type a-SiC:H

It is well known that the open circuit voltage V_{oc} and the short circuit current density J_{sc} strongly depend upon the thickness of a p-layer in a p-i-n a-Si solar cell²³⁾. This dependency is caused by homogeneity and large optical absorption of a p-type a-Si:H. a-SiC:H has a larger optical band gap than a-Si:H so that the photovoltaic performance dependence on the thickness of p-type a-SiC:H may be different from the case of a p-type a-Si:H. Figure 4-7 shows the photovoltaic performance dependence on the thickness of p-type a-SiC:H having $E_{g(opt)}$ of 1.86eV. In this case, the short circuit current density J_{sc} is influenced by the thickness of p-layer as well as a-Si:H, and decreases as the increase of p-layer thickness. The open circuit voltage V_{oc} increases as the increase of p-layer thickness.

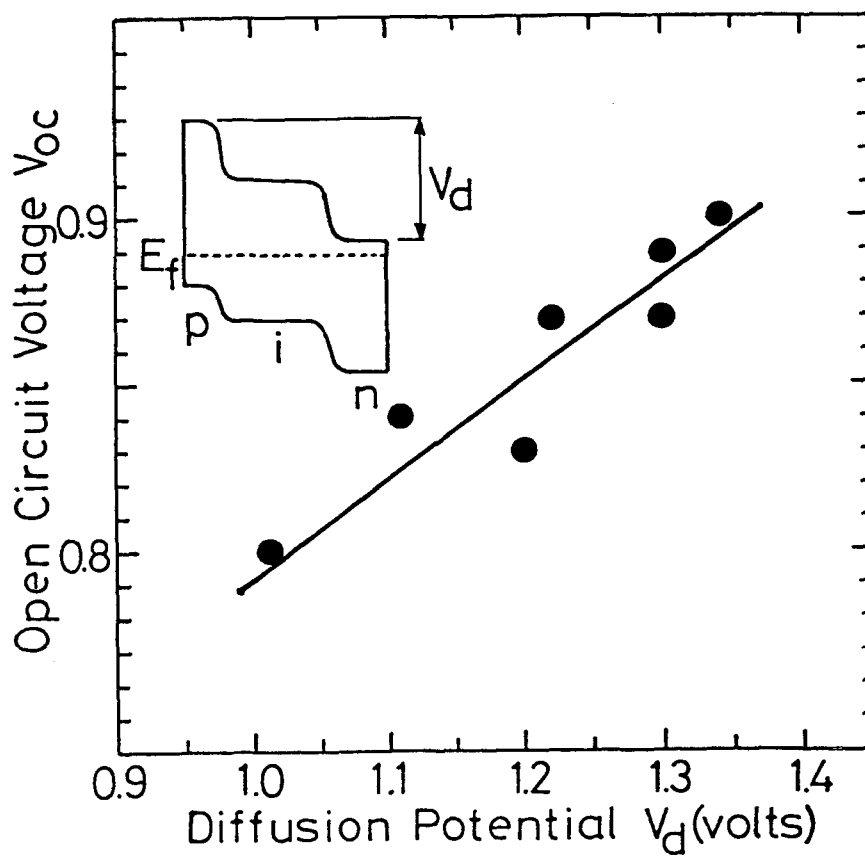


Fig. 4-6. Correlation between the open circuit voltage V_{oc} and the diffusion potential V_d in a-SiC:H/a-Si:H heterojunction solar cells.

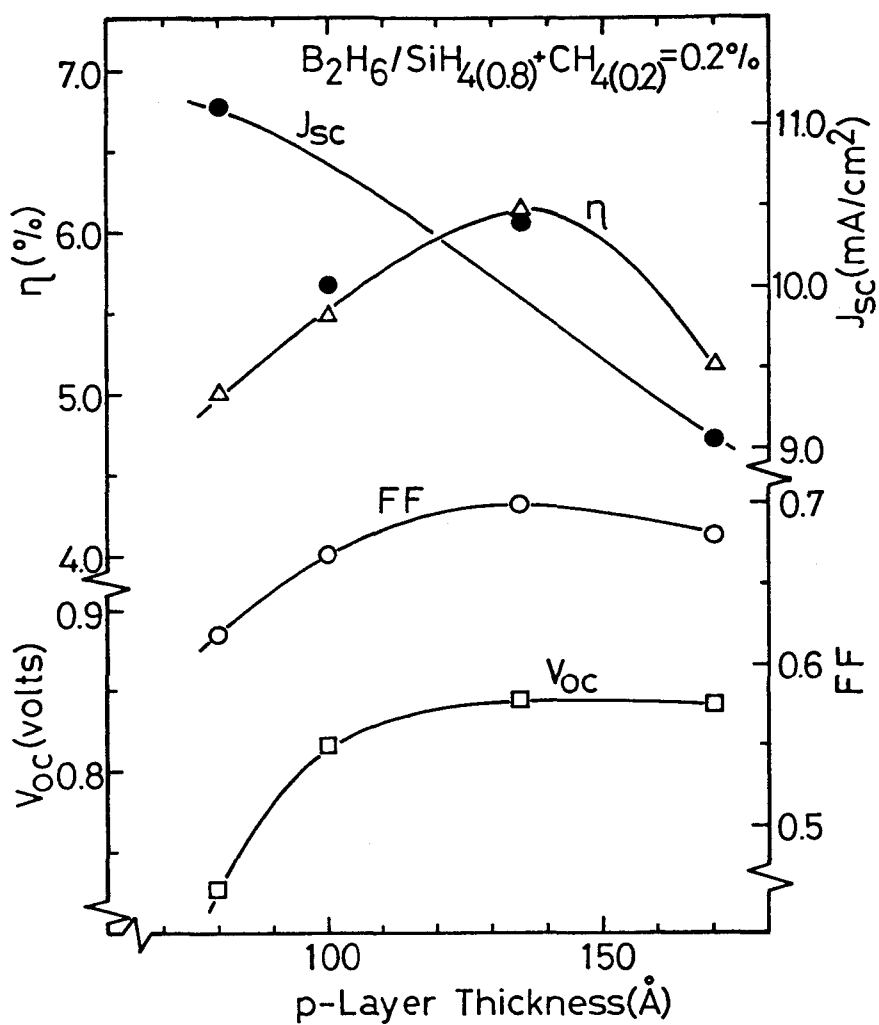


Fig. 4-7. Photovoltaic performances of a-SiC:H/a-Si:H heterojunction solar cells as a function of thickness of p-type a-SiC:H with $E_{g.(opt)}$ of 1.86 eV.

Therefore, the optimum thickness in this case appears at about 130\AA . In this case, we can make p-layer thicker than the case of a-Si:H cells, so that the higher open circuit voltage V_{oc} of 0.845volts has been obtained.

On the other hand, the photovoltaic performance dependence on the thickness of p-layer having $E_{g(opt)}$ of 2.05eV exhibits a different tendency, as shown in Fig. 4-8. The short circuit current density J_{sc} increases with increasing the thickness to about 100\AA , and does not exhibit any change even though p-layer thickness is more than 100\AA . It is because the optical absorption of this p-layer is so small that the ineffective absorption can be almost neglected. The open circuit voltage V_{oc} increases up to 0.91volts as the increase of p-layer thickness. However, the increase of p-layer thickness reduces the fill factor FF owing to the effect of series resistance involved in a p-layer. Therefore, the optimum layer thickness of p-layer is about 100\AA .

4-3-4 Typical J-V characteristics of a-SiC:H/a-Si:H heterojunction solar cells.

Through further optimizations of film qualities and cell parameters, the conversion efficiency of an a-SiC:H/a-Si:H heterojunction solar cell has been improved to 7.55%. While, an ordinary p-i-n a-Si:H homojunction solar cell showed the conversion efficiency of 5.7%. Figure 4-9 shows J-V characteristics of this a-SiC:H/a-Si:H heterojunction solar cell and an ordinary p-i-n a-Si:H homojunction solar cell for the comparison. The performance of an a-SiC:H/a-Si:H heterojunction solar cell is $\eta=7.55\%$, $V_{oc}=0.910\text{volts}$, $J_{sc}=13.45\text{mA/cm}^2$

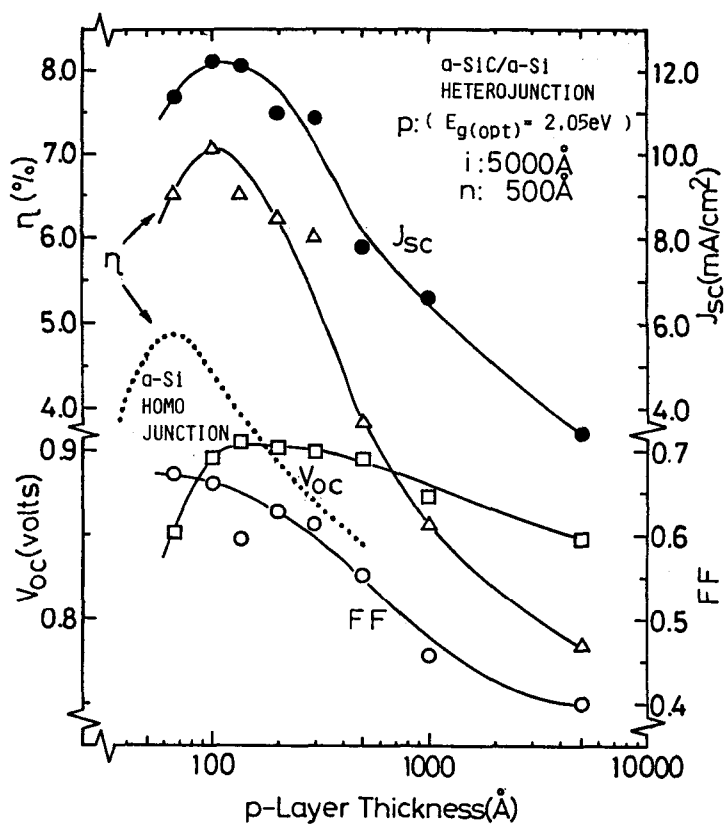
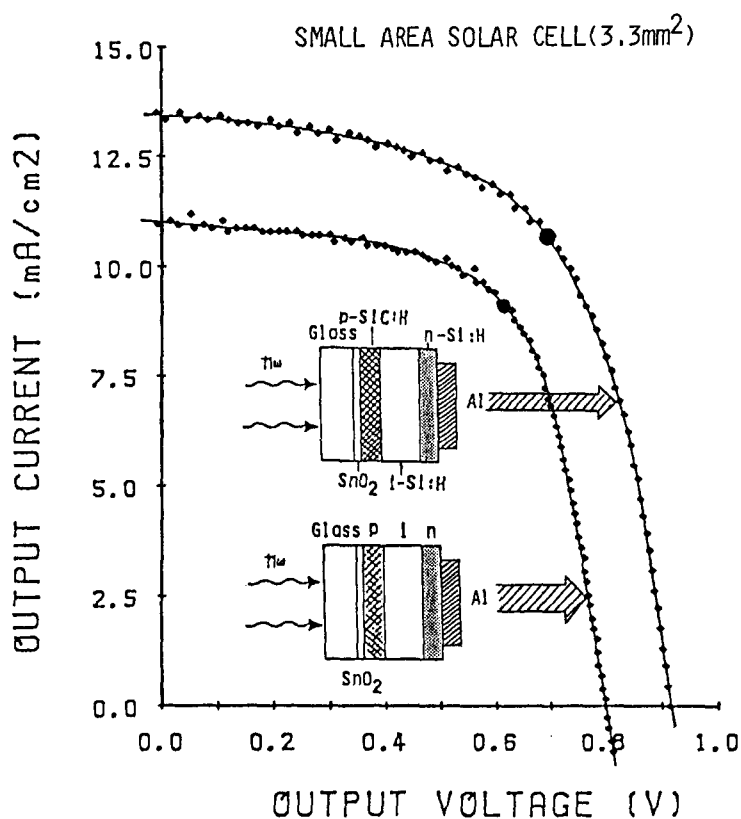


Fig. 4-8. Photovoltaic performances of α -SiC:H/ α -Si:H heterojunction solar cells as a function of thickness of p-type α -SiC:H with $E_{g.(opt)}$ of 2.05 eV.



a-SiC:H/a-Si:H

CELL NO. 56.316-1
 DATE 81.4.17
 $V_{oc} = 0.909$ (V)
 $I_{sh} = 13.45$ (mA/cm²)
 $FF = 61.7$ (%)
 $EFF = 7.55$ (%)
 $P_{in} = 100.0$ (mW/cm²)
 $AREA = 0.033$ (cm²)

a-Si:H

CELL NO. P-10-25
 DATE 81. 3. 3
 $V_{oc} = 0.801$ (V)
 $I_{sh} = 11.02$ (mA/cm²)
 $FF = 64.7$ (%)
 $EFF = 5.71$ (%)
 $P_{in} = 100.0$ (mW/cm²)
 $AREA = 0.033$ (cm²)

Fig. 4-9. Typical J-V characteristics of an a-SiC:H/a-Si:H hetero-junction solar cell (A) and an ordinary p-i-n a-Si:H homojunction solar cell (B).

and FF=61.7%. On the other hand, the conversion efficiency of an ordinary p-i-n a-Si:H solar cell is 5.7% with V_{oc} of 0.801volts, J_{sc} of $11.02\text{mA}/\text{cm}^2$ and FF of 64.7%. As is seen in these data, the performance of an a-SiC:H/a-Si:H heterojunction solar cell is clearly improved by 22% in J_{sc} , 13.5% in V_{oc} and 32% in η as compared with an ordinary p-i-n a-Si:H homojunction solar cell. This remarkable improvement of J_{sc} and V_{oc} is caused by the wide band gap effects of a-SiC:H, that is, the decrease of ineffective absorption in a p-layer and the increase of the diffusion potential in a p-i-n junction. The area of these cells is 3.3mm^2 and so small. As for a large area solar cell(1.0cm^2), the conversion efficiency of 7.11% has been obtained with $J_{sc}=13.3\text{mA}/\text{cm}^2$, $V_{oc}=0.852\text{volts}$ and FF=62.7%, as shown in Fig. 4-10.

Figure 4-11 shows the reflection spectra of these solar cells. As is seen in this figure, the loss by reflection can be estimated to be from 12 to 15%. This can be reduced to less than 5% by the optimization of antireflective coating; then more than 8% conversion efficiency might be obtained with the a-SiC:H/a-Si:H heterojunction solar cell structure.

4-4 Discussion and Summary.

We have conducted a series of experimental investigations on the window effects of a-SiC:H in a-SiC:H/a-Si:H heterojunction solar cells. The results of impurity doping on a-SiC:H imply that there is a good doping efficiency for both donors and acceptors of these impurities.²⁶⁾ Furthermore, doped a-SiC:H has a large optical band gap which can be controllable by methane fraction. These results show us that a-SiC:H is a very useful window material for both p-i-n

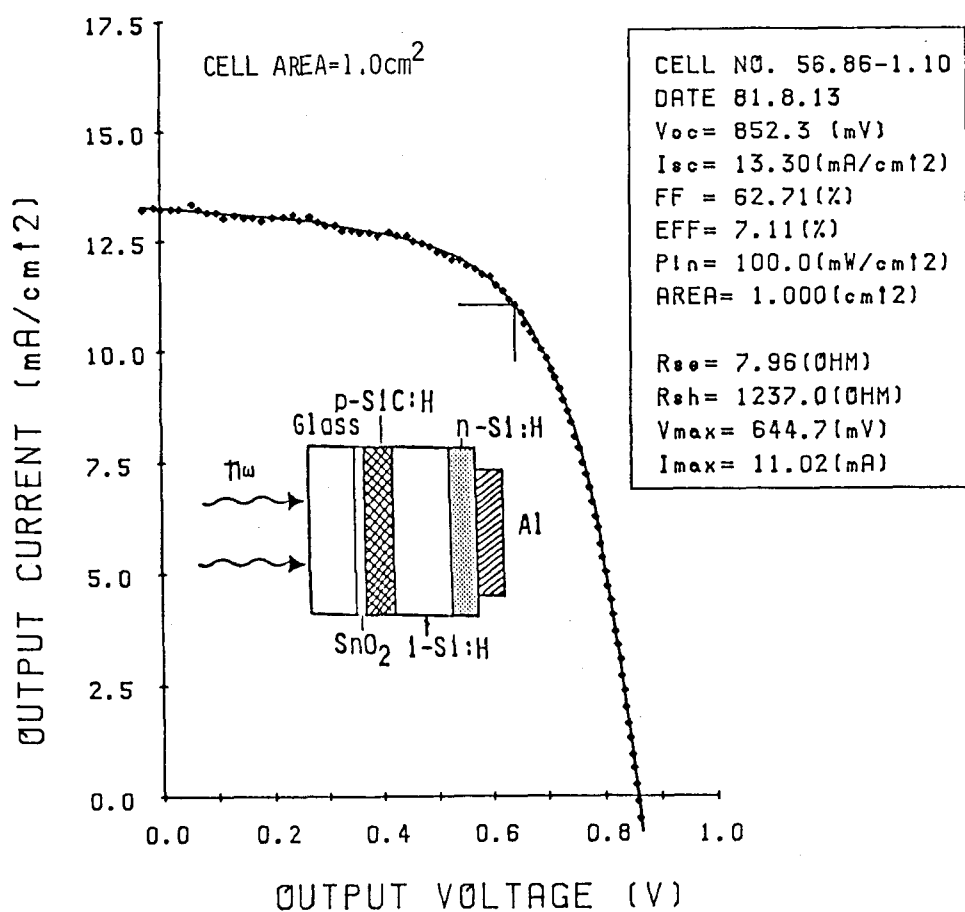


Fig. 4-10. J-V characteristics of a large area (1.0 cm²) a-SiC:H/a-Si:H heterojunction solar cell.

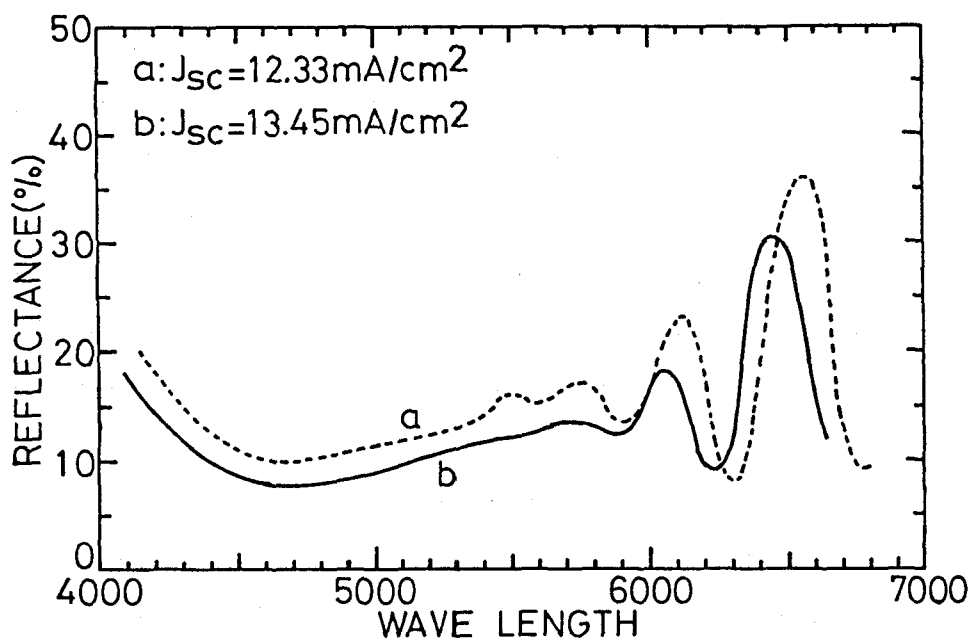


Fig. 4-11. Reflection spectra of typical glass/ SnO_2 /p a-SiC:H/i-n a-Si:H/Al solar cells.

and inverted p-i-n cell constructions. We investigated the window effects of these a-SiC:H in a-SiC:H/a-Si:H heterojunction solar cell. It is clear that not only J_{sc} but also V_{oc} of a-SiC:H/a-Si:H heterojunction solar cell increase with increasing E_{gopt} of a-SiC:H. The collection efficiency of these cells is extremely improved especially near around the peak of solar energy spectrum with increasing E_{gopt} of p-layer. These improvements are caused by the wide band gap effect of a-SiC:H. This is because a-SiC:H reduces the ineffective absorption in a p-layer and increases the internal electric field in a p-i-n junction. As for the increase of V_{oc} , a clear relation can be seen between the open circuit voltage V_{oc} and the diffusion potential V_d . From this linear relation, it is recognized that 1/3 parts of the increase of the diffusion potential contributes to the increase of the open circuit voltage V_{oc} . This result shows that it might be possible to obtain a larger open circuit voltage V_{oc} by the optimization of a-SiC:H. As for the optimum $E_{g(opt)}$ of p-layer, it can be estimated to be about 2eV.

The highest conversion efficiency given by further optimization is 7.55% with J_{sc} of 13.45mA/cm^2 , V_{oc} of 0.910volts and FF of 61.7%. Comparing this cell with an ordinary p-i-n a-Si:H homojunction solar cell, the performance of this a-SiC:H/a-Si:H heterojunction solar cell is clearly improved by 22% in J_{sc} , 13.5% in V_{oc} and 32% in η . As for a large area(1.0cm^2) solar cell, 7.11% conversion efficiency has been obtained with J_{sc} of 13.3mA/cm^2 , V_{oc} of 0.852volts and FF of 62.7%. The loss by reflection of these cells was estimated to be from 12 to 15%. We can reduce this reflection to less than 5% by the optimization of antireflective coating. Therefore, more than 8%

conversion efficiency might be obtained with a-SiC:H/a-Si:H hetero-junction solar cell. This result shows that a-SiC:H is one of the most favorable window side junction material. Additional noticeable merits in the proposed new solar cell are very strong mechanical strength with chemical and thermal stabilities.

REFERENCES

- 1) Y. Hamakawa: Proc. of *9th International Conf. on Amorphous and Liquid Semiconductors, Grenoble(1981)* and J. de Physique 42 (1981), suppl. 10, C4-1131.
- 2) S. R. Ovshinsky: Nature, 276 (1979) 482.
- 3) V. L. Dalal and E. A. Fagen: Proc. of *14th IEEE Photovoltaic Specialists Conf., San Diego(1980)* 1066.
- 4) Y. Tawada, T. Yamaguchi, S. Nonomura, S. Hotta, H. Okamoto and Y. Hamakawa; Jpn. J. Appl. Phys., 20, suppl. 20-2 (1981) 213.
- 5) C. Verie, J. F. Rochette and J. P. Rebonillat: Proc. of *15th IEEE Photovoltaic Specialists Conf., Florida (1981)* to be published.
- 6) H. Okamoto, T. Yamaguchi, Y. Nitta and Y. Hamakawa: J. Non-Cryst. Solids, 35&36 (1980) 201.
- 7) S. Hotta, Y. Tawada, H. Okamoto and Y. Hamakawa: Proc. of *9th International Conf. on Amorphous and Liquid Semiconductors, Grenoble (1981)* and J. de Physique 42 (1981), suppl. 10, C4-631.
- 8) D. E. Carlson: *1980 Photovoltaic Solar Energy Conf., Cannes (1980)*.
- 9) M. Taniguchi, M. Hirose, T. Hamasaki and Y. Osaka: Appl. Phys. Lett., 37 (1980) 787.
- 10) H. Okamoto, Y. Nitta, T. Adachi and Y. Hamakawa; Surface Sci., 86 (1979) 486.
- 11) R.A. Gibson, W. E. Spear, P. G. LeComber and A. J. Snell: J. Non-Cryst. Solids, 35&36 (1980) 725.
- 12) A. Madan, J. MacGill, W. Czubatjy, J. Yang and S. R. Ovshinsky: Appl. Phys. Lett., 37 (1980) 826.
- 13) Y. Hamakawa, H. Okamoto and Y. Nitta: Appl. Phys. Lett., 35 (1979) 187.

- 14) J. J. Hanak, B. Faughnan, V. Korsun and J. P. Pellican: *Proc. of 14th IEEE Photovoltaic Specialists Conf., San Diego (1980)* 1209.
- 15) G. Nakamura, K. Sato, Y. Yukimoto, K. Shirohata, T. Murahashi and K. Fugihara, *Jpn. J. Appl. Phys.*, 20, suppl. 20-1 (1981) 291.
- 16) D. E. Carlson: *Solar Energy Mat.*, 3 (1980) 503.
- 17) Y. Kuwano, M. Ohnishi, H. Nishiwaki, S. Tsuda, H. Shibuya and S. Nakano; *Proc. 15th IEEE Photovoltaic Specialists Conf., Florida (1981)* pp. 698.
- 18) Y. Uchida, T. Ichimura, M. Ueno and M. Ohsawa: *Proc. 9th International Conf. on Amorphous and Liquid Semiconductors, Grenoble (1981)* and *J. de Physique* 42 (1981), suppl. 10, C4-265.
- 19) A. Madan, J. MacGill, J. Yang, W. Czubatjy and S. R. Ovshinsky: *Proc. 9th International Conf. on Amorphous and Liquid Semiconductors, Grenoble (1981)* and *J. de Physique* 42 (1981), suppl. 10, C4-463.
- 20) G. Nakamura, K. Sato, H. Kondo, Y. Yukimoto and K. Shirahata: *Proc. 9th International Conf. on Amorphous and Liquid Semiconductors, Grenoble (1981)* and *J. de Physique* 42 (1981), suppl. 10, C4-483.
- 21) Y. Tawada, M. Kondo, H. Okamoto and Y. Hamakawa: *Proc. 15th IEEE Photovoltaic Specialists Conf., Florida (1981)* 245.
- 22) H. Okamoto, Y. Nitta, T. Yamaguchi and Y. Hamakawa: *Solar Energy Mat.*, 2 (1980) 313.
- 23) Y. Hamakawa, H. Okamoto and Y. Nitta: *Proc. 14th IEEE Photovoltaic Specialists Conf., San Diego (1980)* 1074.
- 24) Y. Tawada, H. Okamoto and Y. Hamakawa: *Appl. Phys. Lett.*, 39 (1981) in press.
- 25) D. A. Anderson and W. E. Spear: *Phil. Mag.*, 35 (1977) 1.

- 26) Y. Tawada, M. Kondo, H. Okamoto and Y. Hamakawa: Proc. 9th
International Conf. on Amorphous and Liquid Semiconductors,
Grenoble (1981) and J. de Physique 42 (1981), suppl. 10, C4-471
- 27) J. C. Knights: Jpn. J. Appl. Phys. 18 (1979) suppl.18-1, 101.
- 28) K. Tanaka et al.: J. Non-Cryst. Solids 35&36 (1980) 385.

V. PROPERTIES AND CHEMICAL BONDING STRUCTURE OF a-SiC:H FILMS FOR HIGH EFFICIENCY a-Si SOLAR CELLS

5-1. Introduction

A hydrogenated amorphous silicon carbide was firstly reported by Anderson and Spear.¹⁾ Since their work, IR^{2,3,4)} and photoluminescence^{5,6)} analysis and a study in the plasma reaction mechanism⁷⁾ of undoped a-SiC:H have been given. However, any informations on the effect of impurity doping on the basic properties of a-SiC:H have not been reported. We have made efforts to control the valency electrons of wide gap materials for the purpose of improving the efficiency of p-i-n a-Si solar cells. Recently, a good valency electron controllability has been found in a hydrogenated amorphous silicon carbide prepared by the plasma decomposition of $[\text{SiH}_4(1-x) + \text{CH}_4(x)]$ gas mixture.^{8,9)}

An a-SiC:H film can be fabricated by the decomposition of silane (SiH_4) and hydrocarbon gas mixture,^{1,7)} or alkylsilane.¹⁰⁾ However, the structural and optoelectronic properties of a-SiC:H films might be significantly dependent upon both carbon sources and deposition conditions. Utilizing ethylene (C_2H_4) and methane (CH_4) as carbon sources, we have fabricated a-SiC:H films and have conducted a series of experimental investigations of the optoelectronic properties in these materials and also examined the relationship between the structural, optical and electrical properties of these films.

It has been found through these investigations that the methane based a-SiC:H is mostly constructed with tetrahedrally coordinated carbons or carbons attached with a hydrogen and is superior to the ethylene based a-SiC:H for a window material in a p-i-n a-Si solar

cell. In this paper, a series of optical and optoelectronic properties, and IR spectra of a-SiC:H films prepared by the decomposition of $[\text{SiH}_{4(1-x)} + \text{CH}_{4(x)}]$ or $[\text{SiH}_{4(1-x)} + \frac{1}{2}\text{C}_2\text{H}_{4(x)}]$ gas mixture are demonstrated and discussed with a view toward adding insight into the structural basis. The photovoltaic performances of a-SiC:H/a-Si:H heterojunction solar cells are also discussed.

5-2. Experimental Details

a-SiC:H films were prepared in the plasma deposition system as described in our previous paper¹¹⁾ by the decomposition of $[\text{SiH}_{4(1-x)} + \text{CH}_{4(x)}]$ or $[\text{SiH}_{4(1-x)} + \frac{1}{2}\text{C}_2\text{H}_{4(x)}]$. Both Corning #7059 glass and high resistive single crystal silicon wafer were used as substrates. They were subjected to standard cleaning techniques and then N_2 plasma bombardment treatment for ten minutes prior to the onset of deposition. Substrate temperature was held at 250 °C, the r.f. power was kept at 35 watts, and the total gas flow was fixed at 100 sccm. The used gas, SiH_4 , CH_4 , C_2H_4 , B_2H_6 and PH_3 were diluted with H_2 . The thicknesses of deposited films were 5000 Å for optical and optoelectronic measurements and were 10000 Å for IR measurement. IR spectra were measured by the double-beam Fourier-Transfer IR spectrometer (FT-IR, Digilab. FTC-15c) to obtain a high resolution. The blank silicon substrate was set in the reference beam.

5-3. Photoconductivity and Optical Band Gap of Undoped and Boron Doped a-SiC:H Films

The optical band gap of a-SiC:H films was determined from the straight line intercept of $(\alpha\hbar\omega)^{-1/2}$ versus $\hbar\omega$ curve at high absorption

region ($\alpha > 10^4/\text{cm}$) following the analysis of Davis and Mott.¹⁴⁾ It seems unreasonable to measure the photoconductivity of a-SiC:H films having optical band gaps ranging from 1.76 to 2.2 eV under the same monochromatic illumination. Therefore, we measured AM-1 photoconductivity (100 mW/cm^2) and also monochromatic photoconductivity under the illumination light of the wave length at which a-SiC:H film has the same optical absorption coefficient ($\alpha = 10^4/\text{cm}$). The monochromatic photoconductivity was normalized to $\eta\mu\tau$ product proposed by Zanzucchi et al.¹⁵⁾ Comparing this $\eta\mu\tau$ product with AM-1 photoconductivity among various compositional a-SiC:H films, an obvious positive correlation has been found between them.⁹⁾ From these results, it is recognized that AM-1 photoconductivity can be used as a convenient characterization tool for the optoelectronic properties of a-SiC:H films.

5-3-1 Optical and optoelectronic properties of methane based a-SiC:H films

Fig. 5-1 shows the AM-1 photoconductivity σ_{ph} and the optical band gap $E_{g.(opt)}$ of undoped and boron doped a-SiC:H films prepared by the decomposition of $[\text{SiH}_4(1-x) + \text{CH}_4(x)]$. AM-1 photoconductivity of undoped a-SiC:H films significantly decreases with increasing the methane fraction. On the other hand, boron doped one shows one or three orders of magnitude larger photoconductivity as compared with undoped one. These photoconductivity recovery effects have been similarly seen in phosphorus doped a-SiC:H films. These effects are accompanied by the decrease of ESR spin density by doping. In other word, boron or phosphorus atoms would compensate the dangling bond in

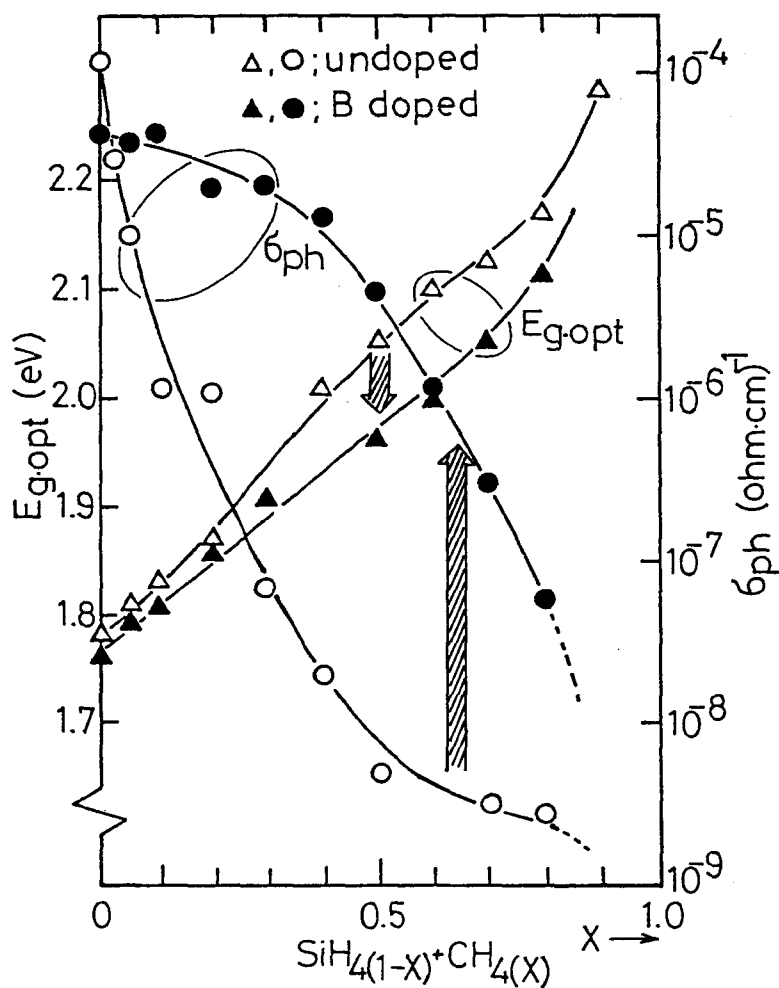


Fig. 5-1. Photoconductivity σ_{ph} and optical band gap $E_{g,(opt)}$ of undoped and boron doped a-SiC:H films prepared by the decomposition of $[SiH_4(1-x) + CH_4(x)]$ gas mixture.

amorphous SiC network and thus enhance the carrier life time.

The optical band gap of undoped and boron doped a-SiC:H increases monotonically with increasing methane fraction, but $E_{g.(opt)}$ of boron doped one is a little bit narrower than undoped one. This narrowing of $E_{g.(opt)}$ by doping is mainly caused by the decrease of hydrogen content attached to carbon.

5-3-2 Optical and optoelectronic properties of ethylene based a-SiC:H films

Fig. 5-2 shows the optical band gap $E_{g.(opt)}$ and AM-1 photoconductivity σ_{ph} of undoped and boron doped a-SiC:H films prepared by $[\text{SiH}_4(1-x) + \frac{1}{2}\text{C}_2\text{H}_4(x)]$ gas mixture. The optical band gap of these ethylene based a-SiC:H films increases from 1.76 to 2.8 eV with increasing ethylene fraction. The reason why the ethylene based a-SiC:H film shows a larger optical band gap in the same gas phase carbon fraction is that the carbon content in the ethylene based a-SiC:H film is larger than that of the methane based a-SiC:H film. It is interesting in this case that $E_{g.(opt)}$ of boron doped a-SiC:H films is larger in the gas fraction less than 0.5 and smaller in the gas fraction more than 0.5 than that of undoped a-SiC:H films. The hydrogen content attached to silicon (Si) is not affected with boron doping but the hydrogen content attached to carbon (C) is affected with boron doping, that is, these narrowing and widening effects are caused by the hydrogen attached to carbon.

In the range where the optical band gap widening occurs, the photoconductivity of boron doped a-SiC:H based on ethylene is only one order larger than that of undoped a-SiC:H. Comparing the

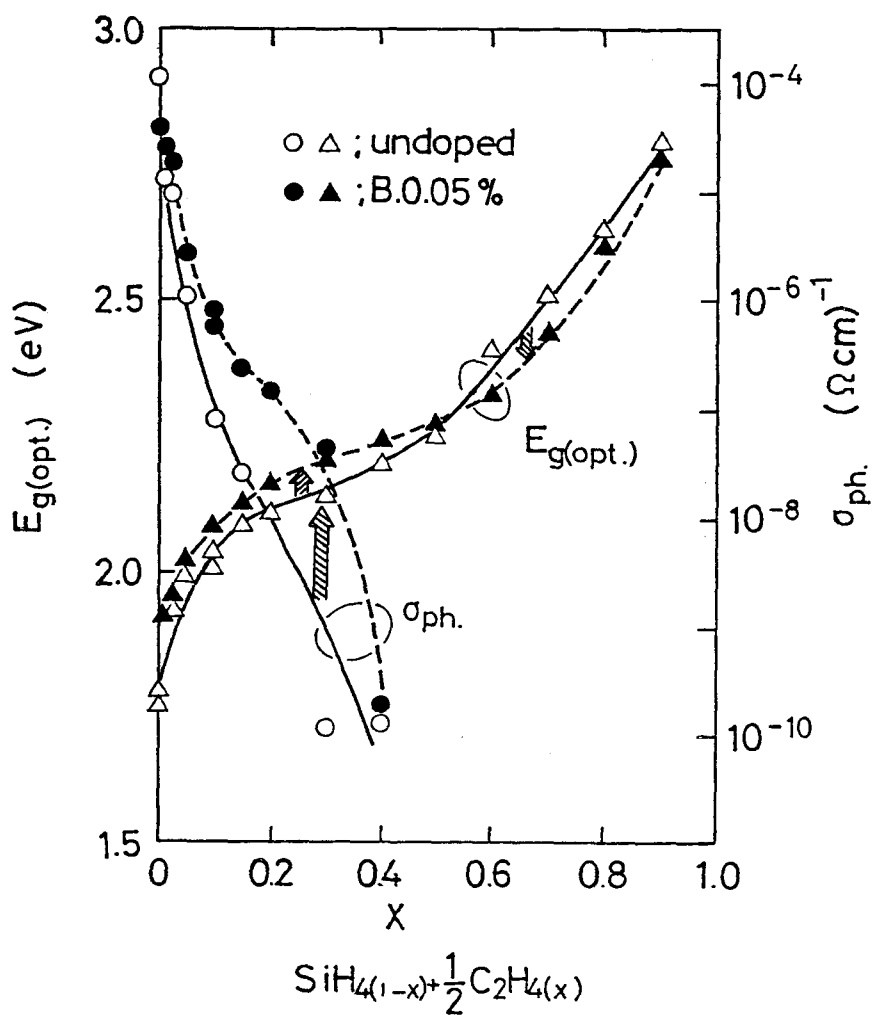


Fig. 5-2. Photoconductivity σ_{ph} and optical band gap $E_{g.(opt)}$ of undoped and boron doped a-SiC:H films prepared by the decomposition of $[SiH_{4(1-x)} + \frac{1}{2}C_2H_{4(x)}]$ gas mixture.

ethylene based a-SiC:H and the methane based a-SiC:H, it is recognized that the methane based a-SiC:H shows one or two orders larger magnitude of photoconductivity recovery effect of boron doping than the ethylene based a-SiC:H. The amount of hydrogen attached to carbon is a factor responsible for these photoconductivity recovery effect.

5-4. IR Spectra Analysis and Chemical Bonding Structure of a-SiC:H

4-4-1. IR spectra analysis of methane based and ethylene based a-SiC:H films

Methane based a-SiC:H films show one or two orders larger magnitude of photoconductivity recovery effect of boron doping than ethylene based a-SiC:H films. To understand the difference between the two, the chemical bonding structure of the methane based and the ethylene based a-SiC:H has been investigated by means of IR spectra. Fig. 5-3 shows the typical IR spectra of boron doped a-SiC:H films. The carbon content of these films might be estimated to be about 12 atm% for Auger electron spectroscopy (AES peak ratio C/Si=0.06, and crystalline SiC standard). a-SiC:H films exhibit four main absorption regions. The absorption band between 2800 and 3000 cm^{-1} is the C-H stretching mode. This absorption band is so weak that each fine peak has not been assigned yet exactly.⁴⁾ There are four peaks in the ethylene based a-SiC:H, that is, 2940, 2910, 2890 and 2870 cm^{-1} . On the other hand, the methane based a-SiC:H film shows only two peaks at 2940 and 2890 cm^{-1} . The 2940 cm^{-1} peak was assigned to the CH_3 stretching by Wieder et al.²⁾ The 2940 and 2890 cm^{-1} peaks can be attributed to CH_3 stretching, because the 1450 cm^{-1} band absorption which could be identified as $-\text{CH}_2-$ bond is seen in the ethylene based a-SiC:H film but not in the methane based

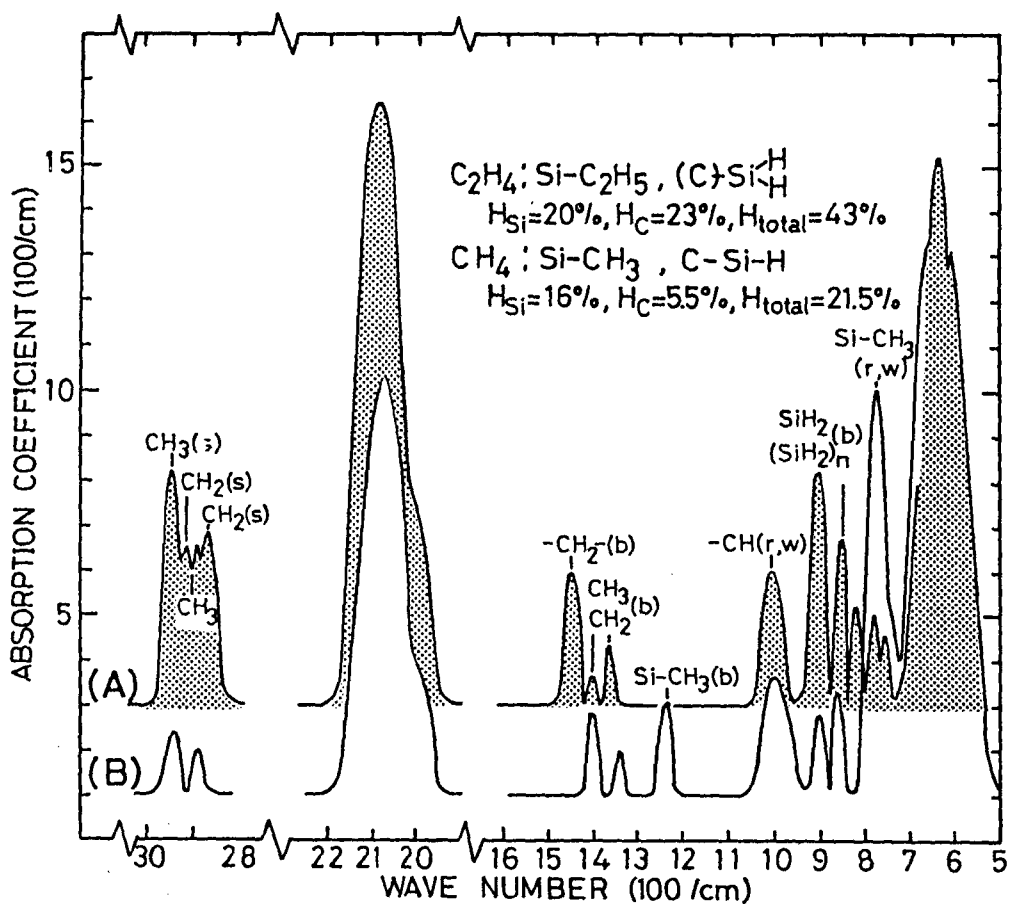


Fig. 5-3. Infra-red spectra of boron doped ethylene based a-SiC:H film (A) and boron doped methane based aSiC:H film (B).

one. While, the CH stretching absorption is very weak in general. Therefore, the 2910 and 2850 cm^{-1} peaks which are observed in ethylene based a-SiC:H might be assigned to CH_2 stretching.

The absorption band between 1500 and 1200 cm^{-1} is the CH_n bending mode. The 1450 cm^{-1} peak which is observed only in the ethylene based a-SiC:H has not been assigned yet. Owing to the analogy from alkylsilane derivatives,¹⁶⁾ the 1450 cm^{-1} peak could be identified as the $-\text{CH}_2-$ bending mode. Another typical peak is the 1250 cm^{-1} which is due to the symmetric bending mode of the CH_3 attached to silicon.²⁾ This peak can be seen only in the methane based a-SiC:H film. It is recognized through these investigations that the ethylene based a-SiC:H film does not contain the $\text{Si}-\text{CH}_3$ bonds.

The strongest feature in these spectra also occurs at 780 cm^{-1} . This peak was assigned to $\text{Si}-\text{CH}_3$ rocking or wagging mode by Wieder et al.²⁾ However, Katayama et al¹⁷⁾ concluded that this peak was assigned to Si-C stretching mode, because this peak could be seen in the sputtered a-SiC without hydrogen. In our experiment, the 780 cm^{-1} peak absorption is four times stronger in the methane based a-SiC:H ($\alpha=900/\text{cm}$) than in the ethylene based a-SiC:H ($\alpha=210/\text{cm}$). If one can assume 780 cm^{-1} to be attributed to $\text{Si}-\text{CH}_3$, this result is well consistent to that of the 1250 cm^{-1} peak.

From the facts described above, we may conclude that carbons are almost incorporated as ethyl ($-\text{C}_2\text{H}_5$) group in the ethylene based a-SiC:H and is incorporated as methyl ($-\text{CH}_3$) group in the methane based a-SiC:H. However, carbon content as $\text{Si}-\text{CH}_3$ bond in the methane based a-SiC:H is only 1 or 2 %.

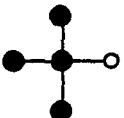

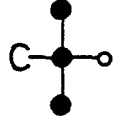

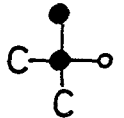

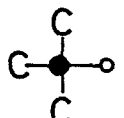
Another strong feature in these spectra can be seen at 860 - 890 cm^{-1} band which is assigned to SiH_2 or $(\text{SiH}_2)_n$ bending mode by Brodsky¹⁸⁾ and Fritzsche.¹⁹⁾ In amorphous silicon films deposited in the same chamber in the absence of carbon sources this band is too weak to detect. This absorption band can be seen in a-SiC:H films, especially in the ethylene based a-SiC:H film. This result shows that carbons promote silicon dihydride bonds in amorphous network. The 890 cm^{-1} peak absorption coefficient of the methane based and the ethylene based a-SiC:H films are 350/cm and 1100/cm, respectively, so that the ethylene based a-SiC:H film contains about three times larger content of silicon dihydride than the methane based a-SiC:H films. Corresponding to this result, the 2000 - 2100 cm^{-1} band is larger in the ethylene based a-SiC:H than in the methane based a-SiC:H film. The 2090 and 2000 cm^{-1} peaks of a-Si:H film was assigned to the SiH_2 and SiH stretching modes.^{18,19)} It is well known that the 2000 cm^{-1} peak shifts to higher wave number region by carbon attached to silicon.²⁾ This shift can be related to the electronegativity of the carbon substituent.²⁰⁾ Using the relation obtained by Lucovsky²⁰⁾ the SiH and SiH_2 stretching frequency in a-SiC:H films can thus be represented as

$$\nu_{\text{SiH}}(\text{cm}^{-1}) = 1740.7 + 34.7 \sum_{i=1}^3 X(R_i) \pm 13$$

$$\nu_{\text{SiH}_2}(\text{cm}^{-1}) = 1956.3 + 25.4 \sum_{i=1}^2 X(R_i) \pm 12$$

From these equations one can estimate the influence of the neighbouring atoms on the frequency of SiH and SiH_2 attached to one, two and three carbon atoms. The results are summarized in Table 5-1. The

Table 5-1. Calculated Si H Stretching Mode Frequency

SiH (cm^{-1})	SiH ₂ (cm^{-1})
 2013	 2092
 2054	 2119
 2095	 2149
 2135	

●=Si ○=H

2090 cm^{-1} peak is inferred any of SiH_2 , and SiH attached with one or two carbons to silicon. Considering that the carbon content of these films is rather small (AES peak ratio $\text{C/Si}=0.06$), it might be possible that the 2090 cm^{-1} peak is assigned to the stretching mode absorption of SiH attached with one carbon to silicon.

a-SiC:H films deposited at room temperature show the 2120 cm^{-1} peak which might be due to the stretching absorption of SiH_2 attached with one carbon atom to silicon. From the result of the SiH_2 bending mode absorption, it is assumed that the 2090 cm^{-1} peak in the ethylene based a-SiC:H film is contained a larger amount of SiH_2 bond ($\nu_{\text{SiH}_2} = 2090 \text{ cm}^{-1}$ and $\nu_{\text{C-SiH}_2} = 2120 \text{ cm}^{-1}$) than in the methane based a-SiC:H film.

5-4-2 Hydrogen content and chemical bonding structure of a-SiC:H films

The hydrogen content of a-SiC:H films was evaluated with the following expression.¹⁸⁾

$$N_H = A_S \int \nu \frac{\alpha(\nu)}{\nu} d\nu$$

with $A_S = 1.4 \times 10^{20} (\text{cm}^{-2})$ for SiH_n ²¹⁾ and $A_S = 1 \times 10^{21} (\text{cm}^{-2})$ for CH_n .²²⁾

The results are summarized in Fig. 5-3. The content of hydrogen attached to Si is 20 atm% and 16 atm% for the ethylene based and the methane based a-SiC:H, respectively, and the content of hydrogen attached to C is 23 atm% and 5.5 atm% for the ethylene based and the methane based a-SiC:H films, respectively. The most important feature can be seen in the carbon attached with hydrogen which is four times larger amount in the ethylene based a-SiC:H than in the

methane based one. Assuming that carbons are incorporated as C_2H_5 group in the ethylene based a-SiC:H and as CH_3 group in the methane based one, one can estimate amount of Si- C_2H_5 and Si- CH_3 bond: 9.2 atm% carbons are incorporated as $-C_2H_5$ group in the ethylene based a-SiC:H film and 1.8 atm% carbons are incorporated as $-CH_3$ group in the methane based a-SiC:H film, and other carbons (about 10 %) are incorporated as tetrahedrally bonded carbons or carbons attached with one hydrogen (C-H) in the methane based a-SiC:H. From these investigations, we propose the structural models of ethylene based and methane based a-SiC:H as shown in Fig. 5-4.

It is recognized from these investigations that the methane based a-SiC:H is a rather ideal amorphous SiC alloy in contrast to the ethylene based a-SiC:H which is an organosilane like structure. It might be basically caused by these structural difference between the two that the methane based a-SiC:H film shows one or two orders larger magnitude of photoconductivity recovery effect of doping than the ethylene based one. Furthermore, this structural difference affects the photovoltaic performances of a-SiC:H/a-Si:H heterojunction solar cells. The results are discussed in the following section.

5-5. Effect of Methane Based and Ethylene Based a-SiC:H on the Photovoltaic Performances

5-5-1. Fabrication of methane based and ethylene based a-SiC:H/a-Si:H heterojunction solar cells

The structure and the optoelectronic properties of glow discharge produced a-SiC:H films are strongly dependent upon the carbon sources as is discussed in the previous sections. To confirm a wide gap

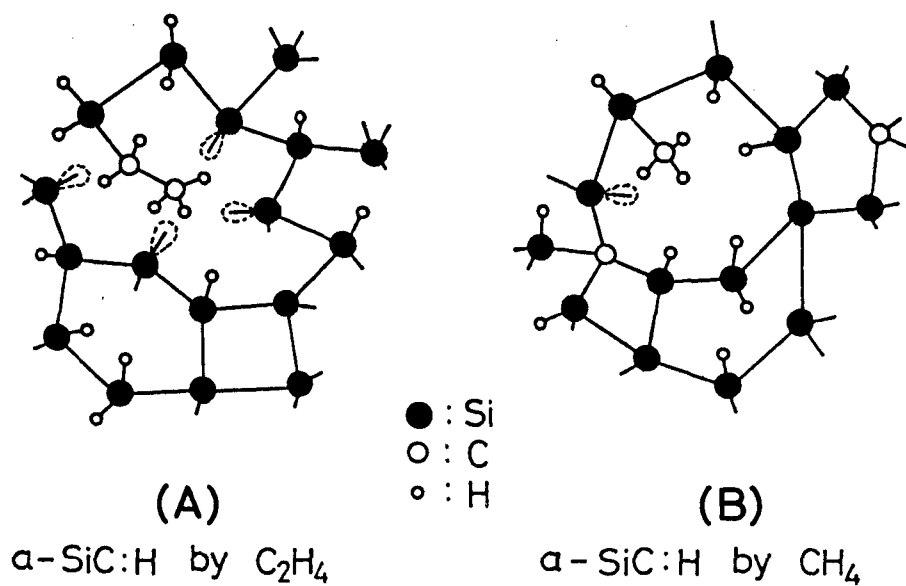


Fig. 5-4. Structural models of $\alpha\text{-SiC:H}$. (A)= ethylene based $\alpha\text{-SiC:H}$, (B)=methane based $\alpha\text{-SiC:H}$.

window effect of a-SiC:H, we have fabricated a-SiC:H/a-Si:H hetero-junction solar cells. The cell structure is glass/SnO₂/p a-SiC:H/i-n a-Si:H/Al. The substrate temperature is about 250°C, and the layer thicknesses of p a-SiC:H, undoped a-Si:H and n a-Si:H are 100, 5000 and 500 Å, respectively. The deposition conditions of undoped and phosphorus doped (PH₃/SiH₄=0.5%) a-Si:H were described in our previous report.¹³⁾ The activation energy and the conductivity of p-layer in p-i-n a-Si solar cells are generally required to be less than 0.6 eV and more than 10⁻⁷ (Ω·cm)⁻¹, respectively. Therefore, the p-type methane based and the ethylene based a-SiC:H having a band gap ranging from 1.8 to 2.2 eV were adopted, whose activation energy and conductivity were settled about 0.55 eV and on the order of 10⁻⁷(Ω·cm)⁻¹, respectively. The sensitive area of solar cells is 3.3 mm² which were carefully evaluated to be about 5 % larger than the deposited aluminum bottom electrode (3.14 mm²) by taking account of experimentally confirmed edge effects to photo-current.⁸⁾ J-V characteristics measurements were carried out under AM-1 solar illumination (100 mA/cm²).

5-5-2. Photovoltaic performances of methane based a-SiC:H/a-Si:H heterojunction solar cells

Fig. 5-5 shows the photovoltaic performances of a-SiC:H/a-Si:H heterojunction solar cells as a function of the optical band gap $E_{g.(opt)}$ of p-type methane based a-SiC:H. As is seen in this figure, not only the short circuit current density J_{sc} but also the open circuit voltage V_{oc} increase as the increase of the optical band gap of p-layer. An essential matter required to increase the

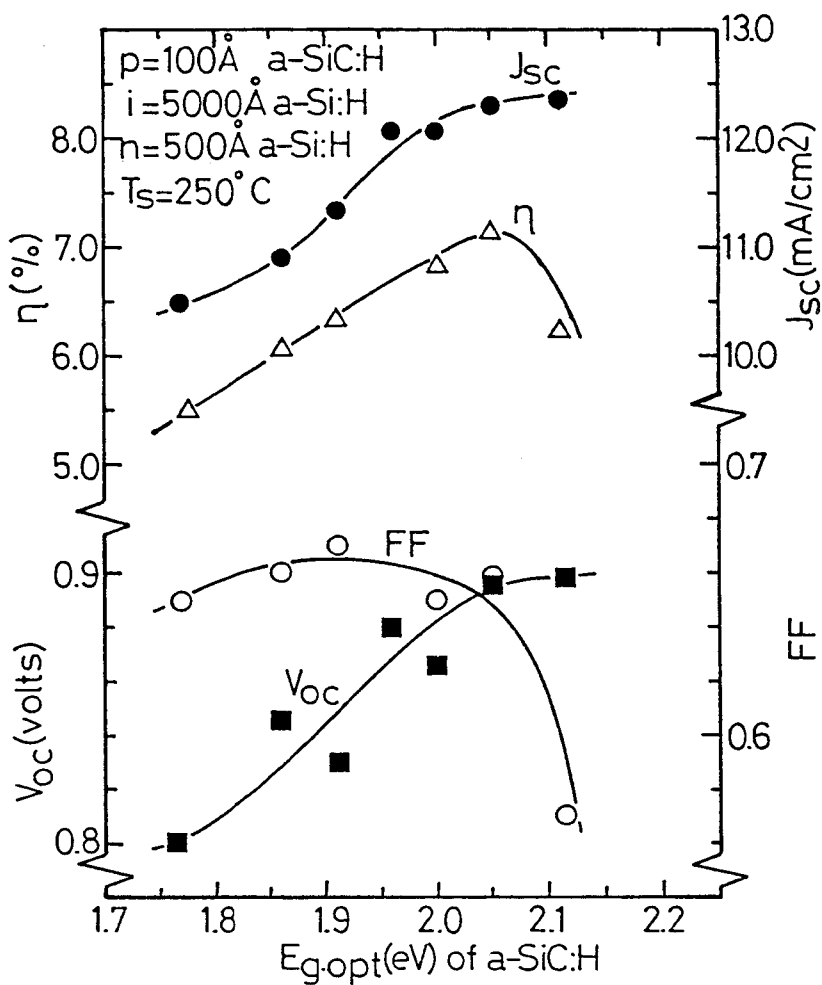


Fig. 5-5. Photovoltaic performances of methane based a-SiC:H/a-Si:H heterojunction solar cells as a function of the optical band gap $E_{g,\text{(opt)}}$ of p-type methane based a-SiC:H.

short circuit current density is to effectively introduce the incident photons into i-layer, where the photocurrent is mainly produced.²³⁾ The increase of J_{sc} is first of all due to the wide gap window of a-SiC:H. Another effect of the increased band gap in p-layer is a corresponding increase in the blocking barrier for electron at p-i interface. The alignment of conduction band in a-SiC:H/a-Si:H heterojunction structure, as shown in Fig. 5-6(A), was chosen so that the discontinuity in the band edge at p-i interface. Therefore, the back diffusion of electrons from the i-layer into p-layer might be practically blocked. This blocking barrier effect is remarkable, especially in the short wave length region of the incident photons. The experimental evidence can be seen in the collection efficiency spectra. Fig. 5-7 shows the collection efficiency data of an ordinary p-i-n a-Si:H homojunction solar cell and methane based and ethylene based a-SiC:H/a-Si:H heterojunction solar cells. The collection efficiency of this methane based heterojunction solar cell is improved by more than two times at the short wave length region as compared with the homojunction solar cell, while this improvement is only 20 % at the wave length of 550 nm. It is concluded that the increase of collection efficiency at the short wave length region is mainly caused by the blocking barrier in the p-i interface of a-SiC:H/ a-Si:H heterojunction solar cell.

The increase of the open circuit voltage is also caused by a wide gap window effect due to the potential profile steepened with a wide gap a-SiC:H. This point will be discussed later.

5-5-3. Photovoltaic performances of ethylene based a-SiC:H/a-Si:H heterojunction solar cells

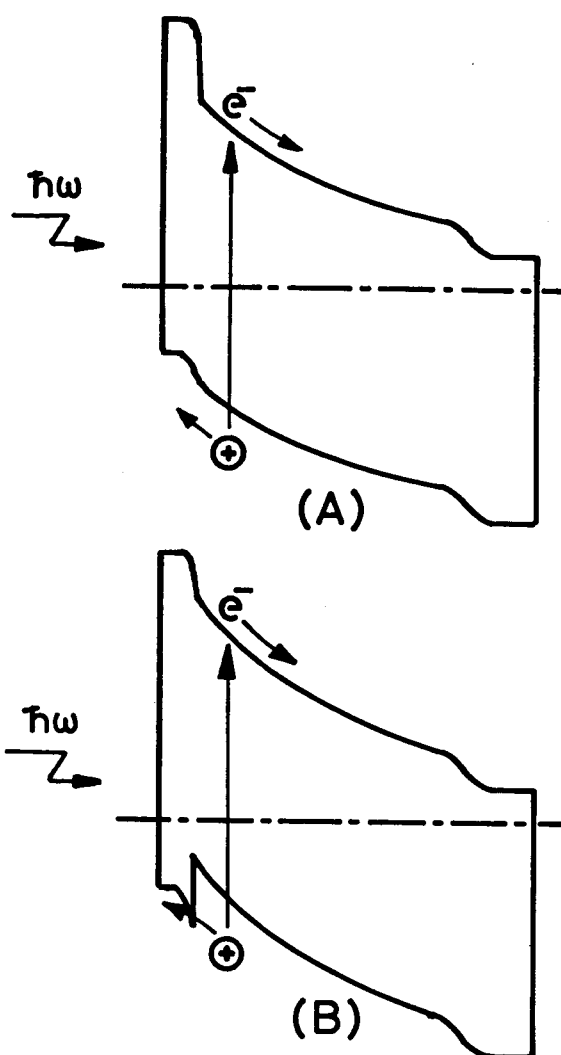


Fig. 5-6. Schematic band profile of p-i-n heterojunctions. (A)=methane based a-SiC:H/a-Si:H heterojunction, (B)=ethylene based a-SiC:H/a-Si:H heterojunction.

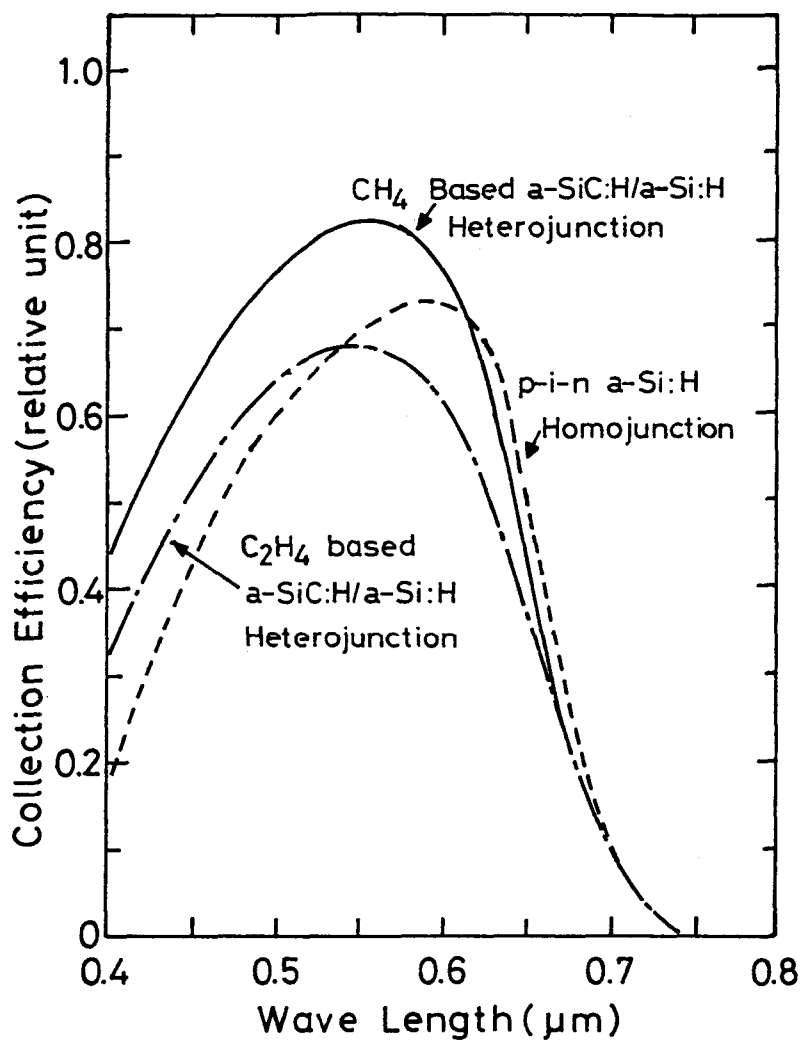


Fig. 5-7. Collection efficiency of an ordinary p-i-n a-Si:H homojunction solar cell and a typical a-SiC:H/a-Si:H heterojunction solar cell.

5-5-3. Photovoltaic performances of ethylene based a-SiC:H/a-Si:H heterojunction solar cells

Fig. 5-8 shows the photovoltaic performances of a-SiC:H/a-Si:H heterojunction solar cells as a function of the optical band gap $E_{g.(opt)}$ of the ethylene based a-SiC:H. In spite of the optical band gap increase of p-layer, the short circuit current density J_{sc} of these cells is smaller in the range from 1.9 to 2.13 eV than that of the p-i-n a-Si:H homojunction solar cell ($E_{g.(opt)}=1.76$ eV). In the ethylene based a-SiC:H/a-Si:H heterojunction cell, it seems that a energy spike exists at the p-i interface in valence band edge as shown in Fig. 5-6(B). Because holes could not traverse freely into p-layer, the photocurrent might be limited in the ethylene based a-SiC:H/a-Si:H heterostructure. Collection efficiency spectrum of ethylene based a-SiC:H/a-Si:H heterojunction solar cell, as is seen in Fig. 5-7, suggests an existence of energy spike at p-i interface.

The distinction of the photocurrent between the methane based and the ethylene based a-SiC:H/a-Si:H heterojunction solar cell may be due to the structural difference as is discussed above, and it comes to the conclusion that wide gap amorphous materials are not always useful as a window side junction material and the structure of these materials is an important factor for the junction formation.

5-5-4. Voltage factor of a-SiC:H/a-Si:H heterojunction solar cells

As for the voltage factor of a-SiC:H/a-Si:H heterojunction solar cells, we found a clear correlation between the open circuit voltage V_{oc} and the diffusion potential V_d in the methane based a-SiC:H/a-Si:H heterojunction solar cells.^{13, 24)} In the ethylene

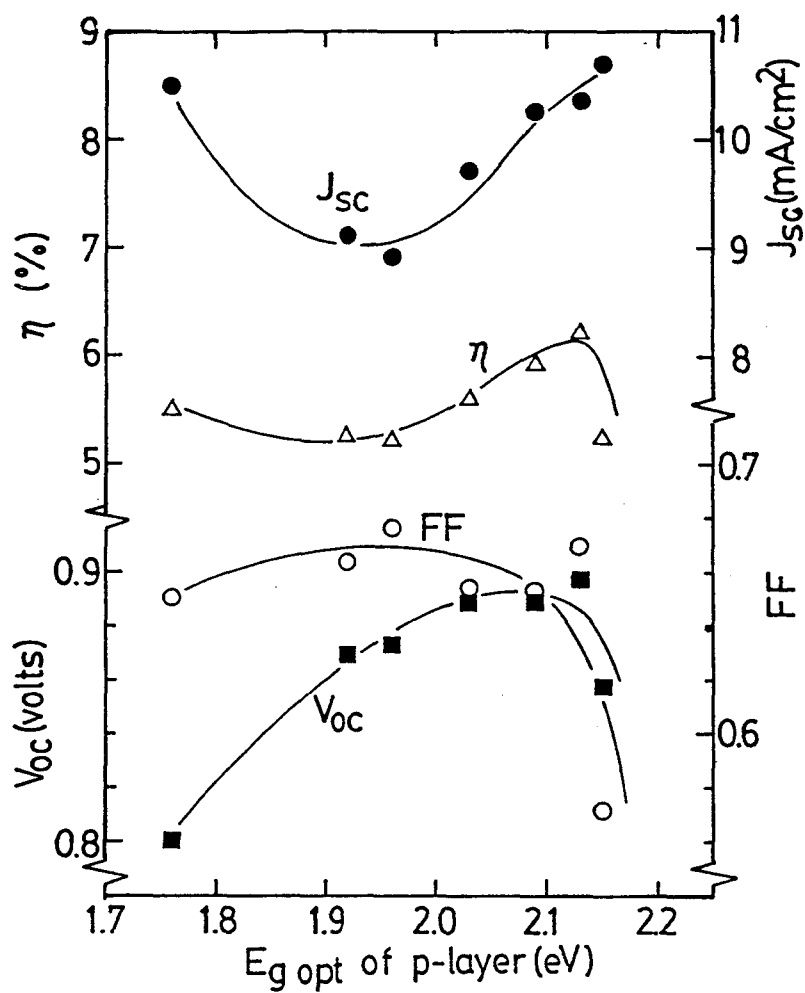


Fig. 5-8. Photovoltaic performances of ethylene based a-SiC:H/aSi:H heterojunction solar cells as a function of the optical band gap $E_{g, \text{(opt)}}$ of p-type ethylene based a-SiC:H.

based a-SiC:H/ aSi:H heterostructure, the open circuit voltage increases as the increase of the optical band gap of the ethylene based a-SiC:H. The same correlation can also be seen in this case, as shown in Fig. 5-9. The diffusion potential V_d can be changed with controlling the doping fraction and the r.f. power in the deposition of p-layer. The open circuit voltage of these cells is plotted on the same correlation between V_{oc} and V_d .

The chemical structure of a-SiC:H depends upon a carbon source, doping fraction and preparation condition. Therefore, the voltage factor might be independent on the structure of a-SiC:H, and the correlation between V_{oc} and V_d is consistent in general. It is recognized experimentally from this correlation that 1/3 of the increased diffusion potential contributes to the increase of the open circuit voltage of solar cell.

5-5-5. Typical J-V characteristics of a-SiC:H/a-Si:H heterojunction solar cells

It has been found through these investigations that the methane based a-SiC:H film is a rather ideal amorphous SiC alloy and is superior to the ethylene based one as a window material. Fig. 5-10 shows the typical photovoltaic performances of the methane based and the ethylene based a-SiC:H/a-Si:H heterojunction solar cells which were obtained on the same substrate. The performances of the methane based a-SiC:H/a-Si:H cell are $\eta=7.82\%$, $J_{sc}=13.76\text{ mA/cm}^2$, $V_{oc}=0.903\text{ volts}$ and $FF=62.9\%$. On the other hand, the performances of the ethylene based a-SiC:H/a-Si:H cell are $\eta=6.21\%$, $J_{sc}=10.34\text{ mA/cm}^2$, $V_{oc}=0.897\text{ volts}$ and $FF=67.0\%$. As is seen in these data,

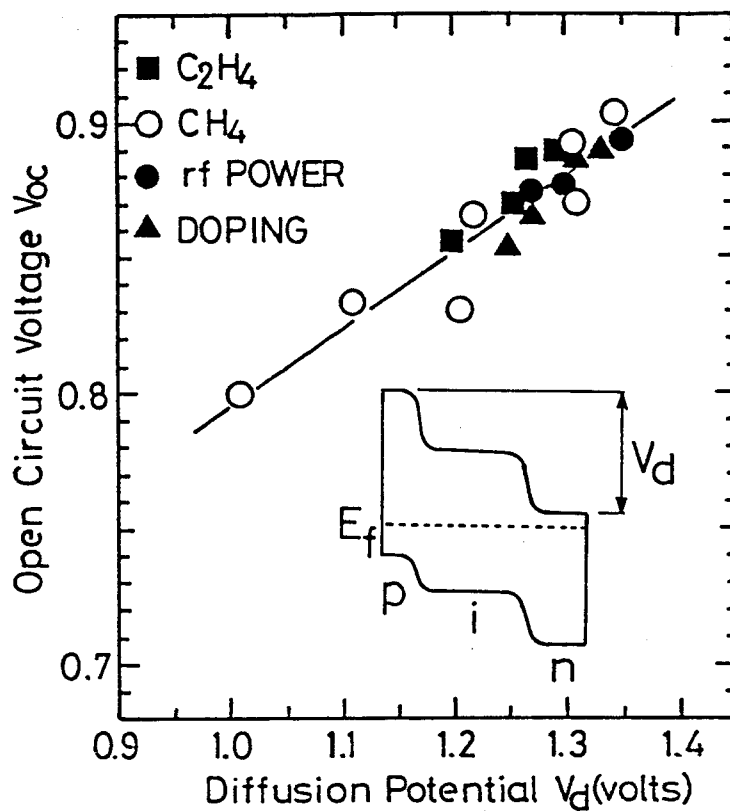


Fig. 5-9. Correlation between the open circuit voltage V_{oc} and the diffusion potential V_d of a-SiC:H/a-Si:H heterojunction solar cells as parameters of carbon sources, r.f. power of p-layer deposition and doping fraction of p-layer.

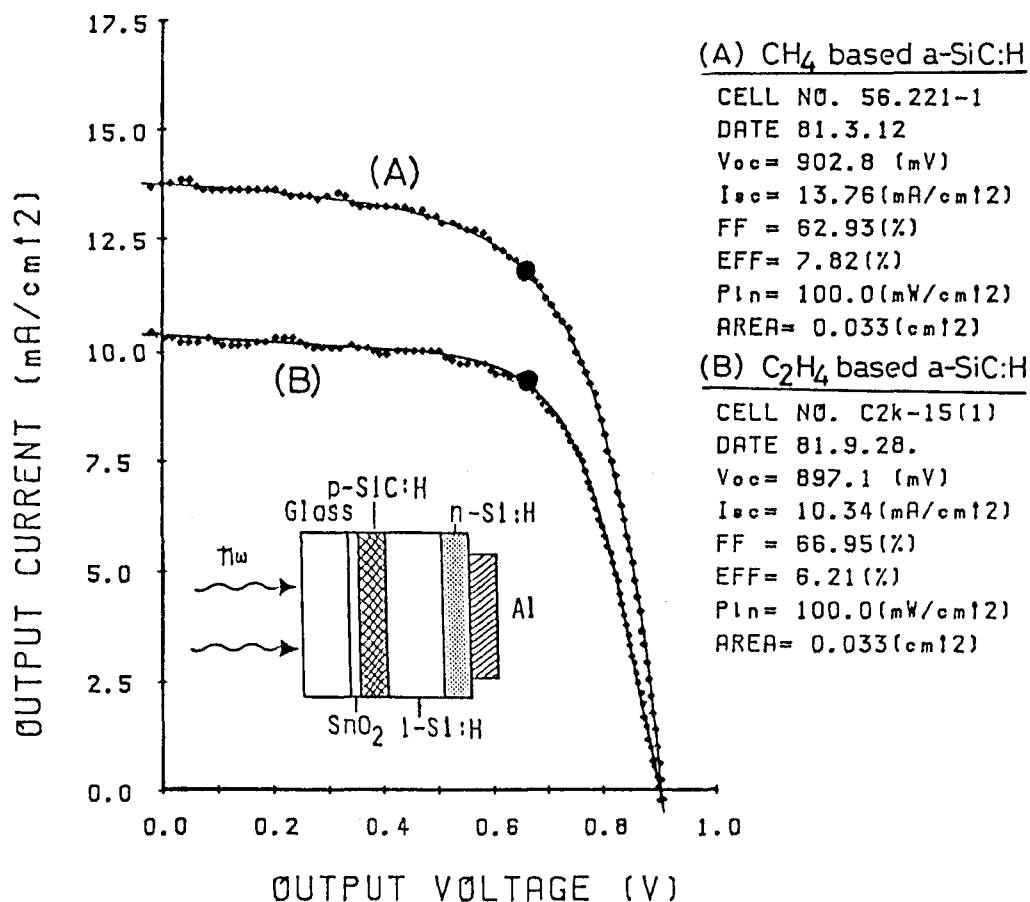


Fig. 5-10. J-V characteristics of a methane based a-SiC:H/a-Si:H heterojunction solar cell (A) and an ethylene based a-SiC:H/a-Si:H heterojunction solar cell (B) with the glass/ SnO_2 substrate. sensitive area= 3.3 mm^2 , $p_{in}=100 \text{ mW/cm}^2$. (A); $V_{oc}=0.903 \text{ volts}$, $J_{sc}=13.76 \text{ mA/cm}^2$, $FF=62.9\%$ and $\eta=7.82\%$. (B); $V_{oc}=0.897 \text{ volts}$, $J_{sc}=10.34 \text{ mA/cm}^2$, $FF=67.0\%$ and $\eta=6.21\%$.

the J_{sc} of the methane based a-SiC:H/a-Si:H heterojunction cell is 33 % larger than the J_{sc} of the ethylene based one.

5-6. Discussion and Summary

Amorphous SiC:H films which have a wide band gap can be fabricated by the plasma decomposition of silane and hydrocarbon gas mixture. However, the optoelectronic properties and the chemical structure of a-SiC:H films might be significantly dependent upon both carbon sources and deposition conditions. The optical band gap can be controlled in the range from 1.8 to 2.2 eV by controlling the gas fraction of $[SiH_{4(1-x)} + CH_{4(x)}]$ and also from 1.8 to 2.8 eV by controlling the gas fraction of $[SiH_{4(1-x)} + \frac{1}{2}C_2H_{4(x)}]$. We have conducted a series of experimental studies of the optoelectronic properties in the methane based and the ethylene based a-SiC:H films, and also examined the relationship between the chemical structure, and the electrical and optical properties of these a-SiC:H films.

The photoconductivity of undoped a-SiC:H films sharply decreases with increasing the carbon fraction. On the other hand, the methane based a-SiC:H films show one or three orders larger magnitude of photoconductivity recovery effect of boron doping. In contrast with this, the ethylene based a-SiC:H films show only one order larger magnitude of photoconductivity recovery effect of boron doping. The photoconductivity recovery effect has been seen also in a phosphorus doped a-SiC:H film, and it is recognized from ESR measurements that this effect is caused by the decrease of ESR spin density; boron and phosphorus atoms compensate the dangling bonds in a-SiC:H network.

The boron doping on the methane based a-SiC:H gives rise to the narrowing of the optical band gap. On the other hand, the boron doping on the ethylene based a-SiC:H give rise to the widening of the optical band gap in the carbon gas phase fraction range less than 0.5 and the narrowing of the optical band gap in the carbon gas phase fraction more than 0.5. These narrowing and widening effects of boron doping are mainly caused by the hydrogen attached to carbon.

To confirm the origin of the optical and optoelectronic differences between the methane based and the ethylene based a-SiC:H films, the chemical structure of these a-SiC:H films has been investigated by IR spectra. It is recognized from the investigation of C-H stretching and bending mode absorption that the ethylene based a-SiC:H film contains $-C_2H_5$ group and the methane based a-SiC:H film contains $-CH_3$ group. On the other hand, the content of hydrogen attached to Si can be estimated to be 20 atm.% and 16 atm.% for the ethylene based and the methane based a-SiC:H, respectively, and the content of hydrogen attached to C can be estimated to be 23 atm.% and 5.5 atm.% for the ethylene based and the methane based a-SiC:H, respectively. Assuming that carbons are incorporated as $-C_2H_5$ group for the ethylene based a-SiC:H and as CH_3 group for the methane based a-SiC:H, we can estimate the Si- C_2H_5 bond and the Si- CH_3 bond: 9.2 % carbons are incorporated as the $-C_2H_5$ group in the ethylene based a-SiC:H, and 1.8 % carbon are incorporated as the $-CH_3$ group in the methane based a-SiC:H. The carbon content of these films might be estimated to be about 12 atm.% from the Auger Electron Spectroscopy (AES peak ratio C/Si=0.06, and crystalline SiC standard). Therefore, carbon atoms are mostly incorporated as $-C_2H_5$

group in the ethylene based a-SiC:H which has a large amount of SiH₂ bond. On the other hand, 1.8 atm.% carbons are incorporated as -CH₃ group and other carbons are incorporated as tetrahedrally bonded atoms in the methane based one. It is recognized from these results that the methane based a-SiC:H is a rather ideal tetrahedrally bonded amorphous SiC alloy in contrast to the ethylene based a-SiC:H which has an organosilane like structure. It might be caused by this structural difference that the methane based a-SiC:H shows one or two orders larger magnitude of photoconductivity recovery effect of doping than the ethylene based a-SiC:H.

To confirm the wide gap window effect of these a-SiC:H films, we fabricated a-SiC:H/a-Si:H heterojunction solar cells. In the methane based a-SiC:H/a-Si:H cell, not only the short circuit current density but also the open circuit voltage increases as the increase of the optical band gap of p-layer. An essential matter required to increase the short circuit current density is to effectively introduce the incident photons into an i-layer, where the photocurrent is mainly produced. The increase of J_{sc} is first of all due to the wide gap window of a-SiC:H. Another effect of a-SiC:H is a corresponding increase in the blocking barrier for electron at p-i interface. The alignment of conduction band in a-SiC:H/a-Si:H heterojunction structure was chosen so that the discontinuity in the band edge at p-i interface. Therefore, the back diffusion of electrons from the i-layer to p-layer might be practically blocked. This experimental evidence can be seen in the collection efficiency, especially in the short wave length region. The collection efficiency of the methane based a-SiC:H/a-Si:H cell is improved to be more than two times at

the short wave length region as compared with that of an a-Si:H p-i-n homojunction cell, while this improvement is only 20 % at the wave length of 0.55 μm .

On the other hand, the short circuit current density of the ethylene based a-SiC:H/a-Si:H cell is smaller in the optical band gap of p-layer ranging from 1.9 to 2.13 eV than the a-Si:H p-i-n homojunction cell, in spite of the wide gap p-layer. In this case, it seems that the energy spike might exist at the p-i interface in the valence band edge and holes could not traverse freely into p-layer. The distinction of the short circuit current density between the ethylene based and the methane based a-SiC:H as a window material may be due to the difference of the chemical bonding structure between the two, as is discussed above. It comes to the conclusion that wide gap materials are not always useful as a window material for p-i-n a-Si solar cells and the chemical bonding structure of these materials is an important factor for junction formation.

As for the voltage factor of a-SiC:H/a-Si:H heterojunction solar cells, we have found a clear correlation between the open circuit voltage and the diffusion potential both in the methane based and the ethylene based a-SiC:H/a-Si:H heterojunction cells. The diffusion potential of these cells can be changed with controlling the doping fraction or the r.f. power in the deposition of p-layer. In this case, this correlation is consistent. Therefore, the voltage factor might be independent on the chemical bonding structure, and it is recognized from this correlation that 1/3 of the increased diffusion potential contributes the increase of the open circuit voltage.

It has been found through these systematic investigations that the methane based a-SiC:H film is a rather ideal amorphous SiC alloy and is superior to the ethylene based one as a window material.

REFERENCES

- 1) D. A. Anderson and W. E. Spear: *Phil. Mag.* 35 (1977) 1.
- 2) H. Wieder, M. Cardona and C. R. Guarnieri: *Phy. Stat. Sol. (b)* 92 (1979) 99.
- 3) A. Guivarch, J. Richard, M. LeContellec, E. Ligeon and J. Fontenille, *J. Appl. Phys.* 51 (1980) 2167.
- 4) Y. Catherine and G. Turban: *Thin Solid Films* 70 (1980) 101.
- 5) D. Engemann, R. Fischer and J. Knecht: *Appl. Phys. Lett.* 32 (1978) 567.
- 6) R. S. Sussmann and R. Ogden: *Phil. Mag.* B44 (1981) 137.
- 7) Y. Catherine, G. Turban and B. Grolleau: *Thin Solid Films* 76 (1981) 23.
- 8) Y. Tawada, H. Okamoto and Y. Hamakawa: *Appl. Phys. Lett.* 39 (1981) 237.
- 9) Y. Tawada, M. Kondo, H. Okamoto and Y. Hamakawa: *Proc. 9th International Conf. on Amorphous and Liquid Semiconductors, Grenoble (1981)* and *J. de Physique* 42 (1981), suppl. 10, C4-471.
- 10) H. Munekata, S. Murasato and H. Kukimoto: *Appl. Phys. Lett.* 37 536.
- 11) Y. Tawada, T. Yamaguchi, S. Nonomura, S. Hotta, H. Okamoto and Y. Hamakawa: *Jpn. J. Appl. Phys.* 20, suppl. 20-2 (1981) 219.
- 12) Y. Tawada, M. Kondo, H. Okamoto and Y. Hamakawa: *Proc. 15th IEEE Photovoltaic Specialists Conf., Florida (1981)* p245.
- 13) Y. Tawada, M. Kondo, H. Okamoto and Y. Hamakawa: *Proc. 13th Conf. on Solid State Devices, Tokyo (1981)* published as *Jpn. J. Appl. Phys.* 21 (1982) suppl. 21-1, 297.
- 14) E.A. Davis and N. F. Mott: *Phil. Mag.* 22 (1970) 903.

- 15) P. J. Zanzuchi, C. R. Wronski and D. E. Carlson: J. Appl. Phys. 48 (1977) 5227.
- 16) K. M. Mackay and R. Watt: Spectrochimica Acta 23A (1967) 2761.
- 17) Y. Katayama and T. Shimada: Jpn. J. Appl. Phys. 19 (1980) suppl. 19-2, 115.
- 18) M. H. Brodsky, M. Cardona and J. J. Cuomo: Phys. Rev. B16 (1977) 3556.
- 19) C. C. Tsai and H. Fritzsche: Solar Energy Mat. 1 (1979) 29.
- 20) G. Lucovsky: Solid State Commun. 29 (1979) 571.
- 21) C. J. Fang, K. J. Gruntz, L. Ley and M. Cardona: J. Non-Cryst. Solids 35 & 36 (1980) 255.
- 22) F. Fujimoto, A. Otsuka, K. Komaki, S. Hashimoto, I. Yamane, H. Yamashita, K. Osawa, Y. Tawada, M. Kondo, H. Okamoto and Y. Hamakawa: Jpn. J. Appl. Phys. Letter (to be published).
- 23) H. Okamoto, Y. Nitta, T. Yamaguchi and Y. Hamakawa: Solar Energy Mat. 2 (1980) 313.
- 24) Y. Tawada, M. Kondo, H. Okamoto and Y. Hamakawa: Solar Energy Mat. 6 (1982) 299.

VI OPTIMIZATION OF a-SiC:H/a-Si:H HETEROJUNCTION SOLAR CELLS

6-1. Introduction

Since Carlson and Wronski first developed an amorphous silicon solar cell in 1976,¹⁾ remarkable progress has been seen in both material science and fabrication technology.²⁾ As a result, the efficiency of a-Si solar cell has been sharply improved: announced conference records are 8.04% with a-SiC:H/a-Si:H heterojunction cells,³⁾ 7.8% with inverted p-i-n cells⁴⁾, 7.7% with a-Si:H/a-SiGe:H tandem cells⁵⁾ and 6.6% with a-Si:F:H MIS cells.⁶⁾

The p-i-n a-Si solar cell might provide better reproducibility as well as being amenable to mass production and design control when put into practical application.⁷⁾ However, the p-i-n cell has one deficiency, that is, a large ineffective optical absorption in the p-layer which has a narrow optical band gap with a high density of nonradiative recombination centers.⁸⁾ Because of this ineffective absorption in the p-layer, the short circuit current density decreases with increasing p-layer thickness contrary to the increase of the open-circuit voltage. Therefore, there exists an optimum thickness of the p-layer in the p-i-n a-Si solar cell, that is, about 80Å.⁹⁾ The ineffective absorption in the p-layer can be estimated to be about 12% at a wave length of 5000Å even if the thickness of p-layer is only 80Å. If the optical absorption coefficient of p-side window material can be reduced to less than 1/10 of that of a-Si:H, this ineffective absorption might become negligibly small and the incident photon flux into an i-layer would increase.

Recently, we have found a good valency electron controllability

in a hydrogenated amorphous silicon carbide (a-SiC:H) prepared by the plasma decomposition of $[\text{SiH}_{4(1-x)} + \text{CH}_{4(x)}]$ gas mixture.^{10, 11, 12)} Using the valency electron controlled a-SiC:H as a window side junction material, a-SiC:H/a-Si:H heterojunction solar cells have been developed.^{13, 14)} Through the optimizations of the preparation conditions and the chemical bonding structure of a-SiC:H, the efficiency of the a-SiC:H/a-Si:H heterojunction solar cell has been improved to be from 6.1%¹⁰⁾ to 7.55%.^{11, 14)} There are several problems to be solved for the further improvement of the efficiency of a-SiC:H/a-Si:H heterojunction solar cells. One of them is related to a transparent electrode and the interface between it and a p-layer. For example, the reflection loss, the reduction of transparent electrode by active hydrogen and the diffusion of reduced elements into p-layer might make some significant affects on the cell performances. The other factors which should be taken into account are in the deposition conditions of p-layer and the design parameters of a-SiC:H/a-Si:H heterojunction cells. In this chapter, a series of experimental investigations on the deposition conditions and the design parameters of a-SiC:H/a-Si:H heterojunction solar cells are presented, mainly in a view point of the interface between the transparent electrode and amorphous layers. Moreover, the actual process how an 8% efficiency barrier has been broken through with an a-SiC:H/a-Si:H heterojunction structure is demonstrated.

6-2. Optimization of Deposition Conditions

6-2-1. rf power dependence

Properties of a-SiC:H films are also influenced by the rf power as well as a-Si:H films.¹⁰⁾ Deposition of a-SiC:H is more complicated than that of a-Si:H, because reactivity of CH₄ is different from that of SiH₄. Carbon content in a-SiC:H films is changed by the deposition conditions, especially by the rf power.

Figure 6-1 shows the rf power dependence of the basic properties in boron doped a-SiC:H films. Gas phase composition in this case is fixed as [SiH₄(0.3) + CH₄(0.7)]. The optical band gap $E_{g(opt)}$ slightly increases with increasing the rf power. The activation energy ΔE also increases and the dark conductivity σ_d sharply decreases as the increase of rf power. This result means that the doping efficiency would decrease with increasing the rf power. Carbon content in these films increases from 6 to 18 atm% with increasing rf power from 25 to 75 watts, as shown in Fig. 6-2. The increase of optical band gap $E_{g(opt)}$ is mainly due to the increase of carbon content in the film. The change of doping efficiency is also influenced by the increase of carbon content.

The performances of p-i-n cells are dependent upon the activation energy and the conductivity of p-layer. Therefore, we examined the influence of p-layer deposition conditions on the performances of a-SiC:H/a-Si:H heterojunction solar cells. Figure 6-3 shows the summary of the results as a function of rf power during the p-layer deposition. The gas phase composition of p-layer is fixed at [SiH₄(0.3) + CH₄(0.7)]. The deposition conditions of i- and n-layer are also fixed. As is seen in this figure, the short circuit current density J_{sc} increases with increasing rf power. This

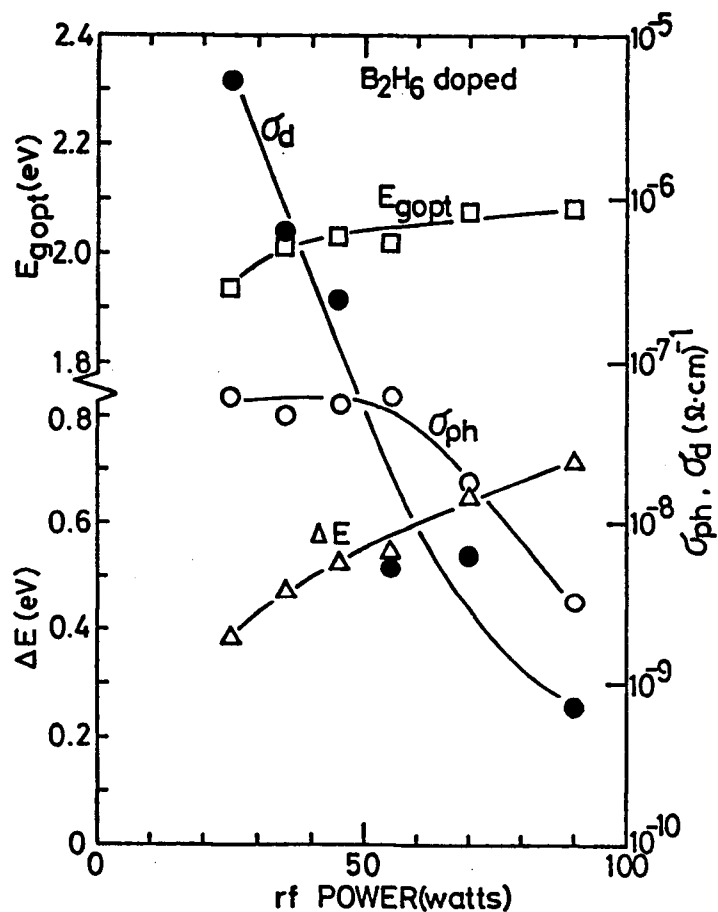


Fig. 6-1. rf power dependence on the film properties of boron doped $a-SiC:H$ prepared by the decomposition of $[SiH_{4(0.3)} + CH_{4(0.7)}]$.

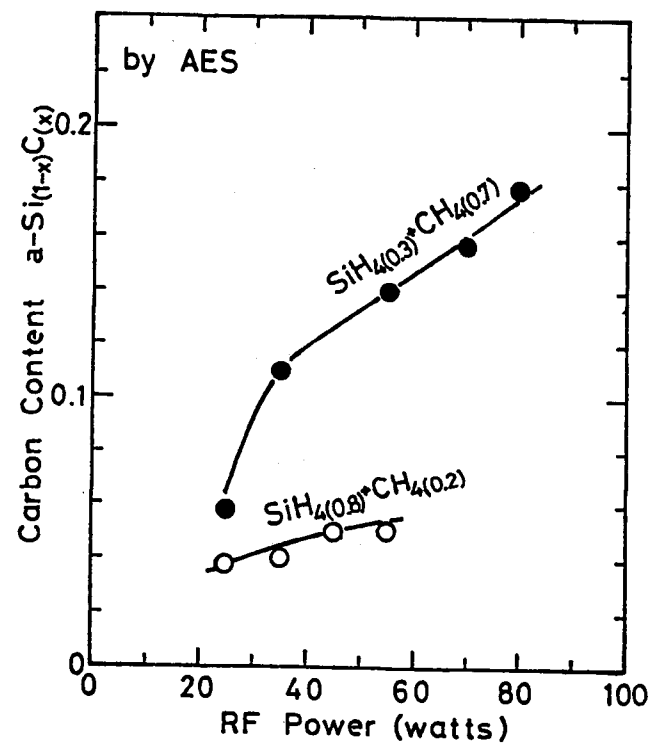


Fig. 6-2. Change of carbon content in $a-SiC:H$ films as a function of rf power.

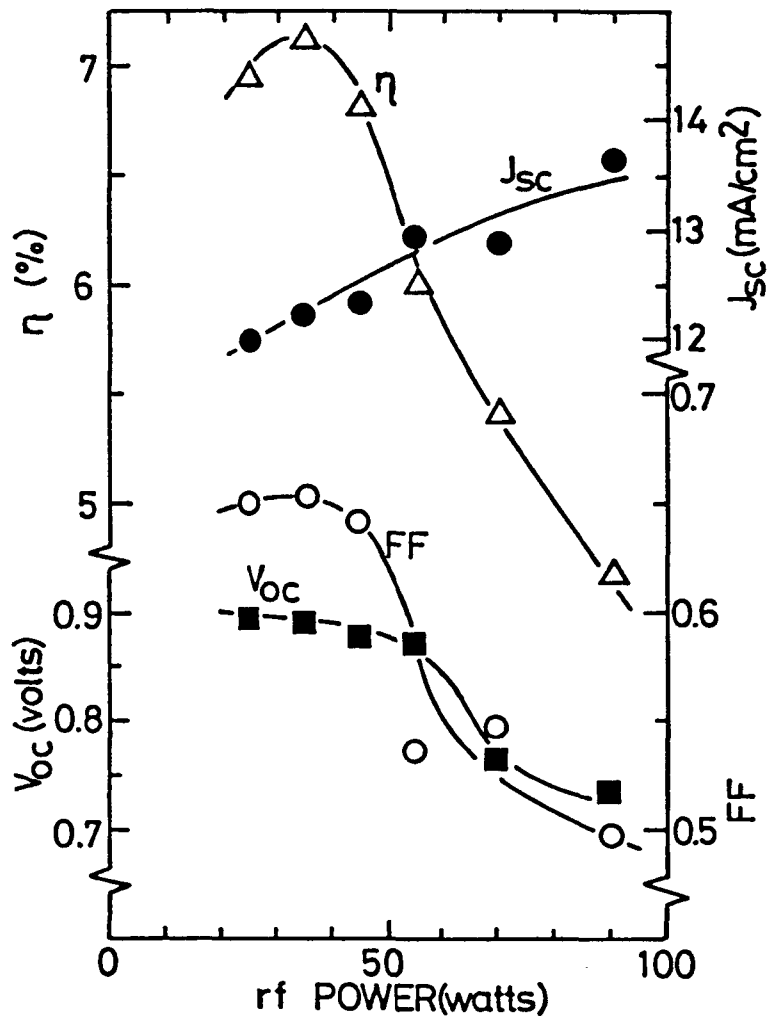


Fig. 6-3. Dependence of p-type a-SiC:H layer on the photovoltaic performances of a-SiC:H/a-Si:H heterojunction solar cells as a function of rf power in p-layer deposition.

increase of J_{sc} is caused by the increase of $E_{g(opt)}$ of p-layer. On the other hand, the open circuit voltage V_{oc} decreases with increasing the rf power. The open circuit voltage V_{oc} depends on the diffusion potential.¹⁴⁾ As the Fermi level of withdraws from the valence band as the increase of rf power, the diffusion potential of p-i-n heterojunction decreases with increasing the rf power during p-layer deposition. The fill factor FF decreases at the rf power of more than 45 watts because of the increase of series resistance of p-layer. From these results, it is recognized that the most desirable rf power of p-layer deposition is near 35 watts.

6-2-2. Substrate temperature dependence

Figure 6-4 shows the substrate temperature dependence on the basic properties of p-type a-SiC:H films. The gas phase composition and the rf power in this case are fixed at $[SiH_4(0.3) + CH_4(0.7)]$ and 35 watts, respectively. The photoconductivity σ_{ph} shows the maximum value at the substrate temperature T_s of 250°C. On the other hand, the dark conductivity σ_d shows the peak value at the $T_s = 280^\circ C$. The optical band gap $E_{g(opt)}$ decreases from 2.13 eV to 1.93 eV with increasing the substrate temperature from 215°C to 300°C. It is expected from this result that the short circuit current density of a-SiC:H/a-Si:H solar cells might decrease by 15 % with increasing the substrate temperature from 215°C to 300°C. The activation energy ΔE also decreases from 0.6 eV to 0.55 eV. However, the change of the optical band gap is larger than that of the activation energy. It is expected from this result that higher open circuit voltage might be obtained at the lower substrate temperature. While, fill factor might decrease with decreasing the substrate temperature.

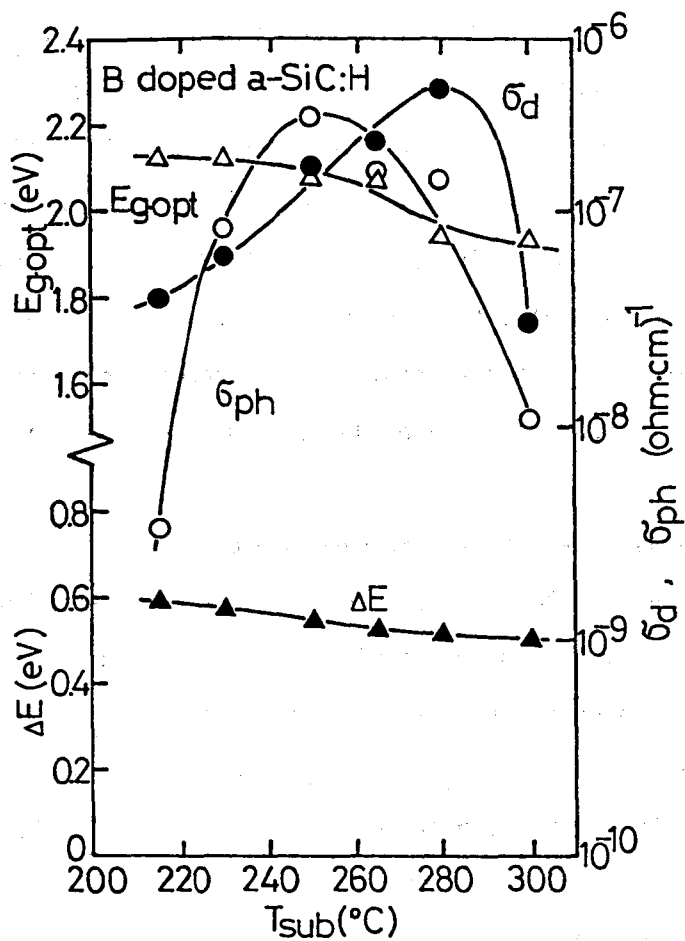


Fig. 6-4. Basic properties of boron doped a-SiC:H films as a function of substrate temperature.

To confirm these forecasts, the substrate temperature dependence on the cell performances has been checked. Figure 6-5 shows the performances of a-SiC:H/a-Si:H heterojunction cells as a function of substrate temperature. As is seen in this figure, the fill factor FF increases and the open circuit voltage V_{oc} decreases with increasing substrate temperature. These results are consistent with above mentioned considerations. However, the short-circuit current density J_{sc} significantly decreases as the increase of the substrate temperature contrary to the expectation. As the optical band gap $E_{g(opt)}$ of a-SiC:H deposited at $T_s=300^\circ\text{C}$ is 1.93 eV, J_{sc} of solar cell deposited at $T_s=300^\circ\text{C}$ is expected to be 11.4 mA/cm^2 . On the contrary, the observed J_{sc} of solar cell deposited at $T_s=300^\circ\text{C}$ is 9.3 mA/cm^2 . The difference between the expected value of J_{sc} and the observed one of solar cells deposited at high substrate temperature originates in the active hydrogen reduction of transparent electrode and the diffusion of reduced element. Figure 6-6 depth profiles near the interface between the transparent electrode (SnO_2) and the p-layer which was deposited at the substrate temperature from 200 to 300°C with a thickness of 100 \AA . As can be seen in this figure, higher the substrate temperature is, larger the diffusion of reduced Sn and the interface region are near the interface between SnO_2 and p-layer. It is recognized that the reduction reaction from SnO_2 to metallic Sn in the plasma and the diffusion of reduced Sn are accelerated by a higher substrate temperature. As the optical transparency of SnO_2 layer decreases with increasing surface reduction of SnO_2 and diffusion region of reduced Sn, the short-circuit current density of solar cell sharply might decrease with increasing the substrate

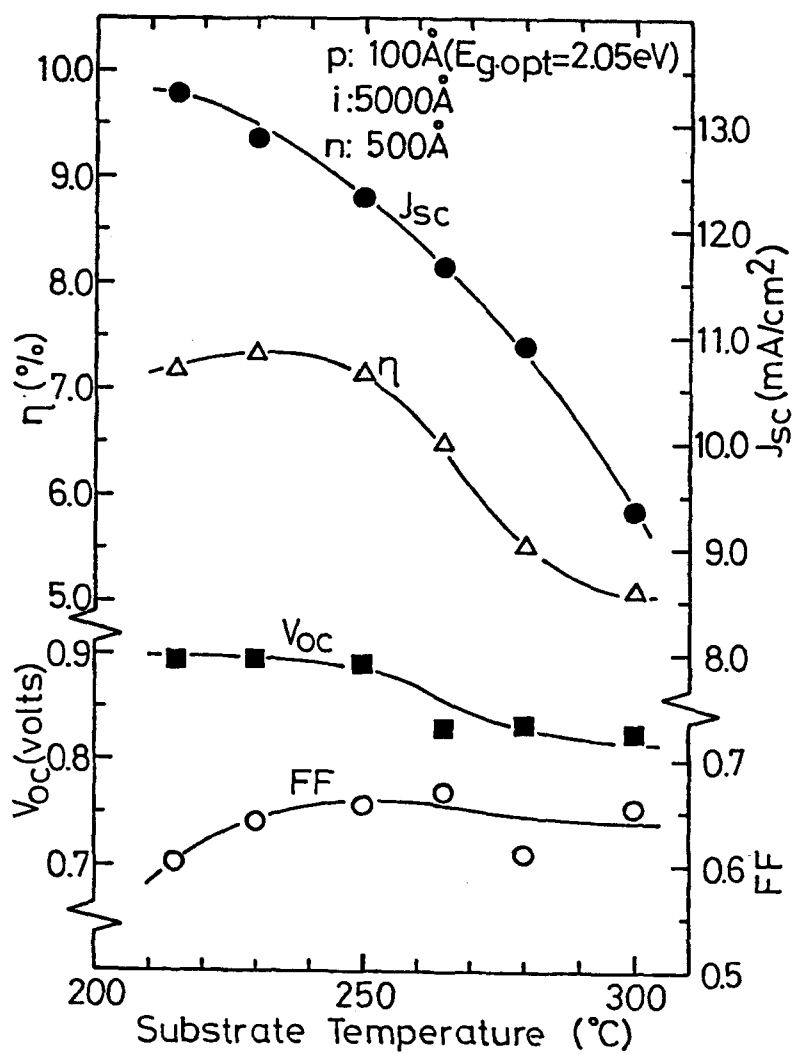


Fig. 6-5. Substrate temperature dependence on photovoltaic performances of a-SiC:H/a-Si:H heterojunction solar cells

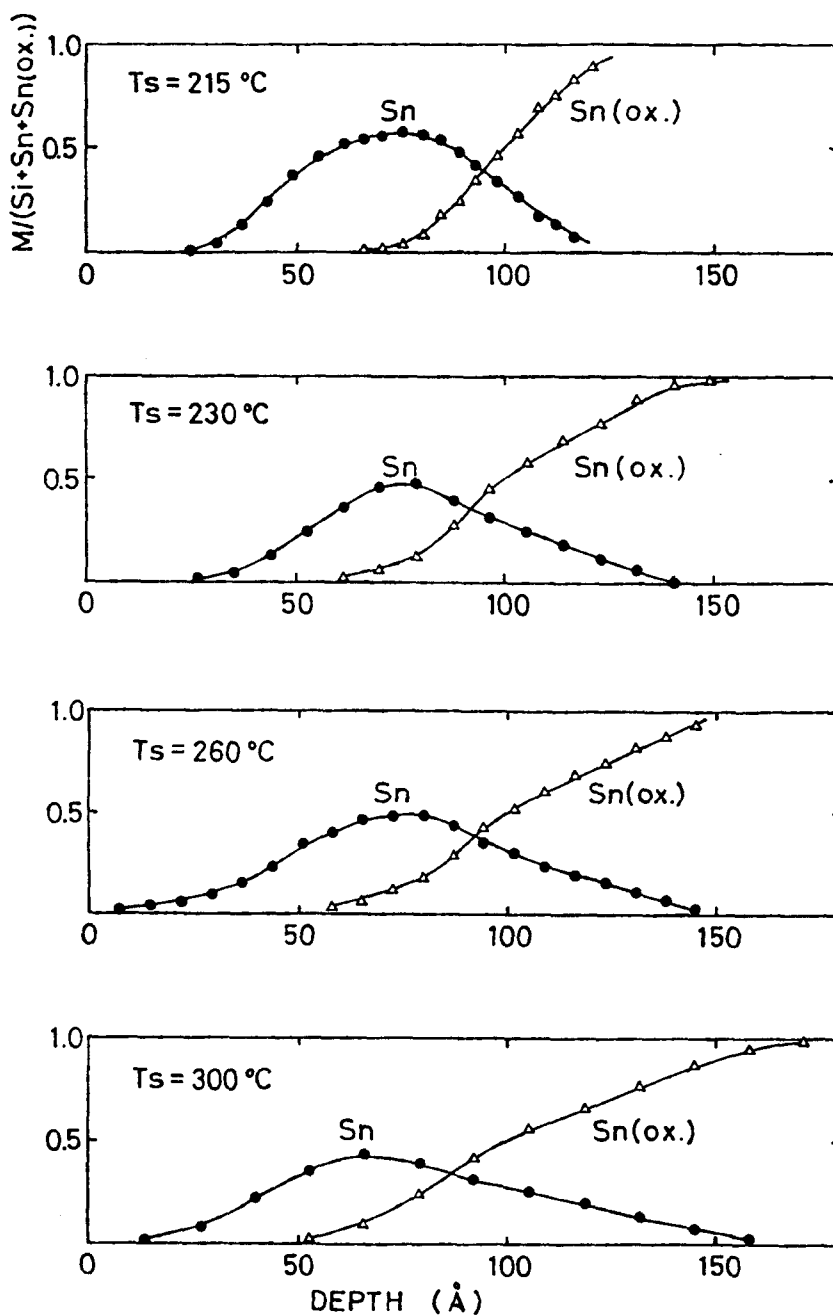


Fig. 6-6. Depth profiles of reduced Sn and oxidized Sn near the interface between SnO_2 layer and p-SiC:H as a parameter of substrate temperature.

temperature. From these results, the optimum substrate temperature is about 230°C at the present stage of the experiments.

6-3. Optimization of Design Parameters of a-SiC:H/a-Si:H Heterojunction Solar Cells

6-3-1. i-layer thickness

Carbon sources, p-layer thickness and deposition conditions of p-type a-SiC:H have been optimized.^{15, 16)} In the p-i-n a-Si solar cell, the i-layer has one of the most important roles not only as an efficient photocarrier generator on the basis of large photoconductivity but also as a carrier separator and a separated carrier accelerator by the diffused built-in field.¹⁷⁾ This point in the roles of i-layer is quite different from the case of single crystalline p-n junction photovoltaic cells where the regions defined by the minority carrier diffusion length in both sides of the junction act as photocurrent generators, and a contribution from the transition region to the photocurrent is usually negligibly small. Therefore, size factors for the determination of i-layer thickness would be width of the region where the built-in field is present and also the diffusion length of the carriers.¹⁸⁾ However, one another restriction for the width of the i-layer in a-Si:H solar cells is an effect of series resistance. That is, the thicker i-layer yields the lowering of J_{sc} and the fill factor FF. Fortunately, these restrictions on the i-layer thickness based upon the remaining finite density of states, short diffusion length of carriers and series resistance effect could be, to some extent, saved by a very short photon penetration depth^{19, 20)} of the order of 1 μm owing to the large absorption coefficient. From

these reasons, optimal thickness of i-layer in p-i-n a-Si homojunction cell has been found at 5000Å.¹⁰⁾ In an a-SiC:H/a-Si:H heterojunction structure, the incident photon flux into i-layer and the internal electric field are enhanced as compared with a-Si:H p-i-n homojunction structure, so that the optimum thickness of i-layer is expected to be larger than that of a-Si:H homojunction structure.

A series of experimental investigations for the effect of i-layer thickness on the photovoltaic performances has been carried out. The substrate temperature of each layer is fixed at 230°C. The layer thicknesses of p- and n-layer are also fixed at 100Å and 500Å, respectively. Figure 6-7 shows a summary of V_{oc} , J_{sc} , FF and η of a-SiC:H/a-Si:H heterojunction solar cells as a function of i-layer thickness. As is seen in the figure, the highest conversion efficiency is obtained at the i-layer thickness of about 6500Å.

From this optimization, the efficiency of a-SiC:H/a-Si:H heterojunction cell is improved to 7.8 %.¹⁵⁾ While, an ordinary p-i-n a-Si:H homojunction cell exhibited the efficiency of 5.7 %.¹⁰⁾ Figure 6-8 shows J-V characteristics of this a-SiC:H/a-Si:H heterojunction cell and an ordinary p-i-n homojunction cell for the comparison. The performances of an a-SiC:H/a-Si:H heterojunction cell is $\eta=7.82\%$, $V_{oc}=0.903$ volts, $J_{sc}=13.76$ mA/cm² and FF=62.9 %. On the other hand, the efficiency of an ordinary p-i-n a-Si:H homojunction cell is 5.7 % with $V_{oc}=0.801$ volts, $J_{sc}=11.02$ mA/cm² and FF=64.7 %. As is seen in these data, the performances of an a-SiC:H/a-Si:H heterojunction cell are clearly improved by 24.9 % in J_{sc} , 13.7 % in V_{oc} and 37 % in η as compared with an ordinary p-i-n a-Si:H homojunction cell. These remarkable improvements of J_{sc} and V_{oc} are caused by the wide gap

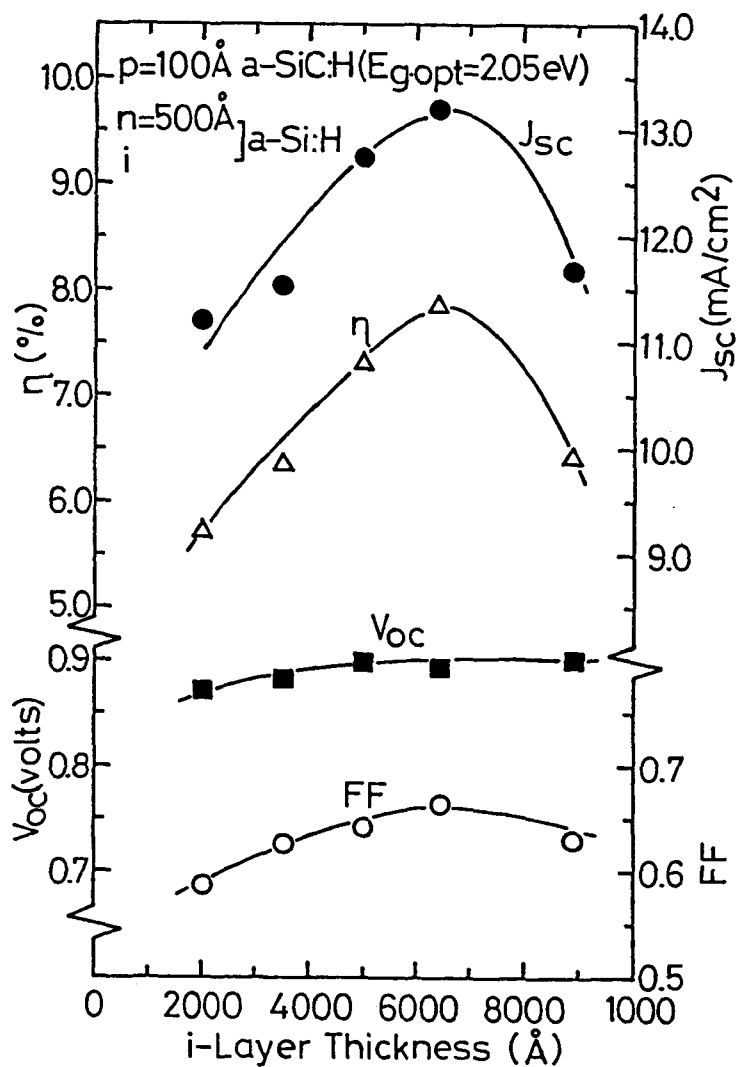


Fig. 6-7. Photovoltaic performances of a-SiC:H/a-Si:H heterojunction solar cells as a function of the i-layer thickness.

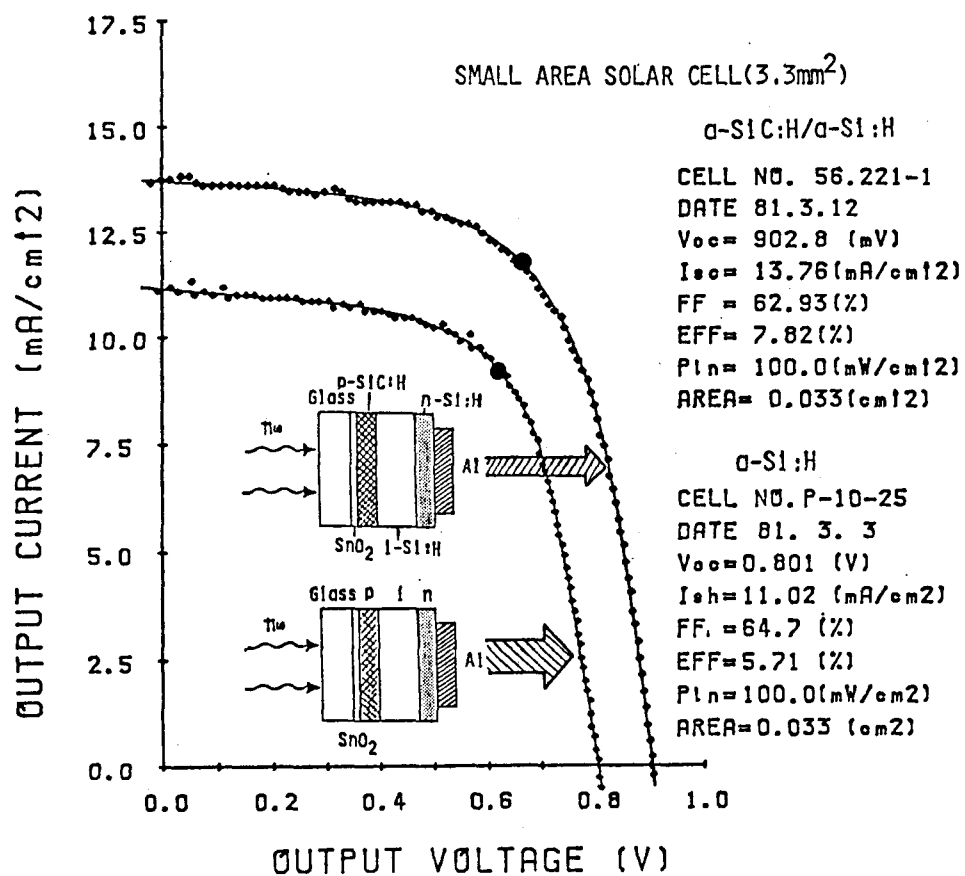


Fig. 6-8. J-V characteristics of (A) a-SiC:H/a-Si:H hetero-junction solar cell and (B) a-Si:H homojunction solar cell.

effects of a-SiC:H, that is, the decrease of ineffective absorption in the p-layer and the increase of the diffusion potential in the p-i-n junction.

6-3-2. Interface between p-layer and transparent electrode

Further improvement of the efficiency necessitates at least well controlled junctions and definite contacts.²¹⁾ Indium thin oxide (ITO) and thin oxide (SnO_2) are very popular transparent electrode. The former one has a low resistivity, but the latter one has a high resistivity. As the low resistivity is necessary to reduce the series resistance in p-i-n cell, glass/ITO substrate is superior to glass/ SnO_2 substrate. However, a solar cell on glass/ SnO_2 shows a higher open circuit voltage than a solar cell on glass/ITO.²²⁾ To analyse this phenomenon, surface analysis such as Auger electron spectroscopy (AES) have been carried out in combination with the ion sputter-etching technique to determine depth distribution of In and Sn near the interface between the transparent electrode and amorphous layer.

Four types of transparent electrode were investigated; Indium thin oxide (ITO), polished ITO, thin oxide (SnO_2) and SnO_2 coated ITO. Glass substrates coated with transparent electrodes were set on the rotating holder and p-layer was deposited on each substrate. Figure 6-9 shows AES spectra for a p-layer (100\AA)/ SnO_2 specimen with different sputtering time (or depth). Two types of Sn (MNN) spectra were observed and from additional examination these peaks are due to the chemical shift and assigned as reduced Sn (428 and 434 eV) and oxidized Sn (422 and 428 eV). It is possible to separately determine the depth profiles of reduced Sn and SnO_2 diffused into p-layer

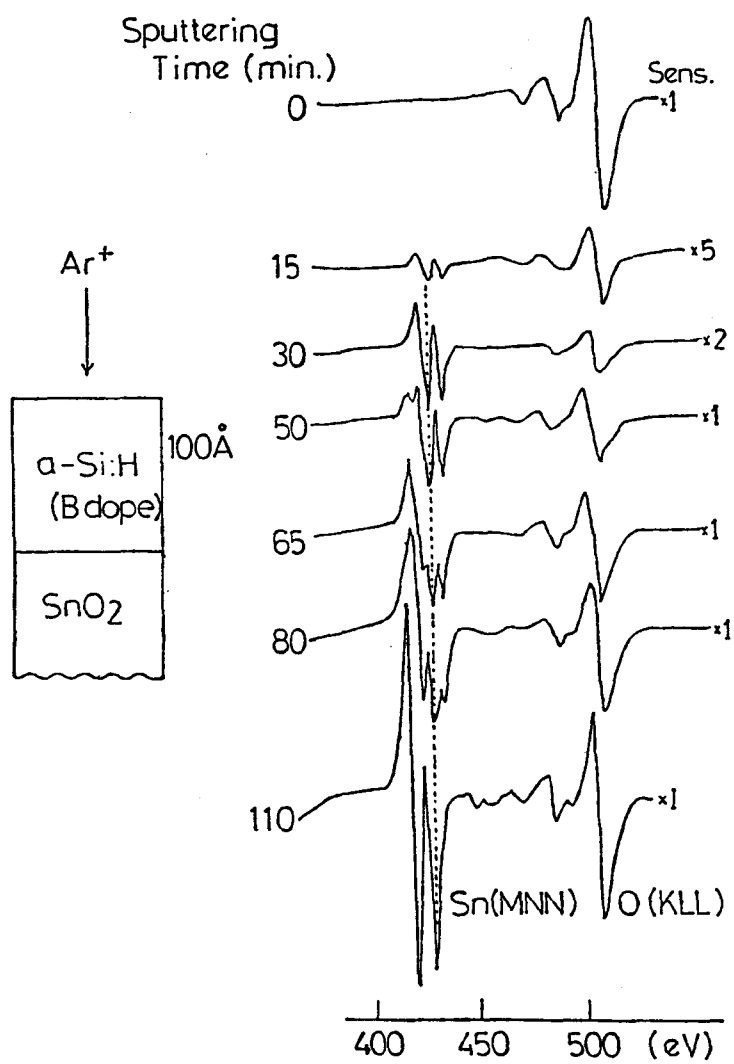


Fig. 6-9. Auger electron spectroscopy (AES) spectra of p-layer (100 Å)/SnO₂ as a parameter of sputtering time

utilizing this chemical shift. Figure 6-10 shows depth profiles of reduced Sn and oxidized Sn with p-layer thickness of 50 and 100 Å. As is seen in this figure, SnO₂ is reduced to metallic Sn which diffuses to p-layer and SnO₂ layer. This reduction is mainly caused by the presence of active hydrogens which are plentifully produced by the plasma decomposition of H₂ or SiH₄. Such a visible chemical shift is not observed in ITO, however the ratio of O/(O+In) reflects this situation of In whether in the reduced or oxidized state. Figure 6-11 shows depth profiles of In and O/(O+In) ratio with 50, 100 and 100 Å of p-layer. Indium also diffuses into p-layer and O/(O+In) ratio in diffusion region is so small. These diffusions of In or Sn influences the cell performances.

Table 6-1 shows the performances of a-SiC:H/a-Si:H heterojunction solar cells deposited on different transparent electrode/glass substrate. There exists an obvious difference in open-circuit voltage. SnO₂ substrate shows a higher open-circuit voltage than

Table 6-1. V_{oc} and η of solar cell deposited on SnO₂, ITO, polished ITO and SnO₂/ITO glass substrate

Electrode	Thickness (Å)	V_{oc} (volts)	η (%)
SnO ₂	2500	0.844	6.37
ITO	1000	0.768	5.64
ITO(polished)	800	0.752	4.93
SnO ₂ /ITO	100/1000	0.840	6.83

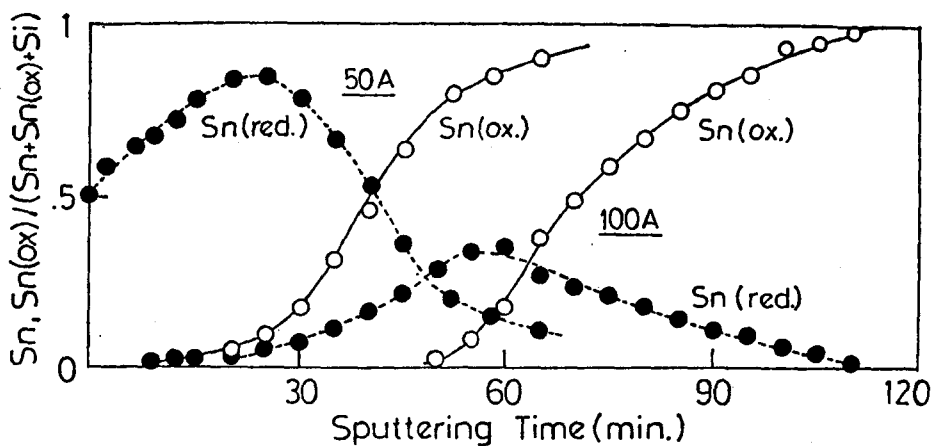


Fig. 6-10. Depth profiles of reduced and oxidized Sn near the interface between p-layer (50 and 100 Å)/SnO₂ as a function of sputtering time.

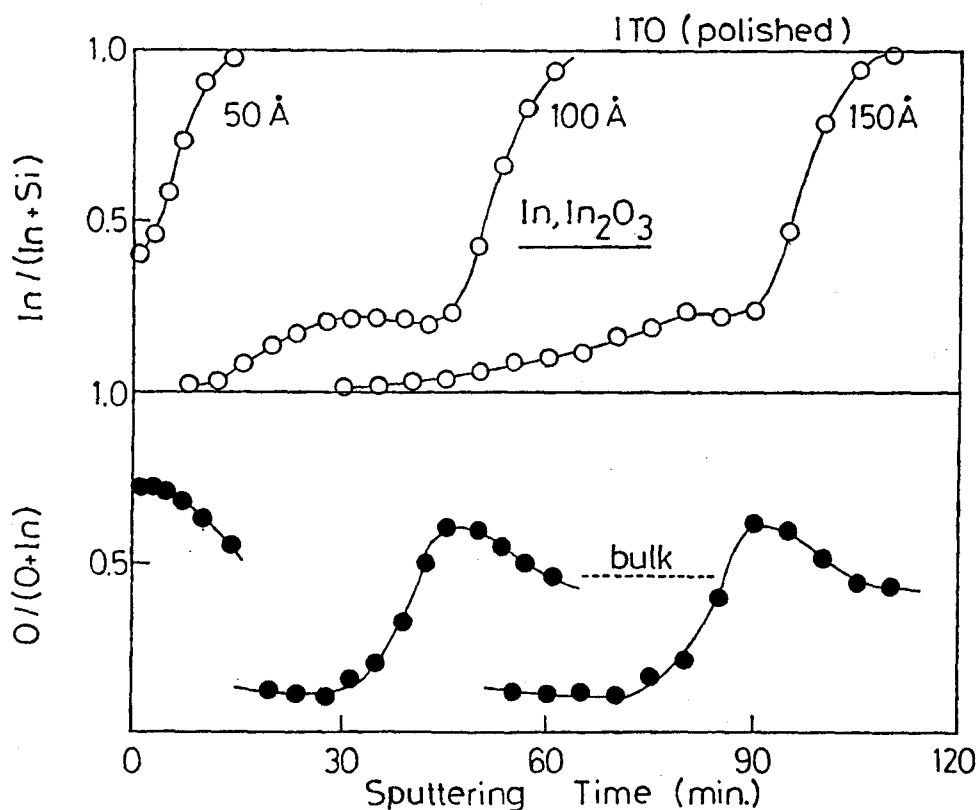


Fig. 6-11. Depth profiles of In and O/(O+In) ratio near the interface between p-layer (50, 100 and 150 Å)/ITO as a function of sputtering time.

ITO substrate. From this result it is recognized that the diffusion of reduced In into p-layer results in harmful influences on cell performances, but Sn does not. In and Sn occupy the coordination numbers of 3 and 4, respectively, so that the diffused In into p-layer might act as electron acceptors. As a result, the enhanced diffusion potential of p-i-n heterojunction might increase the open-circuit voltage. However, the result contradicts this explanation. On the other hand, the SnO_2 seems to be chemically stronger than the ITO. The difference of the open-circuit voltage between the solar cells on SnO_2 and ITO substrate was explained by the chemical resistivity. But, our results show that there is no difference of the chemical resistivity between SnO_2 and ITO in the cell fabrication process.

In order to examine the reason why the open-circuit voltage of the solar cells depends upon the transparent electrode, the X-ray photoemission spectroscopy measurement has been carried out on 100 Å p-layer/transparent electrode. The XPS signal of Si_{2p} is a transition from Si_{2p} to Fermi-level of semiconductor. If the Fermi-level of p-layer is shifted by the diffused Sn and In into p-layer, the change of XPS signal might be observed.

Fig. 6-12 shows the binding energy of Si_{2p} in the p-layer deposited on ITO and SnO_2 substrate determined by XPS method. The binding energy of p-layer deposited on ITO is larger by 0.3 eV than that of p-layer deposited on SnO_2 . The result means that the Fermi-level of p-layer deposited on ITO shifts to the conduction band by 0.3 eV comparing with that of p-layer deposited on SnO_2 and consequently, the diffusion potential of p-i-n junction deposited on ITO is smaller by 0.3 eV than that deposited on SnO_2 . From the corre-

Fermi-Level Shift
Observed by XPS

Structure SnO_2 or ITO / $\alpha\text{-Si:H}$ (150 Å)
B-dope 0.05%

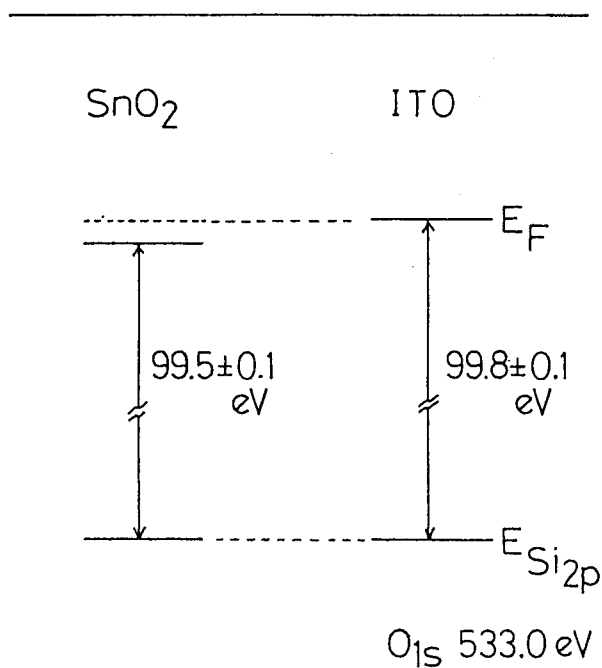


Fig. 6-12. Binding energy from Si_{2p} to Fermi-level of p-layer on SnO_2 and ITO determined by XPS method.

lation between V_{oc} and V_d , as shown in Fig. 5-9, the open-circuit voltage of p-i-n junction deposited on IT0 can be predict to be smaller by about 0.1 volt than that deposited on SnO_2 . The experimental result is just consistent with the above mentioned prediction. That is, it is clearly shown that the diffused methallic In to p-layer acts as the electron donars. From these systematic work, two approaches can be possible to improve the open-circuit voltage; one approach is how to reduce the reduction of IT0, and another one is how to suppress the diffusion of metallic In into p-layer.

I have made some experimantal trials to suppress the reduction of IT0. One of my approaches is to make IT0 which could not be reduced by active hydrogens. IT0 is fabricated by several methods: electron beam evaporation (EB), O_2 plasma assisted EB and sputter (SP). Table 6-2 shows the performances of a-SiC:H/a-Si:H heterojunction solar cells deposited on these substrates. As is seen in this

Table 6-2. Photovoltaic performances of solar cells deposited on EB IT0, O_2 plasma assisted EB IT0 and SP IT0 substrate.

	sheet R ohm/	thickness Å	J_{sc} mA/cm ²	V_{oc} volts	FF %	η %
SnO_2	25	2500	11.67	0.874	61.4	6.26
EB IT0	20	1800	11.7	0.810	60.7	5.75
EB O_2 IT0	20	1380	12.52	0.836	59.5	6.23
EB O_2 IT0	35	860	13.83	0.827	55.4	6.33
SP IT0	40	1280	10.69	0.815	58.2	5.07

table, the open-circuit voltage is influenced by fabrication methods of ITO, and O_2 plasma assisted EB ITO shows a higher open-circuit voltage than other ITO. These results indicate the open-circuit voltage is not dependent upon elements of transparent electrode but upon reduced In. In view of hydrogen reduction, O_2 plasma assisted EB ITO is better material as a transparent electrode.

Another approach is how to suppress the diffusion of In. SnO_2 with the thickness of 50, 100, 200, 500 and 800 Å is deposited on ITO/glass substrate by EB method to stop the diffusion of In. Sheet resistivity and layer thickness of ITO are 20 Ω/\square and 1000 Å, respectively. Figure 6-13 shows depth profiles of In and Sn into p-layer deposited on these substrates. As is seen in this figure, SnO_2 layer acts as the barrier for diffusion of In to p-layer. Using these substrates, a-SiC:H/a-Si:H heterojunction solar cells were fabricated. Figure 6-14 shows the photovoltaic performances of these cells. In accordance with the result of open-circuit voltage, the performance of this cell is improved by using only 100 Å SnO_2 layer. This SnO_2 /ITO multilayer transparent electrode is better than SnO_2 or ITO to obtain a large area solar cells.

6-3-3. Typical photovoltaic performances of a-SiC:H/a-Si:H heterojunction solar cells

Through the optimizations of the deposition conditions and design parameters, the performance of a-SiC:H/a-Si:H heterojunction solar cells is improved to be more than 7.8 % with SnO_2 substrate. As the reflection loss of these cells is estimated to be 12 - 15 %, we optimized the thickness of transparent electrode as the anti-reflective

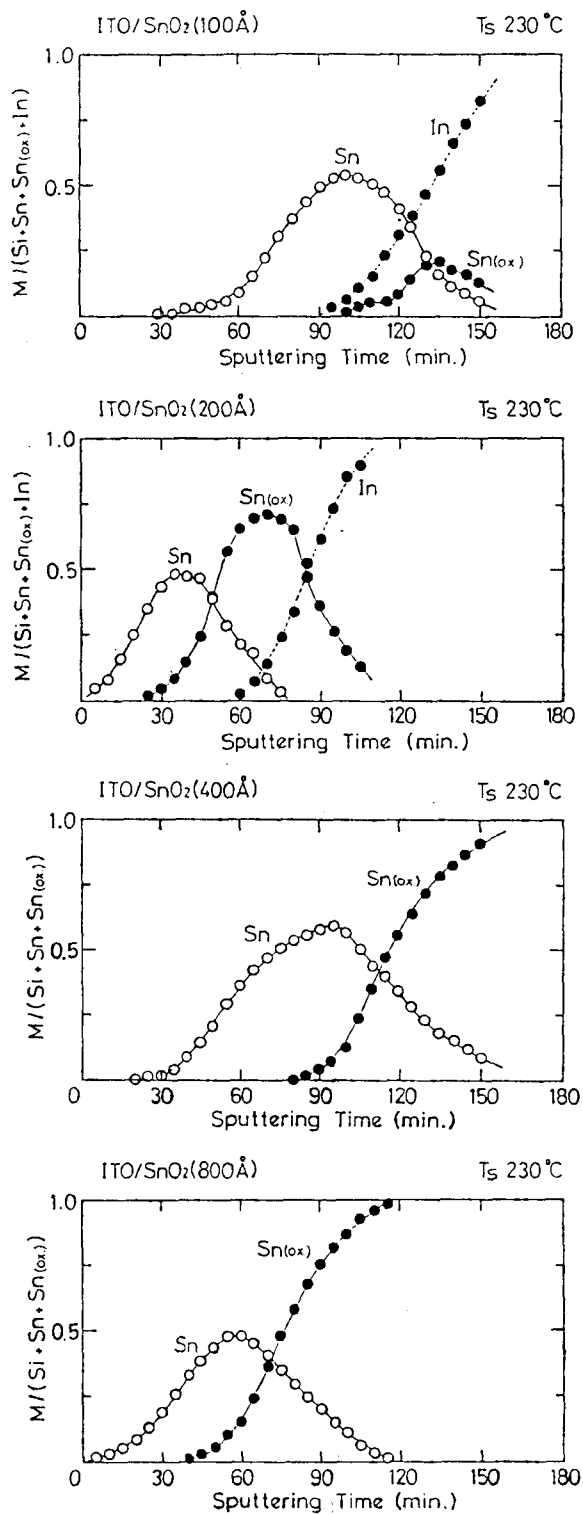


Fig. 6-13. Profiles of reduced and oxidized Sn, and In near the interface between p-layer and SnO₂ coated ITO.

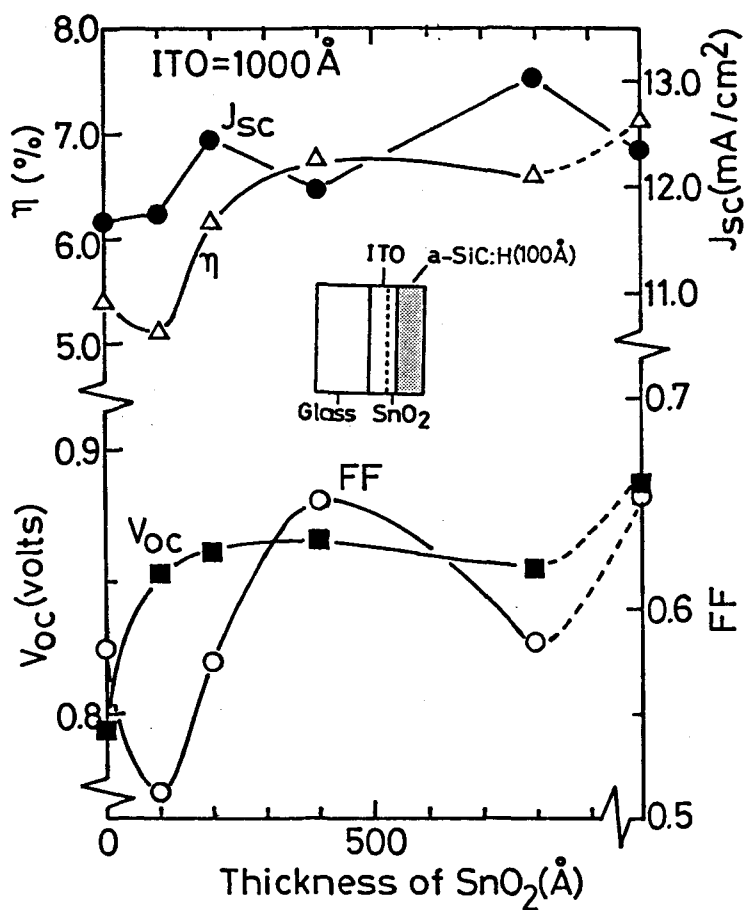


Fig. 6-14. Photovoltaic performances of a-SiC:H/a-Si:H heterojunction solar cells deposited on $\text{SnO}_2/\text{ITO}(1000\text{\AA})/\text{glass}$ substrate as a function of SnO_2 layer thickness.

coating. When the thickness of ITO is about 850 \AA , the reflection of a-Si cell on the ITO/ glass substrate is expected to be less than 5 %. Therefore, a series of experimental investigations to suppress the reduction of ITO has been made with ITO (850 \AA)/glass substrate. Finally, we have succeeded to break through an 8 % efficiency barrier. Typical performances of this cell are J_{sc} of 15 mA/cm^2 , V_{oc} of 0.88 volts, FF of 66.9 % and η of 8.84 % with a sensitive area of 3.3 mm^2 , as shown in Fig. 6-15. As for a large area solar cells, $\text{SnO}_2(100\text{\AA})/\text{ITO}(1000\text{\AA})/\text{glass}$ substrate has been developed. Employing this substrate, 7.7 % efficiency with a sensitive area of 1.0 cm^2 has been obtained as shown in Fig. 6-16. The corresponding performances are $J_{sc}=14.06 \text{ mA/cm}^2$, $V_{oc}=0.88 \text{ volts}$ and $\text{FF}=62.4 \text{ \%}$.

6-4. Realistic Estimations of Conversion Efficiency

In view point of the low cost photovoltaic R&D project, the forecasting of realistic limit of conversion efficiency in the a-Si solar cell would be of a prime importance for the balance of system consideration in the total system. A series of theoretical estimations of the a-Si cell efficiencies have made on both ideal and non-ideal cell parameters, and the obtained numbers are 14 -15 %, 17 -18 % by Carlson et al.,^{23, 24)} 8 % by Debney²⁵⁾ and 12 % by Hamakawa.²⁾ However, no definite numeral to be realized by the present stage of film quality has not appeared yet.

The major contribution to the photovoltaic process in the a-Si solar cell is due to the carrier drifting within the i-layer rather than diffusion.²⁶⁾ To make a concrete feature of geminate recombination

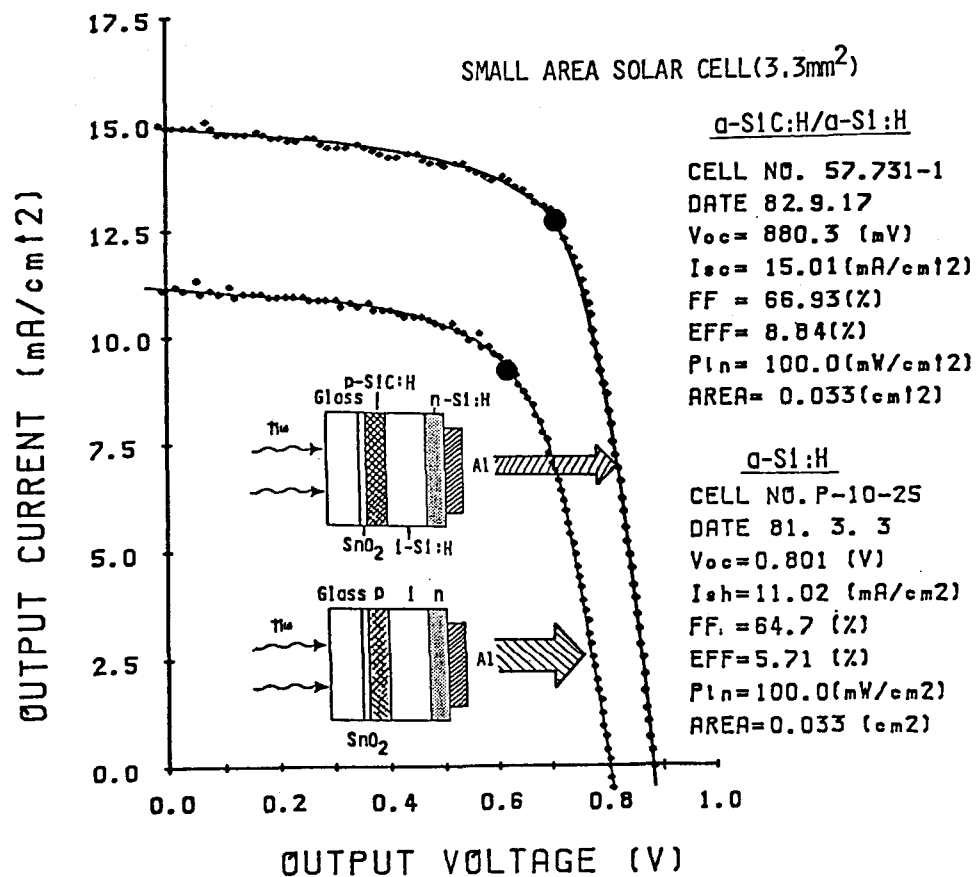


Fig. 6-15. Typical J-V characteristics of the highest efficiency a-SiC:H/a-Si:H heterojunction solar cell having a sensitive area of 3.3 mm² deposited on anti-reflective ITO/glass substrate

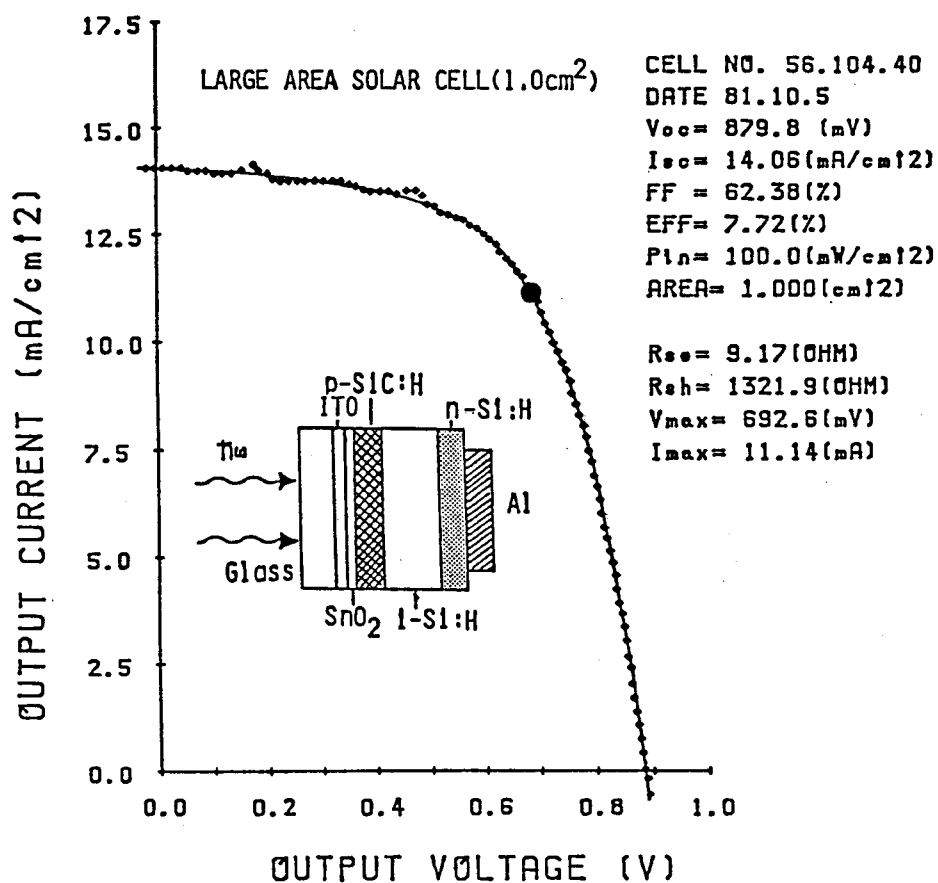


Fig. 6-16. J-V characteristics of a large area a-SiC:H/a-Si:H heterojunction solar cell (area=1.0 cm²) deposited on SnO₂(100 Å)/ITO(1000 Å)/glass substrate.

region L_{GM} , a series of experimental and theoretical investigations on the p-i-n based a-Si solar cells have been conducted by Silver et al.,²⁷⁾ Okamoto et al.²⁹⁾ and Wronski et al.¹⁰⁾

Figure 6-17 shows a result of theoretical estimations on a realistic limit of cell efficiency made by Y. Hamakawa.²⁾ The calculations have been made as a function of i-layer thickness, $W_p + W_{GM} + W_n$, with the parameters of localized state of densities G_{min} , on the basis of real film quality and cell performances experimentally obtained from a-SiC:H/a-Si:H heterojunction cells with the technological level of 1981 at Hamakawa laboratory. It is seen from this result that realistic limit of cell efficiency for our film quality is 10 % with $V_{OC}=0.91$ volts and $J_{SC}=18.3 \text{ mA/cm}^2$ with $FF=0.6$, and 12.5% for $V_{OC}=0.91$ volts and $J_{SC}=18.3 \text{ mA/cm}^2$ with $FF=0.75$ by assuming $g_{min}=10^{16}/\text{cm}^3 \cdot \text{eV}$.

Furthermore, the top data of J_{SC} , V_{OC} and FF separately obtained in a-SiC:H/a-Si:H heterojunction solar cells are 16.4 mA/cm^2 , 0.91 volts and 0.75 , respectively, as shown in Fig. 6.18. If we assume these realistic top data will become a typical routine performances on one cell, the efficiency of 11.2% might be obtained in a near future with this a-SiC:H/a-Si:H heterojunction structure developed in the present work.

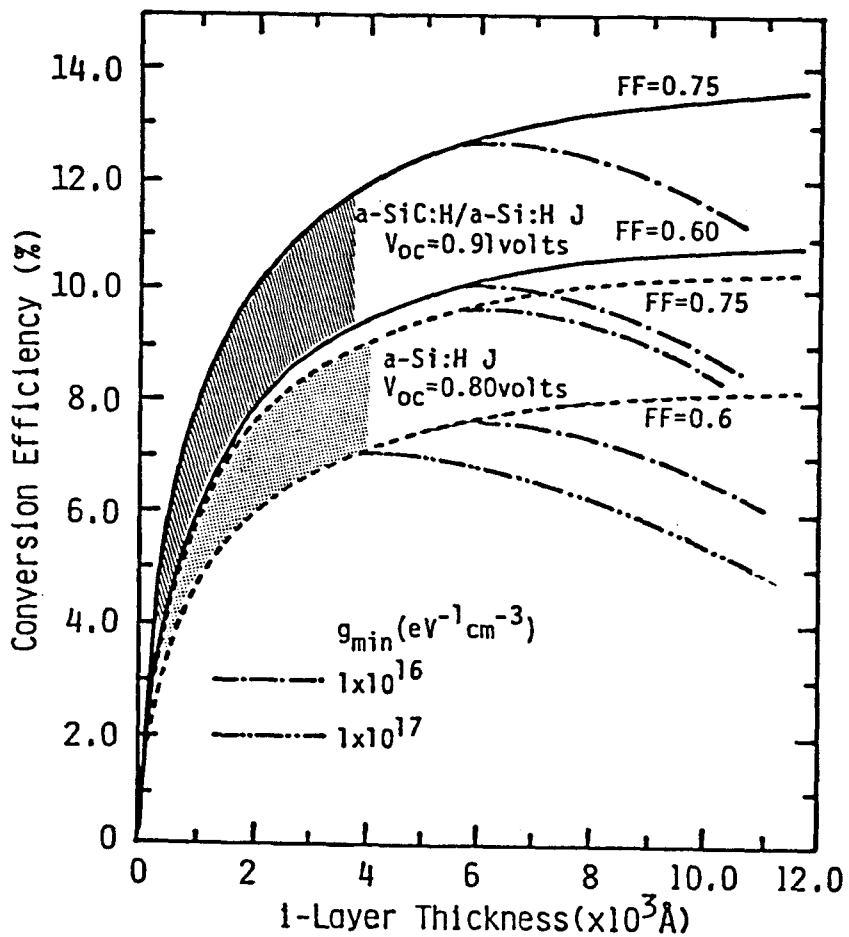


Fig. 6-17. Realistic conversion efficiency vs i-layer thickness as a parameter of minimum localized density of state g_{min} in a-Si:H p-i-n homojunction solar cell and a-SiC:H/a-Si:H heterojunction solar cell.

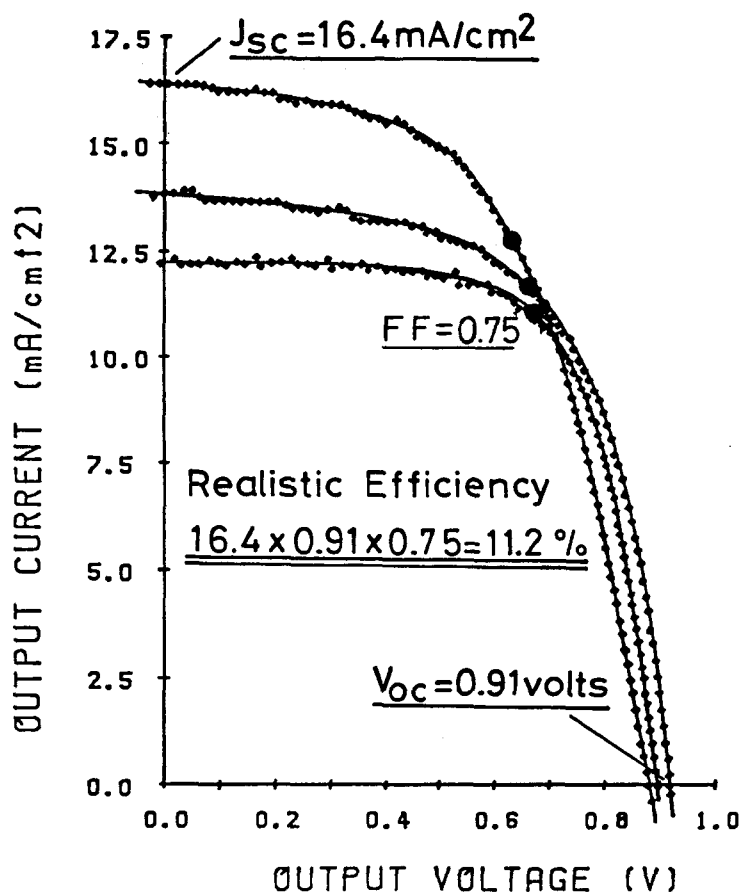


Fig. 6-18. Separately obtained highest values of J_{sc} ($16.4 \text{ mA}/\text{cm}^2$) FF (0.75) and V_{oc} (0.91 volts) and the realistic limit of efficiency ($16.4 \text{ mA}/\text{cm}^2 \times 0.71 \times 0.91 \text{ volts} = 11.2\%$).

6-5. Discussion and Summary

There are several factors to improve the efficiency of a-SiC:H/a-Si:H heterojunction solar cells. One of them is how to improve the interface between a transparent electrode and p-layer. For example, the reflection loss, the reduction of transparent electrode and the diffusion of In or Sn to p-layer might bring about some harmful influences in cell performances. Another factors are the deposition conditions and the design parameters of a-SiC:H/a-Si:H heterojunction cells.

First of all, we optimized rf power of p-layer deposition and substrate temperature. The short-circuit current density of a-SiC:H/a-Si:H heterojunction cells increases with increasing rf power of p-layer deposition. The increase of J_{sc} is caused by the increase of $E_{g(opt)}$ of p-layer. On the other hand, the open-circuit voltage decreases with increasing rf power. As the open-circuit voltage depends on the diffusion potential and the Fermi level of p-layer moves from the vicinity of valence band toward the conduction band as the increase of p-layer, the diffusion potential of p-i-n heterojunction decreases with increasing rf power of p-layer deposition. The fill factor decreases at the rf power of more than 45 watts, because of the increase of series resistance of p-layer. From these results, it is recognized that the most desirable rf power of p-layer deposition is 35 watts.

From the investigations of substrate temperature dependence of p-type a-SiC:H film properties, it is expected that the higher open-circuit voltage might be obtained at the lower substrate temperature. On the other hand, fill factor might decrease with decreasing the

substrate temperature. To confirm the forecasts, we investigated the substrate temperature dependence on the cell performances. The fill factor FF increases and the open-circuit voltage V_{oc} decreases with increasing the substrate temperature. These results are consistent with the considerations of properties of a-SiC:H. However, the short-circuit current density significantly decreases as the increase of the substrate temperature contrary to the expectation. The difference between the expectation and the observed value of J_{sc} of solar cell deposited at high temperature originates in the reduction of transparent electrode and the diffusion of reduced element. As the optical transparency of SnO_2 layer decreases with increasing the surface reduction of SnO_2 and the diffusion of reduced Sn, the short-circuit current density of solar cell might decrease with increasing the substrate temperature. From the result, the optimum substrate temperature is about 230°C at the present stage of the experiment.

Under the optimized deposition condition, experimental investigation for the effect of i-layer thickness on the photovoltaic performances has been carried out, and the highest conversion efficiency is obtained at the i-layer thickness of about 6500 Å. From this i-layer thickness optimization, the efficiency of a-SiC:H/a-Si:H heterojunction solar cells is improved to 7.8 %. While, an ordinary p-i-n a-Si:H homojunction solar cell showed the efficiency of 5.7 %. Comparing the p-i-n a-Si:H homojunction solar cell, the performances of a-SiC:H/a-Si:H heterojunction cell are clearly improved by 24.9 % in J_{sc} , 13.7 % in V_{oc} and 37 % in η .

Further improvement of the efficiency necessitates at least well controlled junctions and definite contact. Surface analysis such as

Auger electron spectroscopy (AES) has been carried out to determine depth distribution of In or Sn near the interface between the transparent electrode and amorphous layer. From this analysis, it has been found that SnO_2 or ITO are reduced to metallic Sn or In by hydrogen plasma and reduced Sn or In diffuses to p-layer. A cell deposited on SnO_2 substrate shows a higher open-circuit voltage than a cell on ITO substrate. From this result it is recognized that the diffusion of metallic In into p-layer results in harmful influence on cell performances, but Sn does not. Possible explanation for the different effect of metallic In and Sn is that these elements occupy coordination number of 3 and 4, respectively.

To suppress the reduction and the diffusion of ITO, glass/ITO/ SnO_2 substrate has been developed. SnO_2 layer with only 100 Å thickness acts as the barrier for the diffusion of In to p-layer and improves the open-circuit voltage. This SnO_2 /ITO multilayer transparent electrode is better structure than SnO_2 or ITO to obtain a large area solar cell. Furthermore, the thickness of transparent electrode has been optimized as the anti-reflective coating. After a series of experimental investigations to suppress the reduction of ITO (850 Å), we have succeeded to break through an 8 % efficiency barrier. Typical performances of the cell are $J_{\text{SC}}=15 \text{ mA/cm}^2$, $V_{\text{OC}}=0.88 \text{ volts}$, $\text{FF}=0.669$ and $\eta=8.84 \%$. As for a large area solar cell, 7.7 % efficiency with a sensitive area of 1.0 cm^2 has been obtained. The corresponding performances are $J_{\text{SC}}=14.06 \text{ mA/cm}^2$, $V_{\text{OC}}=0.88 \text{ volts}$ and $\text{FF}=0.624$.

It is seen from the theoretical calculations that a realistic limit of a-SiC:H/a-Si:H heterojunction cell is 10 % with $V_{\text{OC}}=0.91$

volts, $J_{sc}=18.3 \text{ mA/cm}^2$ and $FF=0.6$, and 12.5 % with $V_{oc}=0.91$ volts, $J_{sc}=18.3 \text{ mA/cm}^2$ and $FF=0.75$ by assuming $g_{min}=10^{16}/\text{cm}^3 \cdot \text{eV}$.

Furthermore, the top data of J_{sc} , V_{oc} and FF separately obtained in a-SiC:H/a-Si:H heterojunction solar cells are 16.4 mA/cm^2 , 0.91 volts and 0.75, respectively. Assuming that these realistic top data will become a typical routine performances on one cell, the efficiency of 11.2% might be obtained in a near future with this a-SiC:H/a-Si:H heterojunction structure developed in the present work.

REFERENCES

- 1) D. E. Carlson and C. R. Wronski: *Appl. Phys. Lett.*, 28 (1976) 671.
- 2) Y. Hamakawa: *Proc. 9th International Conf. on Amorphous and Liquid Semiconductors*, Grenoble (1981) published as *J. du Physique*, C-4 (1981), suppl. 10, 1131.
- 3) Y. Tawada, M. Kondo, H. Okamoto and Y. Hamakawa: *Proc. 15th IEEE Photovoltaic Specialists Conf.*, Florida (1981), p245.
- 4) Y. Uchida, M. Ueno, M. Kamiyama, T. Ichimura and H. Sakai: *42th Fall Meeting of Jpn. Soci. of Appl. Phys.*, Fukui (1981), p441.
- 5) A. Madan, J. MacGill, J. Yang, W. Czubatjy and S. R. Obshinsky: *Proc. 9th International Conf. on Amorphous and Liquid Semiconductors*, Grenoble (1981) published as *J. du Physique*, C-4 (1981), suppl. 10, 463.
- 6) G. Nakamura, K. Sato and Y. Ikumoto: *42th Fall Meeting of Jpn. Soci. of Appl Phys.*, Fukui (1981), p440.
- 7) H. Okamoto, Y. Nitta, T. Adachi and Y. Hamakawa: *Surface Sci.*, 86 (1979) 486.
- 8) H. Okamoto, Y. Nitta, T. Yamaguchi and Y. Hamakawa: *Solar Energy Mat.*, 2 (1981) 313.
- 9) Y. Hamakawa, H. Okamoto and Y. Nitta: *Proc. 14th IEEE Photovoltaic Specialists Conf.*, San Diego (1980), p 1074.
- 10) Y. Tawada, T. Yamaguchi, S. Nonomura, S. Hotta and Y. Hamakawa: *Jpn. J. Appl. Phys.*, 20 (1981), suppl. 20-2, 213.
- 11) Y. Tawada, H. Okamoto and Y. Hamakawa: *Appl. Phys. Lett.*, 39 (1981) 237.
- 12) Y. Tawada, M. Kondo, H. Okamoto and Y. Hamakawa: *Proc. 9th International Conf. on Amorphous and Liquid Semiconductors*, Grenoble (1981) published as *J. du Physique*, C-4 (1981), suppl. 10, 471.

- 13) Y. Tawada, M. Kondo, H. Okamoto and Y. Hamakawa: Proc. *15th IEEE Photovoltaic Specialists Conf.*, Florida (1981), p 245.
- 14) Y. Tawada, M. Kondo, H. Okamoto and Y. Hamakawa: Proc. *13th Conf. on Solid State Devices*, Tokyo (1981) published as Jpn. J. Appl. Phys., 21 (1982), suppl. 21-1, 297.
- 15) Y. Tawada, M. Kondo, H. Okamoto and Y. Hamakawa: Solar Energy Mat., 6 (1982) 299.
- 16) Y. Tawada, K. Tsuge, M. Kondo, H. Okamoto and Y. Hamakawa: J. Appl. Phys., 53 (1982) 5273.
- 17) H. Okamoto, T. Yamaguchi, S. Nonomura and Y. Hamakawa: Proc. *9th International Conf. on Amorphous and Liquid Semiconductors*, Grenoble (1981) published as J. du Physique, C-4 (1981), suppl. 10, 507.
- 18) C. R. Wronski: IEEE Trans. ED-24 (1977), 449.
- 19) D. E. Carlson and C. R. Wronski: Appl. Phys. Lett., 28 (1976) 671.
- 20) W. E. Spear, P. G. LeComber, S. Kimmond and M. H. Brodsky: Appl. Phys. Lett., 28 (1976) 105.
- 21) N. Fukada, T. Imura, A. Hiraki, Y. Tawada, K. Tsuge, H. Okamoto and Y. Hamakawa: Proc. *3rd Photovoltaic Science and Engineering Conf.*, Kyoto (1982) and Jpn. J. Appl. Phys. 21 (1982), suppl. 21-2, 269.
- 22) Y. Tawada, K. Tsuge, M. Kondo, H. Okamoto and Y. Hamakawa: Proc. *4th EC Photovoltaic Solar Energy Conf.*, Stresa, Italy (1982) 698.
- 23) D. E. Carlson: Proc. *14th IEEE Photovoltaic Specialists Conf.*, San Diego (1980), p 291.
- 24) D. E. Carlson: IEEE SSDRC, Denver, Colorado, June 1979.
- 25) B. T. Debney: Solid State and Electronic Devices, 2 (1978) 815.
- 26) H. Okamoto, T. Yamaguchi and Y. Hamakawa: J. Phys. Soci. Japan, 49 (1981) suppl. a, 1213.

- 27) M. Silver, A. Madan, D. Adler and W. Czubytyj: Proc. *14th IEEE Photovoltaic Specialists Conf.*, San Diego (1980), p1062.
- 28) T. Yamaguchi, H. Okamoto, S. Nonomura and Y. Hamakawa: Jpn. J. Appl Phys., 20 (1980), suppl. 20-2, 195.
- 29) C. R. Wronski, G. D. Cody, B. Abeles, R. Stephens, B. Brooks and R. Sherrier; Proc. *15th IEEE Photovoltaic Specialists Conf.*, Florida (1981), p673 and p1030.

VII CONCLUSION

A systematic study has been carried out on the valency control of amorphous silicon carbide and its application to a-SiC:H/a-Si:H heterojunction solar cells. A good valency controllability has been found in methane based a-SiC:H films with a good optical transparency. A series of experimental investigations has been made on the preparations and the characterizations of a-SiC:H films for the purpose of the application to the photovoltaic devices. As a practical application of this new material, a-SiC:H/a-Si:H heterojunction solar cells have been firstly developed. Results obtained in this thesis work are enumerated as follows:

- 1) A series of technical data on the film deposition parameters of the glow discharge process for amorphous semiconductors has been presented. There exist the most favorable rf power and the geometric parameter in our deposition system. The hydrogen radicals are an important factor to explain the geometric effects on the film qualities.
- 2) It has been found that a hydrogenated amorphous silicon carbide (a-SiC:H) prepared by the plasma decomposition of ($\text{SiH}_4 + \text{CH}_4$) gas mixture shows a large photoconductivity recovery effect with boron doping and has a good valency electron controllability.
- 3) The chemical bonding structure of a-SiC:H made of two kinds of carbon source (CH_4 and C_2H_4) has been studied through the infrared absorption measurements on various vibrational modes. By the analysis of clear differences in the absorption spectra and their film qualities, possible bonding structures are identified.

- 4) Utilizing the valency controlled a-SiC:H as a window side p-layer in a p-i-n a-Si solar cell, a-SiC:H/a-Si:H heterojunction solar cells has been developed. A clear improvement of the efficiency has been obtained in the parameters of not only short-circuit current density but also open-circuit voltage as compared with an ordinary p-i-n a-Si:H homojunction solar cell. Comparing with a homojunction cell, the performances of a-SiC:H/a-Si:H heterojunction solar cell are improved by 10 % in V_{oc} and 36 % in J_{sc} .
- 5) Improvement of the short-circuit current density in methane based a-SiC:H/a-Si:H heterojunction cells is mostly due to the wide gap window effect and secondarily caused by an enhanced internal electric field with the electron confinement effect due to the discontinuity of conduction band near in p a-SiC:H/i a-Si:H interface.
- 6) A clear correlationship between the open-circuit voltage and the diffusion potential of a-SiC:H/a-Si:H heterojunction solar cells has been found, and it is experimentally proved that about one thirds of the increased diffusion potential due to the wide gap window junction contributes to the improvement of the open-circuit voltage.
- 7) From the XPS and AES measurement analysis, it has been found that the transparent electrode such as SnO_2 or ITO is reduced to metallic Sn or In by the hydrogen plasma and the diffusion of In into p-layer results in the harmful influence on the cell performances. Suppressing the hydrogen plasma reduction of ITO layer which has an anti-reflective thickness, an 8 % efficiency barrier has first broken through in 1981 with a-SiC:H/a-Si:H heterojunction structure. Typical performances are J_{sc} of 15 mA/cm^2 , V_{oc} of 0.88 volts, FF

of 66.9 % and the conversion efficiency of 8.84 % with a sensitive area of 3.3 mm^2 .

- 8) SnO_2/ITO multilayer substrate which has a low sheet resistivity has been developed for a large area solar cell. Employing the substrate, 7.7 % efficiency has been achieved with a sensitive area of 1.0 cm^2 . The corresponding performances are $J_{\text{sc}}=14 \text{ mA/cm}^2$, $V_{\text{oc}}=0.88 \text{ volts}$ and $\text{FF}=62.4 \%$.
- 9) The theoretical estimation of the cell efficiency has been made on the basis of real cell performances obtained from a-SiC:H/a-Si:H heterojunction solar cells. It is seen that the realistic limit of the efficiency is 12.5 % for $V_{\text{oc}}=0.91 \text{ volts}$ and $\text{FF}=0.75$ by assuming $g_{\text{min}}=10^{16}/\text{cm}^3 \cdot \text{eV}$.
- 10) The top data of J_{sc} , V_{oc} and FF separately obtained in a-SiC:H/a-Si:H heterojunction cells are 16.4 mA/cm^2 , 0.91 volts and 0.75 , respectively. Assuming these realistic top data will become a routine performances on one cell, the efficiency of 11.2 % might be obtained in a near future with this a-SiC:H/a-Si:H heterojunction structure developed in the present work.

VITA

Yoshihisa Tawada was born in Usuki, Ohita, Japan on August 23, 1947. He graduated from Usuki Senior High School, Usuki, Ohita in March 1966 and entered Osaka University, Toyonaka, Osaka in April 1966. He graduated from Osaka University in March of 1970 and entered the Graduate School in April of that year. He recieved his Master of Science degree in Chemistry in March, 1972 from Osaka University. Then he entered Kanegafuchi Chemical Industry Co. Ltd. as a researcher. Since April, 1980, he has joined Semiconductor Laboratory of Electrical Engineering, Faculty of Engineering Science, Osaka University on leave of absence from Kanegafuchi Chemical Industry Co. Ltd.